THE CELL BIOLOGY OF NEK8, DEFECTIVE IN CYSTIC KIDNEY DISEASES

by

Melissa Lin Trapp
BSc, Simon Fraser University, 2005

THESIS SUBMITTED IN PARTIAL FULFILLMENT OF
THE REQUIREMENTS FOR THE DEGREE OF

MASTER OF SCIENCE

In the
Department of Molecular Biology and Biochemistry

SIMON FRASER UNIVERSITY

Summer 2007

APPROVAL

Name: **Melissa Lin Trapp**

Degree: **Master of Science**

Title of Thesis: **The Cell Biology of Nek8, Defective in Cystic Kidney Diseases**

Examining Committee:

Chair: **Dr. Peter J. Unrau**
Assistant Professor of Molecular Biology and Biochemistry

Dr. Lynne M. Quarmby
Senior Supervisor
Associate Professor of Molecular Biology and Biochemistry

Dr. Esther M. Verheyen
Supervisor
Associate Professor of Molecular Biology and Biochemistry

Dr. Michel R. Leroux
Supervisor
Associate Professor of Molecular Biology and Biochemistry

Dr. Michael A. Silverman
Internal Examiner
Assistant Professor of Biological Sciences

Date Defended/Approved: July 3, 2007

ABSTRACT

Ciliopathies, which are caused by defects in cilia and basal bodies include the cystic kidney diseases. Mutations in the NIMA-related kinase, Nek8, are associated with the cystic kidney disease, nephronophthisis, and cause renal cysts in juvenile cystic kidney (jck) mice. In this study, I find that Nek8 localizes to cilia in cell culture and in developing mouse kidney. Specifically, Nek8 is expressed in cilia of epithelial cells lining the tubules of the uretic bud lineage. Cystogenic forms of Nek8 show differential ciliary localization, but do not affect ciliogenesis. In jck mouse kidney, ciliary Nek8 localization is reduced. These data indicate Nek8 functions within the cilium and defects in localization are correlated with renal cystogenesis.

Keywords: cilia, cystic kidney disease, NIMA-related kinase, kidney development

Subject Terms: cell biology

To Jason

ACKNOWLEDGEMENTS

Thank you to the many, many people who have supported and encouraged me in my education and research. Thank you to Dr. Lynne M. Quarmby for being a phenomenal senior supervisor. Thank you to Dr. Michel R. Leroux and Dr. Esther M. Verheyen for being on my supervisory committee and Dr. Michael A. Silverman and Dr. Peter J. Unrau for being my internal examiner and defense chair, respectively. I thank the people in the Quarmby and Leroux labs for their expertise and help with experiments. I also thank Michel Leroux and his lab members for the use of their tissue culture facilities and people in the MBB department who have provided technical insight over the years. I also thank Dr. Noham Weinberg and Dr. B. Mario Pinto for introducing me to research early in my undergraduate years.

I thank my collaborators, Dr. David Beier and Danielle Manning at Harvard Medical School, Dr. Friedhelm Hildebrandt and Dr. Edgar Otto at the University of Michigan, and Dr. Norman Rosenblum and Alevtina Galtseva at the University of Toronto. Thank you to the Michael Smith Foundation for Health Research and the Natural Sciences and Engineering Research Council of Canada for supporting my MSc work through graduate fellowships.

Finally, I thank my families for their support –even if they didn't understand anything I was saying– and last, but not least, Jason Trapp for always being there for me, even when science wasn't.

TABLE OF CONTENTS

LIST OF FIGURES

.

LIST OF TABLES

GLOSSARY

Bardet-Biedl syndrome (BBS)	A pleiotrophic disease associated with eye impairment, polydactyly, obesity, and kidney disease.
Centrosome	A centriole-based organelle responsible for organizing microtubules and regulating cell cycle.
Cilia	Hair-like microtubule-based organelles which extend from the cell; usually motile in unicellular organisms.
Ciliogenesis	The assembly and maintenance of cilia.
Cystogenesis	The formation and expansion of cysts.
IFT	Intraflagellar transport; Bidirectional transport along the cilium mediated by microtubule-binding molecular motors.
Kidney tubule	An epithelial tube with lumenal cilia, used to collectively describe the proximal and distal tubules, the Loop of Henle, the collecting duct, and the uretic bud of the kidney.
Mesenchyme	A developmental cell type consisting of non-epithelial, loosely associated cells.
Mouse model	A spontaneously mutated or transgenic mouse that mimics characteristics of human disease.
Nephron	A tubular filtering unit of the kidney.
Nephrogenesis	The development and elongation of nephrons.
Sonic hedgehog (Shh)	A member of the hedgehog family of cholesterol-bound secreted signalling molecules.
Wnt	A secreted signalling molecule that regulates cell-cell interactions; The name is a composite of wingless in *Drosophila* and integration site-1 in the mouse.

CHAPTER 1: INTRODUCTION

Cilia, Signalling and Cell Cycle

The cilium was once an organelle whose sole role was attributed to cell motility. However, increasing amounts of data has caused a renaissance of cilia, implicating this once-forgotten organelle in extracellular sensing, intracellular signalling, and control of the cell cycle. Defects in cilia and their associated basal bodies, have been discovered to be the cause of many seemingly unrelated diseases, highlighting their importance in the cell.

Ciliary Structure and Intraflagellar Transport

The cilium and the eukaryotic flagellum is an organelle that extends from the cell and is composed of a microtubule-based axoneme, surrounded by membrane continuous with the plasma membrane. The axoneme of the cilium projects as a continuation of the centriole-based basal body and is composed of nine doublet microtubules arranged in a ring, with or without a pair of central microtubules (designated 9+2 or 9+0). While the central pair of microtubules are most commonly associated with motility, cilia can be motile and 9+2 (as in *Chlamydomonas reinhardtii*) or 9+0 (as in nodal cilia). Cilia can also be non-motile and 9+0 (as in renal cilia) or 9+2 (as in olfactory neurons)(Rosenbaum and Witman, 2002; Singla and Reiter, 2006; Pazour and Witman, 2003). The axoneme is associated with radial spokes linking the central pair with the outer

microtubule. The microtubules are oriented with minus-ends at the ciliary base and plus-ends at the ciliary tip.

Cilia are assembled and maintained by a process called intraflagellar transport (IFT)(Rosenbaum and Witman, 2002). Protein synthesis occurs in the cell body and ciliary proteins are transported along the flagellum through a plus-end directed kinesin (anterograde transport) and proteins returning back to the cell body are transported through a minus-end directed cytoplasmic dynein (retrograde transport)(Scholey 2003). Proteins assemble into IFT rafts, consisting of core IFT proteins that are biochemically separable as complex A and complex B (Cole 2003). During ciliary elongation, the building blocks of the cilium undergo anterograde transport and are added to the growing microtubule plus-end, and during ciliary resorption, disassembled ciliary proteins undergo retrograde transport back to the cell body (Rosenbaum and Witman, 2002).

Compared to the cell body, the cilium is distinct in its protein composition, and genomic and proteomic approaches have identified the complement proteins in the cilium. In 2004, Li *et al.* estimated the genes specific to the cilium and basal body by subtracting the ciliated genomes of *Homo sapiens* and *C. reinhardtii* with the non-cilated *Arabidopsis thaliana* genome. The resulting set of sequences were specifically expressed in ciliated cells and were called the flagellar and basal body proteome (Li *et al.* 2004). In 2005, Pazour *et al.* and Keller *et al.* reported the content of the ciliary proteome resulting from biochemical isolation of *C. reinhardtii* flagella. In addition to structural

components of the axoneme, they found numerous enzymes, receptors, and signalling molecules within the cilium.

Model organisms used to study cilia include the unicellular green alga *C. reinhardtii*, the soil nematode *C. elegans*, the protozoan *Tetrahymena thermophila*, unicellular parasites *Leishmania major* and *Trypanosomas bruceii*, zebrafish *Danio renio*, as well as the mammalian models of *Mus musculus* and *Ratticus norvegicus*. Cilia are absent on most fungi, including yeast, and most plants.

Ciliary Signalling

Cilia are ubiquitous in mammals, present on almost every cell in the human body, with the notable exception of blood cells. In photoreceptor cells of the eye, connecting cilia function to transport components to the outer segment, where light-sensing rhodopsin is located (Marszalek *et al.* 2000). In the developing embryo, motile nodal cilia create a flow of morphogenic determinants, thereby breaking left-right asymmetry (Raya and Belmonte, 2006). The primary cilia of the kidney epithelia function as mechanosensors, sensing urine fluid flow and transduction the signalling through calcium influx (Praetorius and Spring 2001, Nauli *et al.* 2003).

It is perhaps not surprising that defects in cilia can lead to disease with pleiotrophic pathology, collectively called ciliopathies. A number of diverse diseases have been categorized in this group and include primary cilia dyskinesia, Bardet-Biedl syndrome, the cystic kidney diseases, orofaciodigital

syndrome, and Meckel-Gruber Syndrome (Badano *et al.* 2006). Phenotypes of these diseases include renal cysts, retinal degeneration, obesity, mental retardation, *situs inversus*, polydactyly, and hydrocephalus (Badano *et al.* 2006). Many of the proteins mutated in ciliopathies localize to the cilia or centrosome, suggesting these organelles function in maintaining cellular homeostasis.

A particularly unexpected role of cilia has been revealed in sonic hedgehog (Shh) signalling. The *Tg737* hypomorphic mouse which is defective in IFT88/Polaris, resembled defects associated with Shh signalling including abnormal dorsoventral patterning of the neural tube (Huangfu and Anderson, 2006; Huangfu *et al.* 2003). An IFT152 mutant mouse also showed Shh-associated defects with misexpression of downstream morphogenic effectors (Huangfu *et al.* 2003). Further localization studies have indicated that smoothened (Smo), the Shh receptor, is found in cilia, along with its downstream effectors, the Gli2 and Gli3 transcriptional regulators. (May *et al.* 2005; Haycraft *et al.* 2005) The model of cilia-dependent Shh signalling suggests that the presence of the cilium allows for sequestration of Gli proteins, and upon Smo binding of Shh, allows cleavage of Gli2 and Gli3 and subsequent transcriptional control (Liu *et al.* 2005).

Cilia have also been implicated in planar cell polarity (PCP) pathway, which is responsible for establishing and maintaining cell polarity within an epithelial layer (Wang and Nathans, 2007). Inversin, a protein found in the cilium and is associated with cystic kidney disease, has been found to regulate dishevelled degradation switching from canonical to non-canonical Wnt signalling

in zebrafish (Simons *et al.* 2005). Mice with mutations in Bardet-Biedl syndrome (BBS) genes, necessary for IFT and basal body function, also show characteristic PCP phenotypes (Ross *et al.* 2005). A genetic interaction with a BBS mutant was observed for the PCP gene Van Gogh-like (Vangl2) which also localizes to the cilia and basal body (Ross *et al.* 2005). From this evidence, it seems that the cilium plays a role in mediating epithelial PCP.

Cilia and Cell Cycle

A burgeoning field of cilia research examines the link between cilia and the cell cycle. An intertwined relationship between the two is inherent as cilia need to be resorbed by the cell to allow basal bodies to function as centrioles to form the mitotic spindle. After mitosis is complete, centrioles again become basal bodies and cilia reassemble. While the mechanistic link coordinating ciliary resorption and assembly with the cell cycle is unclear, some key players have been identified.

In addition to core IFT components, the proteins which affect ciliary assembly include VHL (von-Hippel Lindau), Alms1 (Alström gene 1), and duboraya (Thoma *et al.* 2007; Schermer *et al.* 2006; Li *et al.* 2007; Oishi *et al.* 2006). In *C. reinhardtii*, CALK (*Chlamdomonas* Aurora A like kinase) has been found to regulate ciliary resorption (Pan *et al.* dev cell 2004). Deflagellation, the severing of the microtubule axoneme at the base of the cilium, is also important in regulating resorption (Parker and Quarmby, 2003).

Direct links between cilia and the cell cycle have been made with two *C. reinhardtii* NIMA-related kinases (Neks). The Nek, Fa2p (flagellar autotomy 2 protein), which is essential for calcium-mediated axonemal microtubule severing, is located at a specific region of the proximal cilium, the site of flagellar autotomy. Cells that lack Fa2p have a G2/M cell-cycle delay (Mahjoub *et al.* 2004). The Nek, Cnk2p (*Chlamydomonas* Nek 2 protein), is localized to cilia and regulates ciliary length. In addition, Cnk2p affects cell size control (Bradley and Quarmby, 2005). The dual roles of the Fa2p and Cnk2p kinases in addition to mounting evidence suggests that cilia regulate cell cycle and NIMA-related kinases may be key mediators (Quarmby and Parker, 2005).

NIMA-Related Kinases

The founding member Never-in-mitosis-A (NIMA) from *Aspergillus nidulans* is a serine/threonine kinase identified in a genetic screen for mitotic mutants (Oakley and Morris, 1983; Osmani *et al.* 1988). NIMA-related kinases (Neks) contain an N-terminal kinase domain followed by C-terminal domains which vary in length and composition (O'Connell *et al.* 2003). Neks are evolutionarily conserved and seem to be expanded in species containing ciliated cells that divide (Parker *et al.* submitted).

Mammals have 11 Neks, of which Nek2 is the most studied member and is most similar to *Aspergillus* NIMA (O'Connell *et al.* 2003). Nek2 localizes to the centrosomes, where it mediates centrosome separation during mitotic entry (Hayward and Fry 2006). Nek3 is predominantly cytoplasmic and functions in cell motility (Miller *et al.* 2007, Miller *et al.* 2005; also see appendix 5). Nek6 and

Nek7 localize to centrosomes and are regulated by phosphorylation of Nek9 (Yissachar *et al.* 2006; Belham *et al.* 2003). Nek9 is both cytoplasmic and nuclear, binds bicaudal D, and is involved in interphase progression (Holland *et al.* 2002; Tan and Lee, 2004). Nek1 localizes to centrosomes and has been identified as the causal mutation in the *kat* (kidney, anemia, testes) mouse model of cystic kidney diseases (Uphadya *et al.* 2000; Mahjoub *et al.* 2005; see Chapter 2).

Nek8 was first identified as carrying a spontaneous mutation causing the *jck* mouse model of polycystic kidney disease (Liu *et al.* 2002). With recessive inheritance, the *jck* mouse develops enlarged cystic kidneys that are palpable by 6 weeks of age (Atala *et al.* 1993). The mouse Nek8 2,097 bp transcript encodes a 698 amino acid protein and its C-terminal domain contains five predicted RCC1 (regulator of chromatin condensation-1) repeats (Liu *et al.* 2002). The RCC1 domain is a beta-propeller protein-protein interaction domain and the G448V rnissense mutation in the *jck* mouse is in this domain (Liu *et al.* 2002).

The *jck* mouse has many of the cellular characteristics of polycystic kidney disease, including aberrant apical-basal polarity, and increased proliferation, apoptosis, and cyclic AMP (cAMP) levels (Smith *et al.* 2006). However the *jck* phenotype is genetically modified by unidentified genes on chromosome 1 and 4, suggesting that Nek8 function depends on other gene products (Kuida and Beier, 2000). Kidneys of *jck* mice have increased levels of galectin-1, a soluble beta-galactoside-binding lectin; sorcin, a small cytosolic calcium-binding protein; and vimentin, a component of intermediate filaments (Valkova *et al.* 2005). Human

Nek8 is overexpressed in breast cancer and is associated with decreased actin protein and increased levels of cdk1/cyclinB1 (Bowers and Boylan, 2004). However, the substrates and protein interactors of Nek8 remain unknown.

Cystic Kidney Diseases

Renal cysts are hallmarks in a wide variety of diseases, including polycystic kidney disease (PKD), nephronophthisis (NPHP), tuberous sclerosis, von Hippel-Lindau syndrome, medullary cystic kidney disease, Bardet-Biedl syndrome (BBS), and Meckel-Gruber syndrome (Bisceglia *et al.* 2006). Nek8 has been found to be associated with PKD and NPHP, and the pathology and molecular genetics of these two diseases are discussed below.

Polycystic Kidney Disease

The pathology of PKD involves enlarged kidneys due to cysts throughout and is categorized by genetic inheritance. Autosomal dominant PKD (ADPKD) results from a germline mutation followed by a "second-hit" somatic mutation at the cellular level and disease onset varies between 30 and 60 years of age (Torres and Harris, 2007). Autosomal recessive PKD (ARPKD) causes cysts and enlargement of the kidney during fetal development (Harris and Rossetti, 2004).

ADPKD (Online Mendelian Inheritance in Man [OMIM] #173900) is one of the most common monogenetic diseases with a prevalence estimated at 1:1000 (Harris, 1999). ADPKD usually manifests itself after the third decade of life with symptoms including enlarged cystic kidneys, with extrarenal cysts in the liver and pancreas. Renal cyst formation occurs in all regions of the nephron and is

characterized by increased cell proliferation and apoptosis (Torres and Harris, 2007). However, disease severity, age of onset, and extrarenal manifestations are highly variable between individuals (Pei, 2005). Currently PKD is treatable only by kidney dialysis or organ transplantation.

In 85% of cases, ADPKD is caused by a mutation in PKD1 and in 15% of cases, it is caused by a mutation in PKD2 (Harris, 1999). PKD1 is located on human chromosome 16p13.3 (chromosome 17 in mouse) and the 14.5kb transcript encodes a 4,302 amino acid membrane glycoprotein (polycystin-1) containing a large extracellular N-terminus containing many non-conserved domains, followed by 11 transmembrane domains, and a short intracellular C-terminus (International consortium, 1995 and Hughes et al. 1995). Polycystin-1 localizes to the plasma membrane, cilia, and cell junctions (Ibraghimov-Beskrovnaya *et al.* 2000, Grimm *et al.* 2003, Yoder et al. 2002) and is likely to function as a receptor responsible for mediating cell-cell or cell-matrix interactions. PKD1 is developmentally expressed as early as the morula stage, with differential expression levels in various tissues/organs throughout development. Expression is highest in the early kidney, and is highly regulated in the neural tube, neural crest, chondrogenic tissue, metanephros, and lung (Guillanume *et al.*, 1999).

PKD2 is located on human chromosome 4q21 (chromosome 5 in mice) and the 2.9kb open reading frame encodes a 968 residue membrane glycoprotein (polycystin-2 or TRPP2) with 6 membrane-spanning domains and intracellular N and C termini, which is homologous to the transient receptor

potential (TRP) protein superfamily, a diverse group of voltage-independent cation-permeable channels expressed in most mammalian cells (Mochizuki *et al.* 1996). Polycystin-2 localizes to cilia, but predominantly to the ER, and is required for entry of calcium into the cell upon mechanosensation (Pazour *et al.*2002; Nauli et al. 2003). PKD2 is strongly expressed in ovary, fetal, and adult kidney, testis, and small intestine (Mochizuki *et al.* 1996).

Polycystin-1 and polycystin-2 interact at the plasma membrane through their C-termini and polycystin-1 is necessary for polycysin-2-mediated calcium entry (Tsiokas *et al.* 1997; Hanaoka *et al.* 2000). Disease-associated mutations of either polycystin-1 or polycystin-2 prevent association and channel activity (Hanaoka *et al.* 2000). Interestingly, overexpression of polycystin-1 also causes renal cysts, suggesting that the precise regulation of polycystin-1 levels is required for proper nephron maintenance (Pritchard *et al.* 2000). The C-terminus of polycystin-1 undergoes proteolytic cleavage, and the fragment translocates to the nucleus and interacts with STAT6 and p100 to regulate gene transcription in the absence of flow (Low *et al.* 2006).

The recessive form of PKD, autosomal recessive PKD (ARPKD, OMIM #263200) has pathogenically similar characteristics of ADPKD, with enlarged cystic kidneys that develop *in utero* and is often accompanied by hepatic fibrosis and cysts (Bergmann *et al.* 2004). ARPKD has a prevalence of 1:20,000 people and is caused by a mutation in PKHD1 (polycystic kidney and hepatic disease gene 1; Zerres *et al.* 1998; Ward *et al.* 2002; Onuchic *et al.* 2002). The large transcript encodes a 4074 amino acid receptor-like protein (called fibrocystin or

polyductin) with an extracellular N-terminus consisting of multiple copies of an Ig-like domain, followed by a single transmembrane domain, and a cytoplasmic C-terminus with no conserved domains (Harris and Rossetti, 2004).

Fibrocystin localizes to the primary cilia (Ward et al. 2003) and undergoes proteolysis at both N- and C-termini which requires intracellular calcium and protein kinase C (Hiesberger *et al.* 2006). The C-terminal fragment then translocates to the nucleus (Hiesberger *et al.* 2006). Fibrocystin associates with polycystin-2 through an IFT kinesin and modulates polycystin-2 channel activity (Wu *et al.* 2006; Wang *et al.* 2007).

Nephronophthisis

Nephronophthisis (NPHP) has a prevalence of 1:80,000 in the general population but is the most common genetic cause of end-stage renal disease under the age of thirty (Hildebrandt and Otto, 2005). NPHP is classified as adolescent, juvenile or infantile. NPHP differs from PKD in that renal cysts are restricted to the corticomedullary region, the kidneys are normal or slightly smaller in size, and fibrosis occurs in the tubular interstitial space (Saunier *et al.* 2005). Nephronophthisis is accompanied with retinal degeneration in Senior-Loken syndrome (SLSN), and with both retinal degeneration and cerebellar malformation in Joubert syndrome (JBTS). Seven genes have been identified as mutated in NPHP: NPHP1/nephrocystin-1, NPHP2/inversin, NPHP3, NPHP4/nephroretinin, NPHP5/IQCB1, NPHP6/CEP290, and in collaboration with this work, Nek8 (See Chapter 3; Table 1-1).

Table 1-1 Causal genes for NPHP

Gene	Locus	# of mutations identified (type)	Protein	Domains	Cellular localization	Interacting proteins	Extrarenal associations	References
NPHP1	2q13	>20 (nonsense, null deletions, missense)	Nephrocystin-1	CC, SH3, nephrocystin homology domain	Cilia, centrosome, cell-cell junctions, focal adhesions	Pyk2, tensin, p130Cas, filamin, nephrocystins-3 & -4, inversin	Cerebellar	Hildebrandt *et al.* 1997, Saunier *et al.* 1997, Otto *et al.* 2000, Donaldson *et al.* 2000 and 2002, Benzing *et al.* 2001
NPHP2	9q31	9 (nonsense, frameshift, missense)	Inversin or nephrocystin-2	ANK, IQ, D box, NLS	Cilia, centrosome, cell-cell junctions, nucleus	Nephrocystin-1, β-tubulin,APC, N-cadherin, catenins, calmodulin	*situs inversus*	Otto *et al.* 2003 and Simons *et al.* 2005, Nürnberger *et al.* 2002, Morgan *et al.* 2002a, Morgan *et al.* 2002b
NPHP3	3q22	9 (nonsense, deletion, missense)	Nephrocystin-3	CC, TTL, TPR	Cilia, connecting cilia	Nephrocystin-1	RD, LF	Olbrich *et al.* 2003
NPHP4	1p36	5 (nonsense, frameshift, missense)	Nephroretinin or nephrocystin-4	No conserved, Pro-rich region	Cilia, centrosome, cell-cell junctions	Nephrocystin-1, BCAR1, Pyk2	RD associated with SLSN	Mollet *et al.* 2002 and 2005
NPHP5	3q13	9 (nonsense, frameshift)	IQCB1 or nephrocystin-5	IQ, CC	Cilia, connecting cilia	Calmodulin, RPGR	RD	Otto *et al.* 2005
NPHP6	12q21	9 (nonsense, frameshift)	CEP290 or nephrocystin-6	CC, TMH, KID, NLS, P-loop	Centrosome, nucleus, connecting cilia	ATF4	RD, cerebellar, associated with SLSN, JBTS	Sayer *et al.* 2006
Nek8	17q11	3 (missense)	NEK8	Ser/Thr kinase, RCC1	Cilia	?	-	Otto *et al.* Submitted.

Abbreviations: ANK, ankyrin repeat domain; APC, anaphase promoting complex; ATF4, activating transcription factor 4; BCAR1, breast cancer anti-oestrogen resistance 1; CC, coiled-coil domain; D box, Apc2-binding domain; IQ, IQ calmodulin binding domain; JBTS, Joubert syndrome; LF, liver fibrosis; KID, RepA/Rep^{+} protein KID; NLS, nuclear localization signal; P-loop, ATP/GTP binding site motif; Pyk2, protein tyrosine kinase 2; RCC1, regulator of chromatin condensation; RD, retinal degeneration; RPGR, retinitis pigmentosa GTPase regulator; SH3, Src-homology 3 domain; SLSN, Senior-Loken syndrome; TMH, tropomyosin homology domain; TPR, tetratricopeptide repeat domain; TTL, tubulin-tyrosine ligase domain;

Collectively called the nephrocystins, these proteins localize to cilia and/or centrosomes, but are not required for ciliogenesis (reviewed in Saunier *et al.* 2005; Hildebrandt and Otto, 2005). In addition, some nephrocystins localize to cell-cell junctions, focal adhesions, and the nucleus (Table 1-1). Nephrocystin-1 also interacts with inversin, NPHP3, and nephroretinin, suggesting that a common mechanistic pathway exists. Taken together with the different subcellular localizations and interacting proteins, it appears that nephrocystins are involved in mediating signalling from cilia, centrosomes, cell-cell junctions, and focal adhesions and defects in this signalling cause NPHP.

Pathogenic Mechanisms of Cystic Kidney Diseases

Although the exact pathways downstream of causal mutations of genes responsible for cystic kidney disease remains enigmatic, studies have pieced together some of the processes involved. Cystogenesis involves increased proliferation (especially in PKD), increased apoptosis, non-planar cell division, dilation of kidney tubules, delamination from the epithelial layer, aggregation of cystic epithelium, loss of apical-basal polarity, and secretion of fluid into the cyst lumen (Simons and Walz 2006; Nauli and Zhou, 2004).

Cystic kidney diseases involve abnormalities in cellular growth and death. PKD results in enlarged kidneys due to increased proliferation of cystic epithelia. Unexpectedly, this is also accompanied by increased apoptosis as shown in cystic and non-cystic kidney tubules of sectioned kidneys (Woo 1995; Edelstein 2005) and in *bcl-2* knockout mice displaying polycystic kidneys (Nagata *et al.*

1996). These data suggest abnormal control of cell cycle control leads to renal cystogenesis.

Cystic kidney disease is also associated with increased cAMP levels, and decreased intracellular calcium levels. These second messengers affect a wide number of cellular processes, including gene regulation, enzyme control, cell proliferation, and apoptosis (Parekh and Putney, 2005; Alberts *et al.* 2002). Inhibitors of vasopressin and somatostatin receptors attenuate PKD progression in murine models by decreasing cAMP levels (Torres and Harris, 2007). Cells isolated from cystic kidneys of *PKD1* and *PKD2* mutant mice are unable to respond to mechanosensation through calcium influx (Nauli *et al.* 2003). Store-operated calcium influx and cAMP pathways converge on mitogen-activated protein kinase/extracellulary regulated kinase (MAPK/ERK) pathway, which is also abnormal in cystic kidney diseases (Torres and Harris, 2007).

Cystogenesis also involves the planar cell polarity (PCP), as evident by mouse mutant in *Tcf2/HNF1β*, a transcription factor essential for PKD1 and PKD2 expression. The *Tcf2/HNF1β* mutant mouse shows misoriented mitotic cell division during tubular elongation in epithelial cells of the nephron and this precedes cystogenesis (Fischer *et al.* 2006). In addition, BBS proteins and inversin also affect PCP, indicating that oriented cell division and maintenance of an epithelial plane is crucial for renal tubule morphology (Ross *et al.* 2005; Simons *et al.* 2005).

The extracellular matrix is an intergral part of developing and maintaining kidney structure. The role of the extracellular matrix in cystogenesis is

highlighted in polycystic kidneys of mice mutant for xylosyltransferease, an enzyme responsible for biosynthesis of glycosaminoglycans, the side chains of proteoglycans of the extracellular matrix (Condac *et al.* 2007). In addition, the expression of the secreted matrix metalloprotease, matrilysin, is upregulated in *jck* and *wnt4* mutant mice (Surendran *et al.* 2004).

Despite the many cellular processes involved in cystogenesis, the primary cause of cystic kidney diseases is a defect in ciliogenesis or ciliary signalling (Pazour, 2004). Almost all of the proteins defective in cystic kidney diseases localize to the cilium and/or centrosomes (Hildebrandt and Otto, 2005). A model of cyst formation has been proposed and hypothesizes that, under normal physiological conditions, renal epithelial cells can sense luminal fluid flow through a primary cilium. Mutation in cystogenic genes would result in failure of this mechanosensory mechanism, causing the loss of a differentiated phenotype, initiation of cell proliferation, and formation of a new tubule without restricted lumen size, i.e. a cyst (Nauli & Zhou 2004).

Hints to the etiology of cystogenesis involve other proteins identified from mouse and rat models of cystic kidney disease including bicaudal C (Bicc1) (*bpk* and *jcpk* mice), cystin (*cpk* mice), SamCystin (*Pkdr1* rat), as well as the BBS proteins (Guay-Woodford, 2003; Tobin and Beales 2007). The cause and effect relationships of these genes with the cellular processes remain to be fully elucidated. The defective processes identified in cystic kidney diseases appear to be broad homeostatic mechanisms, and may be primary or secondary results

of cystogenesis. Clearly the mechanism of renal cystogenesis is complex and further identification of the pathways involved is required.

Kidney Development

The kidney functions to excrete metabolic by-products, maintain pH and electrolyte homeostasis, and regulate fluid volume. The functional unit of the kidney is the nephron, an epithelial tubule responsible for filtration, selective resorption, and secretion of solutes, water, and macromolecules. Within the outer cortex of the kidney, blood flows from the renal arteriole into the capillary network, the glomerulus, and blood serum is pressure filtrated into the Bowman's capsule of the nephron. The filtrate passes into the proximal tubule of the nephron where active and passive transporters cause reuptake of filtered protein, carbohydrates, and electrolytes. Fluid then flows into the loop of Henle, which descends into the kidney medulla and undergoes active transport of sodium. The impermeability of the tubule in the ascending Loop of Henle allows for diffusion of water. The distal tubule then selectively secretes waste and resorbs water, thus concentrating the urine. The nephron drains into collecting ducts, which further resorbs water in the medulla, and ultimately the concentrated urine exits the kidney through the ureter and empties into the bladder (Silverthorn *et al.* 2004; Figure 1-1A).

The mammalian kidney has been extensively studied in organogenesis, and involves many important developmental processes including reciprocal induction between mesenchyme and epithelia, branching morphogenesis,

mesenchymal-to-epithelial transition, and control of cell proliferation and differentiation (Davies and Bard, 1998).

Mammalian kidney development is an example of ontogeny recapitulating phylogeny, where three forms of excretory systems develop, in a rostral-to-caudal progression. Two are transient and primitive structures (the pronephros, found in frogs and fish, and the mesonephros, present in chicken) and the remainder becomes the permanent kidney (the metanephric kidney). In the mouse, the pronephros forms adjacent to the Wolffian (nephric) duct at embryonic day 8.5 (E8.5) but without any apparent function and subsequently degenerates. Concomitantly with the pronephros degeneration, the mesonephros is formed by invasion of the Wolffian duct into the mesonephric blastema inducing the formation of nephrons at E9. These transiently function to filter blood, but degenerate by E11 with the advent of the metanephric kidney (Kuure *et al.* 2000).

Mouse metanephric kidney development begins at E10.5 where the uretic bud forms in the Wolffian duct adjacent to the uninduced metanephric blastema (Figure 1-1B). The uretic bud extends and invades the metanephric mesenchyme, inducing it to differentiate into prenephrogenic and prestromal components. The former includes stem cells that localize to the peripheral cortex of the developing kidney and form nephrons, and the latter remains in the medulla of the kidney and give rise to stromal cells, necessary for signalling to maintain kidney structure. In turn, the induced metanephric mesenchyme causes the uretic bud to bifurcate and continue growing, forming the branching collecting

duct tree. In this way, the uretic bud (which is of epithelial origin) and metanephric mesenchyme undergoes reciprocal induction (Davies and Bard, 1998).

The prenephrogenic mesenchyme condenses around the uretic bud tip at E12.5 and undergoes a mesenchymal-to-epithelial transition to form renal vesicles or cysts, in which apical cilia project into the lumen. Nephrogenesis continues as the cyst sprouts two buds, one furthest from the uretic bud, forming the proximal tubule and glomerulus, resulting in a comma-shaped body, and one closest to the uretic bud which becomes the distal tubule, forming an S-shaped body (Figure 1-1B). The distal tubule fuses with the adjacent uretic bud connecting the nephron with the collecting duct. Through poorly defined mechanisms, the tubule elongates and undergoes patterning to form the complete functioning nephron.

Figure 1-1 Metanephric kidney development

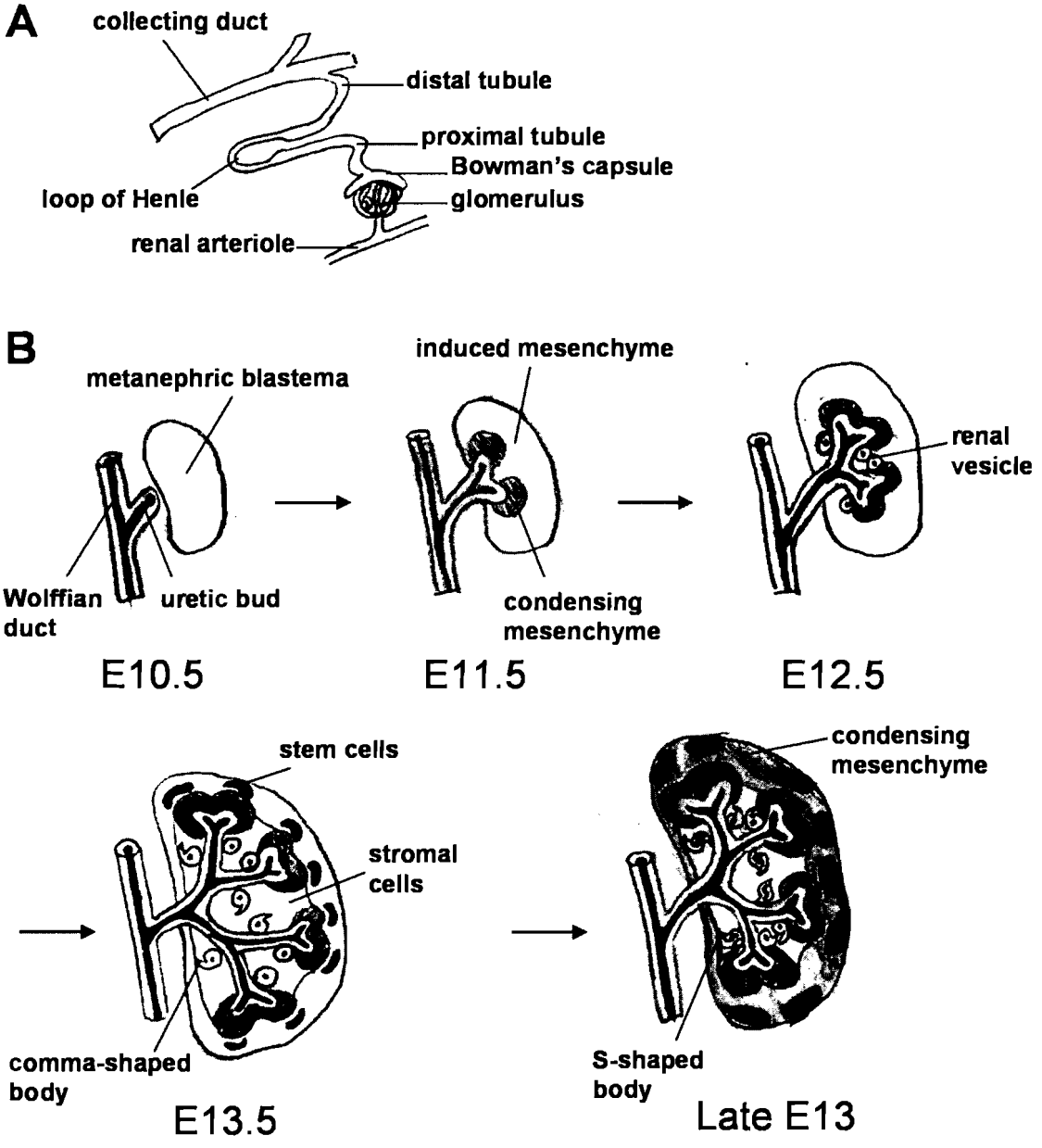

(A) Schematic of a functioning nephron. **(B)** Schematic of mouse renal development. See text for description. Drawings not to scale.

Fuelled by the proliferation of cortical stem cells, subsequent reiterations of uretic bud branching and mesenchymal condensation create the network of collecting ducts and nephrons. During E13.5 to E16, the kidney doubles in size

every 9 hours. Interestingly, the nephrons that formed earlier in development and are located in the inner kidney start to filter blood serum while the periphery of the kidney is still developing. As kidney development draws to an end a few days after birth, growth slows, the stromal cells undergo apoptosis and allow invasion of the Loop of Henle into the renal medulla, and finally, the cortical stem cells are lost. The end result is the metanephric kidney containing thousands of nephrons, a great proliferative feat considering that the uninduced metanephric blastema consisted of only a few thousand cells.

Human kidney development proceeds similarly to the mouse, with the exceptions of a longer developmental period, more nephrons, the division of the kidney into lobes, and the completion of renal development 6 weeks before birth.

Many signaling pathways are involved in kidney development, markedly the FGF (fibroblast growth factor), Wnt, BMP (bone morphogenetic protein), and Shh (sonic hedgehog) families (Schedl and Hastie, 2000; Gill and Rosenblum, 2006). In fact, over 300 genes have been found to be expressed at different stages and about 80 receptor-ligand pairings have been identified (Bard 2002). The objective of this work is not to provide a complete summary of these pathways, and the reader is referred to several excellent reviews (Schedl and Hastie, 2000; Bard 2002; Dressler 2006; Karihaloo *et al.* 2005). Signals include autocrine and paracrine pathways, often with redundancy as evident in knockout studies in mice. Various pathways function to induce the metanephric mesenchyme to undergo differentiation and epithelialisation, cause branching of the uretic bud to form the collecting duct arborisation, expand and maintain the

stem cell population, cause epithelialized cells to undergo nephrogenesis, and develop the glomerulus (Dressler 2006). These signals originate through cell-cell and cell-matrix interactions, as well as through diffusible morphogeneic gradients.

It is of note that most research has focussed on the early stages of kidney development, the induction of the metanephric mesenchyme, and the mesenchyme-to-epithelial transition. Little molecular data is known about the formation and elongation of nephrons, ie. nephrogenesis.

Overview

This thesis examines the cell biology of Nek8, which is defective in human nephronophthisis and the *jck* mouse model of polycystic kidney disease. I find that Nek8 co-localizes to cilia of epithelial cells lining the tubules of the uretic bud lineage during mouse kidney development. In the diseased state, Nek8 shows decreased ciliary localization, while not affecting ciliogenesis. These data indicate Nek8 functions within the cilium and defects in localization are correlated with renal cystogenesis.

References

Alberts B, Johnson A, Lewis J, Raff M, Roberts K, Walter P: Cell Communication In: *Molecular Biology of the Cell*, 4th ed., edited by Gibbs S, New York, Garland Science, 2002, pp 854-858

Atala A, Freeman MR, Mandell J, Beier DR: Juvenile cystic kidneys (*jck*): A new mouse mutation which causes polycystic kidneys. *Kidney Int* 43: 1081-1085, 1993

Badano JL, Mitsuma N, Beales PL, Katsanis N: The Ciliopathies: An Emerging Class of Human Genetic Disorders. *Annu Rev Genomics Hum Genet* 7: 125-148, 2006

Bard JBL: Growth and death in the developing mammalian kidney: signals, receptors and conversions. *Bioessays* 24: 72-82, 2002

Belham C, Roig J, Caldwell JA, Aoyama Y, Kemp BE, Comb M, Avruch J: A mitotic cascade of NIMA family kinases. Nercc1/Nek9 activates the Nek6 and Nek7 kinases. *J Biol Chem* 278: 34897-34909, 2003

Benzing T, Gerke P, Hopker K, Hildebrandt F, Kim E, Walz G: Nephrocystin interacts with Pyk2, p130(Cas), and tensin and triggers phosphorylation of Pyk2. *Proc Natl Acad Sci U S A.* 98: 9784-9789, 2001

Bergmann C, Senderek J, Kupper F, Schneider F, Dornia C, Windelen E, Eggermann T, Rudnik-Schoneborn S, Kirfel J, Furu L, Onuchic LF, Rossetti S, Harris PC, Somlo S, Guay-Woodford L, Germino GG, Moser M, Buttner R, Zerres K: PKHD1 mutations in autosomal recessive polycystic kidney disease (ARPKD). *Hum Mutat* 23: 453-463, 2004

Bisceglia M, Galliani CA, Senger C, Stallone C, Sessa A: Renal Cystic Diseases. *Adv Anat Pathol* 13: 26-56, 2006

Bowers AJ, Boylan JF: Nek8, a NIMA family kinase member, is overexpressed in primary human breast tumors. *Gene* 328: 135-142, 2004

Bradley BA, Quarmby LM: A NIMA-related kinase, Cnk2p, regulates both flagellar length and cell size in *Chlamydomonas. J Cell Sci* 118: 3317–3326, 2005

Cole DG: The intraflagellar transport machinery of *Chlamydomonas reinhardtii. Traffic* 4: 435–442, 2003

Condac E, Silasi-Mansat R, Kosanke S, Schoeb T, Towner R, Lupu F, Cummings RD, Hinsdale ME: Polycystic disease caused by deficiency in xylosyltransferase 2, an initiating enzyme of glycosaminoglycan biosynthesis. *Proc Natl Acad Sci U S A* 104: 9416-9421, 2007

Davies JA, Bard JBL: The development of the kidney. *Curr Top Dev Biol* 39: 245-301, 1998

Donaldson JC, Dempsey PJ, Reddy S, Bouton AH, Coffey RJ, Hanks SK: Crk-associated substrate p130(Cas) interacts with nephrocystin and both proteins localize to cell-cell contacts of polarized epithelial cells. *Exp Cell Res* 256:168-178, 2000

Donaldson JC, Dise RS, Ritchie MD, Hanks SK: rocystin-conserved domains involved in targeting to epithelial cell-cell junctions, interaction with filamins, and establishing cell polarity. *J Biol Chem* 277: 29028-29035, 2002

Dressler GR: The cellular basis of kidney development. *Annu Rev Cell Dev Biol* 22: 509-29, 2006

Edelstein CL: What is the role of tubular epithelial cell apoptosis in polycystic kidney disease (PKD)? *Cell Cycle* 4: 1550-1554, 2005

Fischer E, Legue E, Doyen A, Nato F, Nicolas JF, Torres V, Yaniv M, Pontoglio M: Defective planar cell polarity in polycystic kidney disease. *Nat Genet* 38: 21-23, 2006

Gill PS, Rosenblum ND: Control of murine kidney development by sonic hedgehog and its GLI effectors. *Cell Cycle* 5: 1426-1430, 2006

Grimm DH, Cai Y, Chauvet V, Rajendran V, Zeltner R, Geng L, Avner ED, Sweeney W, Somlo S, Caplan MJ: Polycystin-1 distribution is modulated by polycystin-2 expression in mammalian cells. *J. Biol. Chem.* 278: 36786-36793, 2003

Guay-Woodford LM: Murine models of polycystic kidney disease: Molecular and therapeutic insights. *Am J Physiol Renal Physiol* 285: F1034–F1049, 2003

Guillaume R, D'Agati V, Daoust M, Trudel M: Murine *Pkd1* Is a Developmentally Regulated Gene From Morula to Adulthood: Role in Tissue Condensation and Patterning. *Dev. Dyn.* 214: 337–348, 1999

Hanaoka K, Qian F, Boletta A, Bhunia AK, Piontek K, Tsiokas L, Sukhatme VP, Guggino WB, Germino GG: Co-assembly of polycystin-1 and -2 produces unique cation-permeable currents. *Nature* 408: 990-994, 2000

Harris PC, Rossetti S: Molecular genetics of autosomal recessive polycystic kidney disease. *Mol Genet Metab* 81: 75-85, 2004

Harris PC: Autosomal dominant polycystic kidney disease: clues to pathogenesis. *Hum. Mol. Genet.* 8: 1861–1866, 1999.

Haycraft CJ, Banizs B, Aydin-Son Y, Zhang Q, Michaud EJ, Yoder BK: Gli2 and Gli3 localize to cilia and require the intraflagellar transport protein polaris for processing and function. *PLoS Genet* 1:e53, 2005

Hayward DG, Fry AM: Nek2 kinase in chromosome instability and cancer. *Cancer Lett* 237: 155-166, 2006

Hiesberger T, Gourley E, Erickson A, Koulen P, Ward CJ, Masyuk TV, Larusso NF, Harris PC, Igarashi P: Proteolytic cleavage and nuclear translocation of fibrocystin is regulated by intracellular Ca2+ and activation of protein kinase C. *J Biol Chem* 281: 34357-34364, 2006

Hildebrandt F, Otto E, Rensing C, Nothwang HG, Vollmer M, Adolphs J, Hanusch H, Brandis M: A novel gene encoding an SH3 domain protein is mutated in nephronophthisis type 1. *Nat Genet* 17:149-153, 1997

Hildebrandt F, Otto E: Cilia and centrosomes: A unifying pathogenic concept for cystic kidney disease? *Nat Rev Genet* 6: 928-940, 2005

Holland PM, Milne A, Garka K, Johnson RS, Willis C, Sims JE, Rauch CT, Bird TA, Virca GD: Purification, cloning, and characterization of Nek8, a novel NIMA-related kinase, and its candidate substrate Bicd2. *J Biol Chem* 277: 16229-16240, 2002

Huangfu D, Anderson KV: Signaling from Smo to Ci/Gli: conservation and divergence of Hedgehog pathways from Drosophila to vertebrates. *Development* 133: 3-14, 2006

Huangfu D, Liu A, Rakeman AS, Murcia NS, Niswander L, Anderson KV: Hedgehog signalling in the mouse requires intraflagellar transport proteins. *Nature* 426: 83-87, 2003

Hughes J, Ward CJ, Peral B, Aspinwall R, Clark K, San Millan JL, Gamble V, Harris PC: The polycystic kidney disease 1 (PKD1) gene encodes a novel protein with multiple cell recognition domains. *Nat Genet* 10: 151–160, 1995.

Ibraghimov-Beskrovnaya O, Bukanov NO Donohue LC, Dackowski WR, Klinger KW, Landes GM: Strong homophilic interactions of the Ig-like domains of polycystin-1, the protein product of an autosomal dominant polycystic kidney disease gene, PKD1. *Hum. Molec. Genet.* 9: 1641-1649, 2000

International Polycystic Kidney Disease Consortium: Polycystic kidney disease: the complete structure of the PKD1 gene and its protein. *Cell* 81: 289-298, 1995

Karihaloo A, Nickel C, Cantley LG: Signals which build a tubule. *Nephron Exp Nephrol* 100: e40-e45, 2005

Keller LC, Romijn EP, Zamora I, Yates JR, Marshall WF: Proteomic analysis of isolated *Chlamydomonas* centrioles reveals orthologs of ciliary disease genes. *Curr Biol* 15: 1090-1098, 2005

Kuida S, Beier DR: Genetic localization of interacting modifiers affecting severity in a murine model of polycystic kidney disease. *Genome Res* 10: 49-54, 2000

Kuure S, Vuolteenaho R, Vainio S: Kidney morphogenesis: cellular and molecular regulation. *Mech Dev* 92: 31-45, 2000

Li G, Vega R, Nelms K, Gekakis N, Goodnow C, McNamara P, Wu H, Hong NA, Glynne R: A role for Alström syndrome protein, alms1, in kidney ciliogenesis and cellular quiescence. *PLoS Genet* 2007 3: e8, 2007

Li JB, Gerdes JM, Haycraft CJ, Fan Y, Teslovich TM, May-Simera H, Li H, Blacque OE, Li L, Leitch CC, Lewis RA, Green JS, Parfrey PS, Leroux MR, Davidson WS, Beales PL, Guay-Woodford LM, Yoder BK, Stormo GD, Katsanis N, Dutcher SK: Comparative genomics identifies a flagellar and basal body proteome that includes the BBS5 human disease gene. *Cell* 117: 541-552, 2004

Liu A, Wang B, Niswander LA: Mouse intraflagellar transport proteins regulate both the activator and repressor functions of Gli transcription factors. *Development* 132: 3103-3111, 2005

Liu S, Lu W, Obara T, Kuida S, Lehoczky J, Dewar K, Drummond IA Beier DR: A defect in a novel Nek-family kinase causes cystic kidney disease in the mouse and in the zebrafish. *Development* 129: 5839-5846, 2002

Low SH, Vasanth S, Larson CH, Mukherjee S, Sharma N, Kinter MT, Kane ME, Obara T, Weimbs T: Polycystin-1, STAT6, and P100 function in a pathway that transduces ciliary mechanosensation and is activated in polycystic kidney disease. *Dev Cell* 10: 57-69, 2006

Mahjoub MR, Rasi MQ, Quarmby LM: A NIMA-related kinase, Fa2p, localizes to a novel site in the proximal cilia of *Chlamydomonas* and mouse kidney cells. *Mol Biol Cell* 15: 5172–5286, 2004

Mahjoub MR, Trapp ML, Quarmby LM: NIMA-related kinases defective in murine models of polycystic kidney diseases localize to primary cilia and centrosomes. *J Am Soc Nephrol* 16: 3485-3489, 2005

Marszalek JR, Liu X, Roberts EA, Chui D, Marth JD, Williams DS, Goldstein LS: Genetic evidence for selective transport of opsin and arrestin by kinesin-II in mammalian photoreceptors. *Cell* 2000, 102: 175-187.

May SR, Ashique AM, Karlen M, Wang B, Shen Y, Zarbalis K, Reiter J, Ericson J, Peterson AS: Loss of the retrograde motor for IFT disrupts localization of Smo to cilia and prevents the expression of both activator and repressor functions of Gli. *Dev Biol* 287: 378-389, 2005

Miller SL, Antico G, Raghunath PN, Tomaszewski JE, Clevenger CV: Nek3 kinase regulated prolactin-mediated cytoskeletal reorganization and motility of breast cancer cells. *Oncogene* In Press.

Miller SL, DeMaria JE, Freier DO, Riegel AM, Clevenger CV: Novel association of Vav2 and Nek3 modulates signaling through the human prolactin receptor. *Mol Endocrinol* 19: 939-949, 2005

Mochizuki T, Wu G, Hayashi T, Xenophontos SL, Veldhuisen B, Saris JJ, Reynolds DM, Cai Y, Gabow PA, Pierides A, Kimberling WJ, Breuning MH, Deltas CC, Peters DJ Somlo S: PKD2, a gene for polycystic kidney disease that encodes an integral membrane protein. *Science* 272: 1339-1342, 1996

Mollet G, Salomon R, Gribouval O, Silbermann F, Bacq D, Landthaler G, Milford D, Nayir A, Rizzoni G, Antignac C, Saunier S: The gene mutated in juvenile nephronophthisis type 4 encodes a novel protein that interacts with nephrocystin. *Nat Genet* 32: 300-305, 2002

Mollet G, Silbermann F, Delous M, Salomon R, Antignac C, Saunier S: Characterization of the nephrocystin/nephrocystin-4 complex and subcellular localization of nephrocystin-4 to primary cilia and centrosomes. *Hum Mol Genet* 14: 645-656, 2005

Morgan D, Eley L, Sayer J, Strachan T, Yates LM, Craighead AS, Goodship JA: Expression analyses and interaction with the anaphase promoting complex protein Apc2 suggest a role for inversin in primary cilia and involvement in the cell cycle. *Hum Mol Genet* 11: 3345-3350, 2002b

Morgan D, Goodship J, Essner JJ, Vogan KJ, Turnpenny L, Yost HJ, Tabin CJ, Strachan T: The left-right determinant inversin has highly conserved ankyrin repeat and IQ domains and interacts with calmodulin. *Hum Genet* 110: 377-384, 2002a

Nagata M, Nakauchi H, Nakayama K, Nakayama K, Loh D, Watanabe T: Apoptosis during an early stage of nephrogenesis induces renal hypoplasia in bcl-2-deficient mice. *Am J Pathol* 148: 1601-1611, 1996

Nauli SM, Alenghat FJ, Luo Y, Williams E, Vassilev P, Li X, Elia AE, Lu W, Brown EM, Quinn SJ, Ingber DE, Zhou J: Polycystins 1 and 2 mediate mechanosensation in the primary cilium of kidney cells. *Nat Genet* 33:129-137, 2003

Nauli SM, Zhou J: Polycystins and mechanosensation in renal and nodal cilia. *Bioessays* 26: 844-56, 2004

Nürnberger J, Bacallao RL, Phillips CL: Inversin forms a complex with catenins and N-cadherin in polarized epithelial cells. *Mol Biol Cell* 13: 3096-3106, 2002

Oakley BR, Morris NR: A mutation in Aspergillus nidulans that blocks the transition from interphase to prophase. *J Cell Biol* 96:1155-1158, 1983

O'Connell MJ, Krien MJ, Hunter T: Never say never. The NIMA-related protein kinases in mitotic control. *Trends Cell Biol* 13: 221-228, 2003

Oishi I, Kawakami Y, Raya A, Callol-Massot C, Izpisúa Belmonte JC: Regulation of primary cilia formation and left-right patterning in zebrafish by a noncanonical Wnt signaling mediator, duboraya. *Nat Genet* 38: 1316-1322, 2006

Olbrich H, Fliegauf M, Hoefele J, Kispert A, Otto E, Volz A, Wolf MT, Sasmaz G, Trauer U, Reinhardt R, Sudbrak R, Antignac C, Gretz N, Walz G, Schermer B, Benzing T, Hildebrandt F, Omran H: Mutations in a novel gene, NPHP3, cause adolescent nephronophthisis, tapeto-retinal degeneration and hepatic fibrosis. *Nat Genet* 34: 455-459, 2003

Onuchic LF, Furu L, Nagasawa Y, Hou X, Eggermann T, Ren Z, Bergmann C, Senderek J, Esquivel E, Zeltner R, Rudnik-Schoneborn S, Mrug M, Sweeney W, Avner ED, Zerres K, Guay-Woodford LM, Somlo S, Germino GG: PKHD1, the polycystic kidney and hepatic disease 1 gene, encodes a novel large protein containing multiple immunoglobulin-like plexin-transcription-factor domains and parallel beta-helix 1 repeats. *Am J Hum Genet* 70: 1305-1317, 2002

Osmani SA, Pu RT, Morris NR: Mitotic induction and maintenance by overexpression of a G2-specific gene that encodes a potential protein kinase. *Cell* 53: 237-244,1988

Otto E, Kispert A, Schätzle , Lescher B, Rensing C, Hildebrandt F: Nephrocystin: gene expression and sequence conservation between human, mouse, and Caenorhabditis elegans. *J Am Soc Nephrol* 11: 270-282, 2000

Otto EA, Loeys B, Khanna H, Hellemans J, Sudbrak R, Fan S, Muerb U, O'Toole JF, Helou J, Attanasio M, Utsch B, Sayer JA, Lillo C, Jimeno D, Coucke P, De Paepe A, Reinhardt R, Klages S, Tsuda M, Kawakami I, Kusakabe T, Omran H, Imm A, Tippens M, Raymond PA, Hill J, Beales P, He S, Kispert A, Margolis B, Williams DS, Swaroop A, Hildebrandt F: Nephrocystin-5, a ciliary IQ domain protein, is mutated in Senior-Loken syndrome and interacts with RPGR and calmodulin. *Nat Genet* 37: 282-288, 2005

Otto EA, Schermer B, Obara T, O'Toole JF, Hiller KS, Mueller AM, Ruf RG, Hoefele J, Beekmann F, Landau D, Foreman JW, Goodship JA, Strachan T, Kispert A, Wolf MT, Gagnadoux MF, Nivet H, Antignac C, Walz G, Drummond IA, Benzing T, Hildebrandt F: Mutations in INVS encoding inversin cause nephronophthisis type 2, linking renal cystic disease to the function of primary cilia and left-right axis determination. *Nat Genet* 34: 413-420, 2003

Otto EA, Trapp ML, Schultheiss UT, Quarmby LM, Hildebrandt F: Mutations in NIMA-related kinase NEK8 causes nephronophthisis in humans and affects ciliary and centrosomal localization. Submitted.

Pan J, Wang Q, Snell WJ: An aurora kinase is essential for flagellar disassembly in Chlamydomonas. *Dev Cell* 6: 445-451, 2004

Parekh AB, Putney JW Jr: Store-operated calcium channels. *Physiol Rev* 85: 757-810, 2005

Parker JDK, Bradley BB, Mooers AO, Quarmby LM: Phylogeny of the NIMA-related family of kinases (Neks): an ancient gene family associated with cilia Submitted.

Parker JDK, Quarmby LM: Chlamydomonas fla mutants reveal a link between deflagellation and intraflagellar transport. *BMC Cell Biol* 4: 11, 2003

Pazour GJ, Agrin N, Leszyk J, Witman GB: Proteomic analysis of a eukaryotic cilium. *J Cell Biol* 170: 103-113, 2005

Pazour GJ, San Agustin JT, Follit JA, Rosenbaum JL, Witman GB: Polycystin-2 localizes to kidney cilia and the ciliary level is elevated in orpk mice with polycystic kidney disease. *Curr Biol* 12: R378-R380, 2002

Pazour GJ, Witman GB: The vertebrate primary cilium is a sensory organelle. *Curr Opin Cell Biol* 15:105-110, 2003

Pazour GJ: Intraflagellar transport and cilia-dependent renal disease: The ciliary hypothesis of polycystic kidney disease. *J Am Soc Nephrol* 15: 2528–2536, 2004

Pei Y: Nature and nurture on phenotypic variability of autosomal dominant polycystic kidney disease. *Kidney Int* 67: 1630–1631, 2005

Praetorius HA, Spring KR: Bending the MDCK cell primary cilium increases intracellular calcium. *J Membr Biol* 184: 71-79, 2001

Pritchard L, Sloane-Stanley JA, Sharpe JA, Aspinwall R, Lu W, Buckle V, Strmecki L, Walker D, Ward CJ, Alpers CE, Zhou J, Wood WG, Harris PC: A human PKD1 transgene generates functional polycystin-1 in mice and is associated with a cystic phenotype. *Hum Molec Genet* 9: 2617-2627, 2000

Quarmby LM, Parker JDK: Cilia and the cell cycle? *J Cell Biol* 169: 707–710, 2005

Raya A, Belmonte JC: Left-right asymmetry in the vertebrate embryo: from early information to higher-level integration. *Nat Rev Genet* 7: 283-93, 2006

Roig J, Mikhailov A, Belham C, Avruch J: Nercc1, a mammalian NIMA-family kinase, binds the Ran GTPase and regulates mitotic progression. *Genes Dev* 16: 1640-1658, 2002

Rosenbaum JL, Witman GB: Intraflagellar transport. *Nat Rev Mol Cell Biol* 3: 813-825, 2002

Ross AJ, May-Simera H, Eichers ER, Kai M, Hill J, Jagger DJ, Leitch CC, Chapple JP, Munro PM, Fisher S, Tan PL, Phillips HM, Leroux MR, Henderson DJ, Murdoch JN, Copp AJ, Eliot MM, Lupski JR, Kemp DT, Dollfus H, Tada M, Katsanis N, Forge A, Beales PL. Disruption of Bardet-Biedl syndrome ciliary proteins perturbs planar cell polarity in vertebrates. *Nat Genet* 37: 1135-1140, 2005

Saunier S, Calado J, Heilig R, Silbermann F, Benessy F, Morin G, Konrad M, Broyer M, Gubler MC, Weissenbach J, Antignac C: A novel gene that encodes a protein with a putative src homology 3 domain is a candidate gene for familial juvenile nephronophthisis. *Hum Mol Genet* 6:2317-2323, 1997

Saunier S, Salomon R, Antignac C: Nephronophthisis. *Curr Opin Genet Dev* 15: 324-331, 2005

Sayer JA, Otto EA, O'Toole JF, Nurnberg G, Kennedy MA, Becker C, Hennies HC, Helou J, Attanasio M, Fausett BV, Utsch B, Khanna H, Liu Y, Drummond I, Kawakami I, Kusakabe T, Tsuda M, Ma L, Lee H, Larson RG, Allen SJ, Wilkinson CJ, Nigg EA, Shou C, Lillo C, Williams DS, Hoppe B, Kemper MJ, Neuhaus T, Parisi MA, Glass IA, Petry M, Kispert A, Gloy J, Ganner A, Walz G, Zhu X, Goldman D, Nurnberg P, Swaroop A, Leroux MR, Hildebrandt F: The centrosomal protein nephrocystin-6 is mutated in Joubert syndrome and activates transcription factor ATF4. *Nat Genet* 38: 674-681, 2006

Schedl A, Hastie ND: Cross-talk in kidney development. *Curr Opin Genet Dev* 10: 543-549, 2000

Schermer B, Ghenoiu C, Bartram M, Müller RU, Kotsis F, Höhne M, Kühn W, Rapka M, Nitschke R, Zentgraf H, Fliegauf M, Omran H, Walz G, Benzing T: The von Hippel-Lindau tumor suppressor protein controls ciliogenesis by orienting microtubule growth. *J Cell Biol* 175: 547-554, 2006

Scholey JM: Intraflagellar transport. *Annu Rev Cell Dev Biol* 19: 423–43, 2003

Silverthorn, DU, Ober WC, Garrison CW, Silverthorn AC, Johnson BR: The Kidneys. In: *Human Physiology an Integrated Approach*, 3rd ed., edited by Silverthorn BU, San Francisco, Pearson Benjamin Cummings, 2004, pp 598-624

Simons M, Gloy J, Ganner A, Bullerkotte A, Bashkurov M, Kronig C, Schermer B, Benzing T, Cabello OA, Jenny A, Mlodzik M, Polok B, Driever W, Obara T, Walz G: Inversin, the gene product mutated in nephronophthisis type II, functions as a molecular switch between Wnt signaling pathways. *Nat Genet* 37: 537-543, 2005

Simons M, Walz G: Polycystic kidney disease: Cell division without a c(l)ue? *Kidney Int* 70: 854-864, 2006

Singla V, Reiter JF: The primary cilium as the cell's antenna: signaling at a sensory organelle. *Science* 313: 629-633, 2006

Smith LA, Bukanov NO, Husson H, Russo RJ, Barry TC, Taylor AL, Beier DR, Ibraghimov-Beskrovnaya O: Development of polycystic kidney disease in juvenile cystic kidney mice: insights into pathogenesis, ciliary abnormalities, and common features with human disease. *J Am Soc Nephrol* 17: 2821-2831, 2006

Surendran K, Simon TC, Liapis H, McGuire JK: Matrilysin (MMP-7) expression in renal tubular damage: association with Wnt4. *Kidney Int* 65: 2212-2222, 2004

Tan BC, Lee SC: Nek9, a novel FACT-associated protein, modulates interphase progression. *J Biol Chem* 279: 9321-9330, 2004

Thoma CR, Frew IJ, Hoerner CR, Montani M, Moch H, Krek W: pVHL and GSK3beta are components of a primary cilium-maintenance signalling network. *Nat Cell Biol* 9: 588-595, 2007

Tobin JL, Beales PL: Bardet-Biedl syndrome: beyond the cilium. *Pediatr Nephrol* 22: 926-936, 2007

Torres VE, Harris PC: Polycystic kidney disease: genes, proteins, animal models, disease mechanisms and therapeutic opportunities. *J Intern Med.* 261: 17-31, 2007

Tsiokas L, Kim E, Arnould T, Sukhatme VP, Walz G: Homo- and heterodimeric interactions between the gene products of PKD1 and PKD2. *Proc Natl Acad Sci U S A* 94: 6965-6970, 1997

Upadhya P, Birkenmeier EH, Birkenmeier CS, Barker JE: Mutations in a NIMA-related kinase gene, Nek1, cause pleiotropic effects including a progressive polycystic kidney disease in mice. *Proc Natl Acad Sci* 97: 217-221, 2000

Valkova N, Yunis R, Mak SK, Kang K, Kültz D: Nek8 mutation causes overexpression of galectin-1, sorcin, and vimentin and accumulation of the major urinary protein in renal cysts of jck mice. *Mol Cell Proteomics* 4: 1009-1018, 2005

Wang S, Zhang J, Nauli SM, Li X, Starremans PG, Luo Y, Roberts KA, Zhou J: Fibrocystin/polyductin, found in the same protein complex with polycystin-2, regulates calcium responses in kidney epithelia. *Mol Cell Biol* 27: 3241-3252, 2007

Wang Y, Nathans J: Tissue/planar cell polarity in vertebrates: new insights and new questions. *Development* 134: 647-658, 2007

Ward CJ, Hogan MC, Rossetti S, Walker D, Sneddon T, Wang X, Kubly V, Cunningham JM, Bacallao R, Ishibashi M, Milliner DS, Torres VE, Harris PC: The gene mutated in autosomal recessive polycystic kidney disease encodes a large, receptor-like protein. *Nat Genet* 30: 259-269, 2002

Ward CJ, Yuan D, Masyuk TV, Wang X, Punyashthiti R, Whelan S, Bacallao R, Torra R, LaRusso NF, Torres VE, Harris PC: Cellular and subcellular localization of the ARPKD protein; fibrocystin is expressed on primary cilia. *Hum Mol Genet* 12: 2703-2710, 2003

Woo D: Apoptosis and loss of renal tissue in polycystic kidney diseases. *N Engl J Med* 333: 18-25, 1995

Wu Y, Dai XQ, Li Q, Chen CX, Mai W, Hussain Z, Long W, Montalbetti N, Li G, Glynne R, Wang S, Cantiello HF, Wu G, Chen XZ. Kinesin-2 mediates physical and functional interactions between polycystin-2 and fibrocystin. *Hum Mol Genet* 15: 3280-3292, 2006

Yissachar N, Salem H, Tennenbaum T, Motro B: Nek7 kinase is enriched at the centrosome, and is required for proper spindle assembly and mitotic progression. *FEBS Lett* 580: 6489-6495, 2006

Yoder BK, Hou X, Guay-Woodford LM: The polycystic kidney disease proteins, polycystin-1, polycystin-2, polaris and cystin are co-localized in renal cilia. *J. Am. Soc. Nephrol.* 13: 2508–2516, 2002

Zerres K, Mucher G, Becker J, Steinkamm C, Rudnik-Schoneborn S, Heikkila P, Rapola J, Salonen R, Germino GG, Onuchic L, Somlo S, Avner ED, Harman LA, Stockwin JM, Guay-Woodford LM: Prenatal diagnosis of autosomal recessive polycystic kidney disease (ARPKD): molecular genetics, clinical experience, and fetal morphology. *Am J Med Genet* 76: 137-144, 1998

CHAPTER 2: NIMA-RELATED KINASES DEFECTIVE IN MURINE MODELS OF POLYCYSTIC KIDNEY DISEASES LOCALIZE TO PRIMARY CILIA AND CENTROSOMES

Moe R. Mahjoub*, Melissa L. Trapp*, and Lynne M. Quarmby. *J. Am. Soc. Nephrol.* 16: 3485-3489, 2005

*equal contribution

Rationale and Contribution

In this previously published work, we hypothesized that Nek1 and Nek8, which are defective in mouse models of cystic kidney disease, would show sub-cellular localization to either cilia or centrosomes, consistent with the ciliary hypothesis of cystic kidney disease. Our aim was to determine the endogenous localization of these proteins *in vitro*. My contributions were writing the manuscript and maintaining the cell culture prior to immunofluorescence.

Abstract

A key feature of the polycystic kidney diseases is aberrant cell proliferation, a consequence of dysfunctional ciliary signaling. The NIMA-related kinases (Nek) Nek1 and Nek8 carry the causal mutations of two of the eight established mouse models of polycystic kidneys. Nek proteins have roles in cell cycle and may contribute to coordinate regulation of cilia and cell-cycle progression. Herein is reported that in a mouse kidney epithelial cell line, mNek1

localizes to centrosomes in interphase and remains associated with the mitotic spindle pole during mitosis. In contrast, mNek8 localizes to the proximal region of the primary cilium and is not observed in dividing cells. Knockdown of mNek8 by siRNA does not affect ciliary assembly. Taken together with the phenotypes of the mutant mice, these data suggest that mNek1 and mNek8 provide links between cilia, centrosomes, and cell-cycle regulation.

Introduction

Polycystic kidney disease (PKD) is one of the most common genetic diseases and has a highly variable pathology involving aberrant cell proliferation in the kidney and in other organ systems, such as the liver and the pancreas. Evidence that renal cyst formation is caused by defects in ciliogenesis or ciliary function is substantial (1). Most dramatically, failure to assemble a primary cilium leads to polycystic pathology in mice (2). In addition, several of the proteins that are implicated in renal cyst formation localize to cilia and/or basal bodies, including polycystin-1 and polycystin-2, which are responsible for autosomal dominant PKD, and fibrocystin- 1, which is responsible for autosomal recessive PKD (1).

Murine models that contain spontaneously arising mutations have served to identify many of the genes that are involved in the polycystic pathology and to form causal associations between gene and phenotype. Seven proteins have been implicated in eight of the mouse models: Cystin in *cpk*, bicaudal C in *bpk* and *jcpk*, polaris/IFT88 in *orpk*, inversin in *inv*, NPHP3 in *pcy*, Nek1 in *kat*, and Nek8 in *jck* mice (3). Nek1 and Nek8 are members of the NIMA-related kinase

(Nek) family. Nek are cell cycle kinases that seem to have co-evolved with the bifunctional use of centrioles as spindle poles and basal bodies (4,5). For example, the founding member of the Nek family, NIMA, is essential for mitotic entry in *Aspergillus nidulans* (6), and the mammalian Nek2 is involved in centrosome separation and bipolar spindle formation (7).

The roles of Nek in ciliary regulation have been studied in the unicellular biciliate *Chlamydomonas reinhardtii* and the ciliated protozoan *Tetrahymena thermophila* (4,8). The *Chlamydomonas* Nek Fa2p, which is essential for Ca^{2+}-mediated axonemal microtubule severing, is located at a specific region of the proximal cilium, the site of flagellar autotomy (SOFA) (9). Several *Tetrahymena* Nek and the *Chlamydomonas* Nek Cnk2p are localized to cilia and regulate ciliary length (4,10). In addition to their roles in the regulation of cilia, Fa2p and Cnk2p affect the cell cycle. Cells that lack Fa2p have a G2/M cell-cycle delay and, Cnk2p affects cell size control (8). The dual roles of the Fa2p and Cnk2p kinases, taken together with the murine PKD phenotypes of Nek1 and Nek8 mutations, suggest that Nek are a direct link between cilia and centrosomes and the aberrant cell proliferation of cystic kidneys.

Here we report the localization of endogenous murine Nek1 and Nek8 (mNEK1 and mNEK8) in an inner medullary collecting duct (IMCD-3) cell line. mNek1 was observed in multiple foci associated with the centrosomes during interphase and remained associated with the microtubule organizing center at the mitotic spindle pole. In contrast, the mNek8 signal was restricted to the proximal region of the primary cilia during interphase and was not observed

during mitosis. siRNA knockdown of mNek8 resulted in loss of an immunofluorescence signal at the cilia but did not affect ciliary assembly. These data support the idea that mNek1 and mNek8 are involved in ciliary cell-cycle signaling.

Materials and Methods

Cell Culture, Synchrony, and Immunofluorescence

IMCD-3 cells were grown in a 1:1 mixture of DMEM and Ham's F12 medium supplemented with 10% FBS (all from Life Technologies, BRL, Auckland, New Zealand). For synchrony, cells that were grown to approximately 50% confluence were incubated with 2 mM thymidine for 18 h and then rinsed briefly with PBS. Cells were incubated with regular growth medium for 14 h, and samples were taken at 2-h intervals. For indirect immunofluorescence, cells were fixed with ice-cold methanol and incubated at 20°C for 10 min, then rehydrated in PBS. The primary antibodies used include rabbit polyclonal antimNek1 (diluted 100-fold) and anti-mNek8 (diluted 100-fold [11]), mouse monoclonal anti–γ-tubulin (clone GTU-88, diluted 1000-fold; Sigma-Aldrich, St. Louis, MO), mouse monoclonal anti-acetylated tubulin (clone 6–11B-1, diluted 10,000-fold; Sigma-Aldrich), and human autoimmune serum M4491 (diluted 3000-fold [12]). The secondary antibodies used include Alexa Fluor 488–conjugated goat anti-rabbit IgG (diluted 1000-fold; Molecular Probes, Eugene, OR), Alexa Fluor 594–conjugated goat anti-mouse IgG (diluted 2000-fold; Molecular Probes), Alexa Fluor 594–conjugated goat anti-human IgG (diluted 500-fold; Molecular Probes), and Cy5-conjugated goat anti-mouse IgG (diluted 500-fold; Southern Biotech,

Birmingham, AL). All antibody incubations were done at room temperature for 1 h, followed by a wash in PBS. Cell nuclei were stained with 4'-6-diamidino-2-phenylindole for 10 min and coverslips were mounted using Mowiol (Calbiochem, San Diego, CA). Immunofluorescence microscopy was performed using the Delta Vision system (Applied Precision, Issaquah, WA) as described previously (9).

RNA Interference

The siGENOME SMARTpool reagent that contained four different siRNA duplexes that target mNek8 (Dharmacon catalog no. M-044403-00) was used to transfect IMCD-3 cells according to the manufacturer's instructions. Untransfected and mock-transfected cells were used as negative controls. Cells were transfected for 24, 48, 72, and 96 h; harvested; and processed as described above.

Western Analysis

IMCD-3 cells were grown to confluence, harvested, and resuspended 1x SDS sample buffer. Immunoblot analysis using rabbit anti-mNek1 (diluted 2000-fold) was performed as described previously (9).

Results and Discussion

mNek1 Localizes to Centrosomes during Interphase and Mitosis

IMCD-3 cells that were stained with polyclonal rabbit antimNek1 antibodies showed multiple puncta associated with centrosomes during interphase (Figure 2-1A). In general, we observed more mNek1 foci surrounding

the daughter centriole than the mother centriole, which nucleates a cilium. Similar staining was observed in the mouse fibroblast line NIH 3T3 and in the human embryonic kidney cell line HEK 293 (data not shown). During mitosis, mNek1 staining remained associated with the centrosomes in metaphase, anaphase, and cytokinesis (Figure 2-1A).

The multiple foci of mNek1 suggest that it is not a component of the centriole itself. To resolve whether mNek1 localization was specific to pericentriolar material, IMCD-3 cells were costained with Nek1 and a human autoimmune serum (M4491) that is known to stain the pericentriolar proteins CEP 110, ninein, pericentrin/kendrin, and CEP 250 (12,13). The Nek1 foci appear outside the pericentriolar material (PCM) tube stained by the M4491 serum in IMCD-3 cells (Figure 2-1B) and HeLa cells (data not shown). The spatial localization relative to the M4491- stained PCM tube suggests that mNek1 could be a component of pericentriolar satellites. PCM-1 has been localized to centriolar satellites in a microtubule-dependent manner and is involved in centriolar duplication (14). However, PCM-1 dissociates from centrosomes during mitosis (14), whereas mNek1 remains associated.

Figure 2-1 Murine NIMA-related kinase 1 (mNek1) is localized to centrosomes throughout the cell cycle.

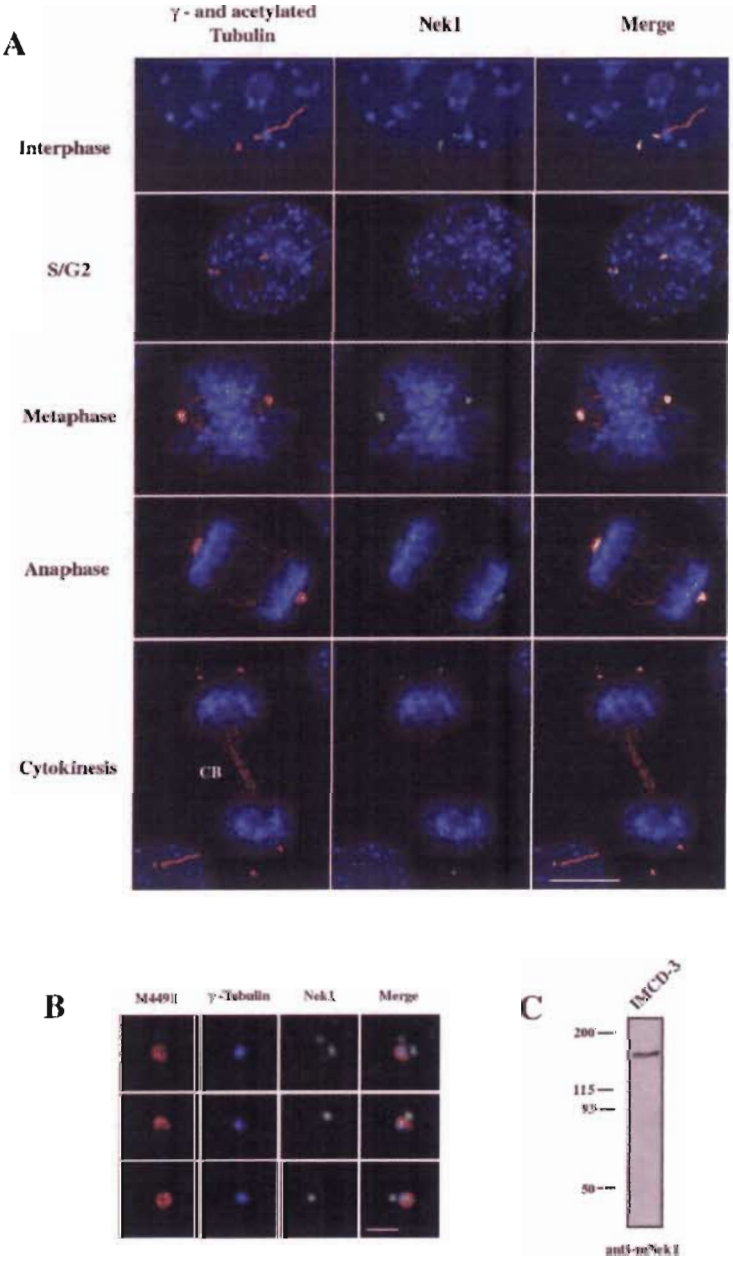

(A) Synchronized inner medullary collecting duct-3 (IMCD-3) cells were stained with antibodies against γ- and acetylated tubulin (red) to mark the positions of the centrioles and the cilia, respectively. mNek1 (green) was detected using a rabbit polyclonal antibody, and DNA was stained with 4'-6-diamidino-2-phenylindole (blue). CB, cytoplasmic bridge. Bar = 5 μm. **(B)** To refine the centrosomal localization of mNek1, IMCD-3 cells were stained with the centrosome-reactive human autoimmune serum M4491 (red), which identifies the pericentriolar material (PCM) tube (12,13). Cells were co-stained with antibodies against γ-tubulin (blue) and mNek1 (green). Bar = 1 μm. **(C)** Western analysis of IMCD-3 cells showing anti-mNek1 antibody specificity. A single band of expected molecular weight (approximately 180 kD) is observed after incubation with the rabbit anti-mNek1 antibody.

mNek8 Localizes to Primary Cilia during Interphase but Is not Observed during Mitosis

Indirect immunofluorescence of endogenous mNek8 revealed a specific signal that usually is restricted to the proximal region of primary cilia in IMCD-3 cells during interphase (Figure 2-2). We observed the same localization in NIH 3T3 cells (data not shown). A quantitative analysis revealed that mNek8 was present in the cilia of 96% of ciliated cells. During mitosis, no specific mNek8 staining was observed in cells that were undergoing metaphase, anaphase, or cytokinesis (Figure 2-2).

The ciliary localization of mNek8 is reminiscent of other proteins that are implicated in PKD. Polycystin-1 and polycystin- 2 are found within primary cilia (15,16), as well as fibrocystin-1 (17,18), polaris, and cystin (16). The localization of mNek8 is also similar to Fa2p, which localizes to the base of the cilia at the SOFA in *Chlamydomonas* and when exogenously expressed in IMCD-3 cells (9). However, the mNek8 signal labels a broader region of the cilium than the tightly focused Fa2p signal.

Figure 2-2 mNek8 is localized to the proximal region of primary cilia during interphase.

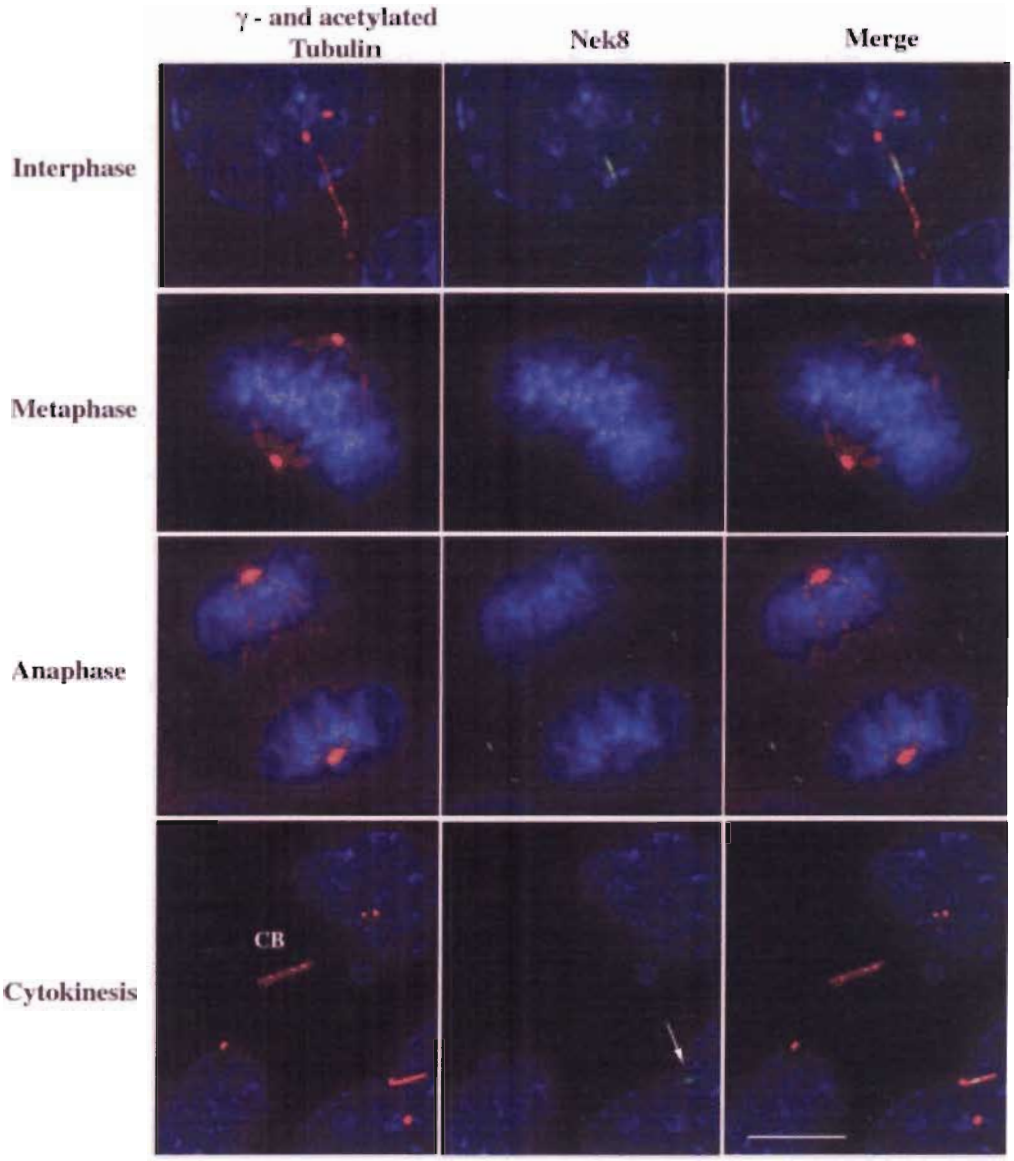

Synchronized IMCD-3 cells were stained for γ- and acetylated tubulin (red), mNek8 (green), and DNA (blue). No mNek8 signal was detected during mitosis and appears only in ciliated cells in interphase (interphase panel and arrow in cytokinesis panel). Bar = 5 μm.

Knockdown of mNek8 Does not Affect Cilia Formation

Renal cyst formation as a result of failure to assemble cilia is often accompanied by pleiotropic pathologies. This is apparent in the *orpk* mouse model, in which a hypomorphic allele of polaris/IFT88, encoding a component of the intraflagellar transport machinery, is defective in ciliary assembly (2). Because mNek8 localized to the cilia, we hypothesized that it could play a role in ciliary assembly. siRNA that targeted Nek8 was transfected into IMCD-3 cells, and mNek8 knockdown was measured at 96 h after transfection. There was a dramatic decrease in the ciliary staining of mNek8 in cells that were treated by siRNA (Figure 2-3A), in which only 34% of ciliated cells contained mNek8 *versus* 96% of untransfected and 94% of mock-transfected cells (Figure 2-3B). However, the percentage of ciliated cells (>90%) in the population did not change when compared with the negative controls. Staining at the plasma membrane was still observed in knockdown cells, suggesting nonspecific staining by the polyclonal mNek8 antibody. Western blot analysis of cellular protein indicated knockdown of mNek8 protein below detectable levels (data not shown).

The mNek8 knockdown indicates that ciliogenesis is unaffected by loss of ciliary mNek8 and suggests that mNek8 function is not essential for cilia assembly. The *jck* mutation is a single amino acid substitution in the C-terminus of mNek8 (11), and only the kidneys are affected (19), unlike other models, in which multiple organ systems are defective. Taken with our findings that mNek8 knockdown does not affect ciliogenesis strongly suggests that mNek8 is involved in a signaling role specific to the kidney.

Our discovery that mNek1 is centrosomal and mNek8 is ciliary completes the subcellular localization studies of the seven proteins identified in the mouse models of cystic kidney disease. It is interesting that mNek1 is the only gene product of these mouse models that does not localize to the primary cilia. Many of the proteins that are implicated in renal cyst formation are not members of conserved protein families; polycystin-1 and fibrocystin-1 are novel integral membrane proteins (20,21), polycystin-2 is a TRP cation channel (22), cystin is a novel lipid-anchored membrane protein (23), and inversin is a novel protein that contains ankyrin repeats and calmodulin-binding motifs (24). PKD is a ciliopathy that results in aberrant cell proliferation; therefore, conserved ciliary and cell-cycle proteins are expected to contribute to the mechanism of disease. mNek1 and mNek8 are excellent candidates because they are members of a cell-cycle kinase family that is conserved throughout ciliated eukaryotes, and, as shown here, they localize to basal bodies and cilia. Considering Fa2p and Cnk2p and their roles in regulating ciliary function and cell-cycle progression, Neks may provide a common link between cilia and cellcycle regulation, although the cellular mechanisms remain to be established.

An important aspect of elucidating the signal transduction pathway may lie in identification of modifying loci, as genetic background greatly influences the variable PKD phenotype. Although PKD1, PKD2, and PKHD1 are the genes that are responsible for PKD, the age of onset and disease severity are highly variable and are affected by additional germline and somatic mutations (25). It is possible that hNek1 and hNek8 are important modifiers of PKD.

Figure 2-3 siRNA knockdown of mNek8 does not affect ciliogenesis.

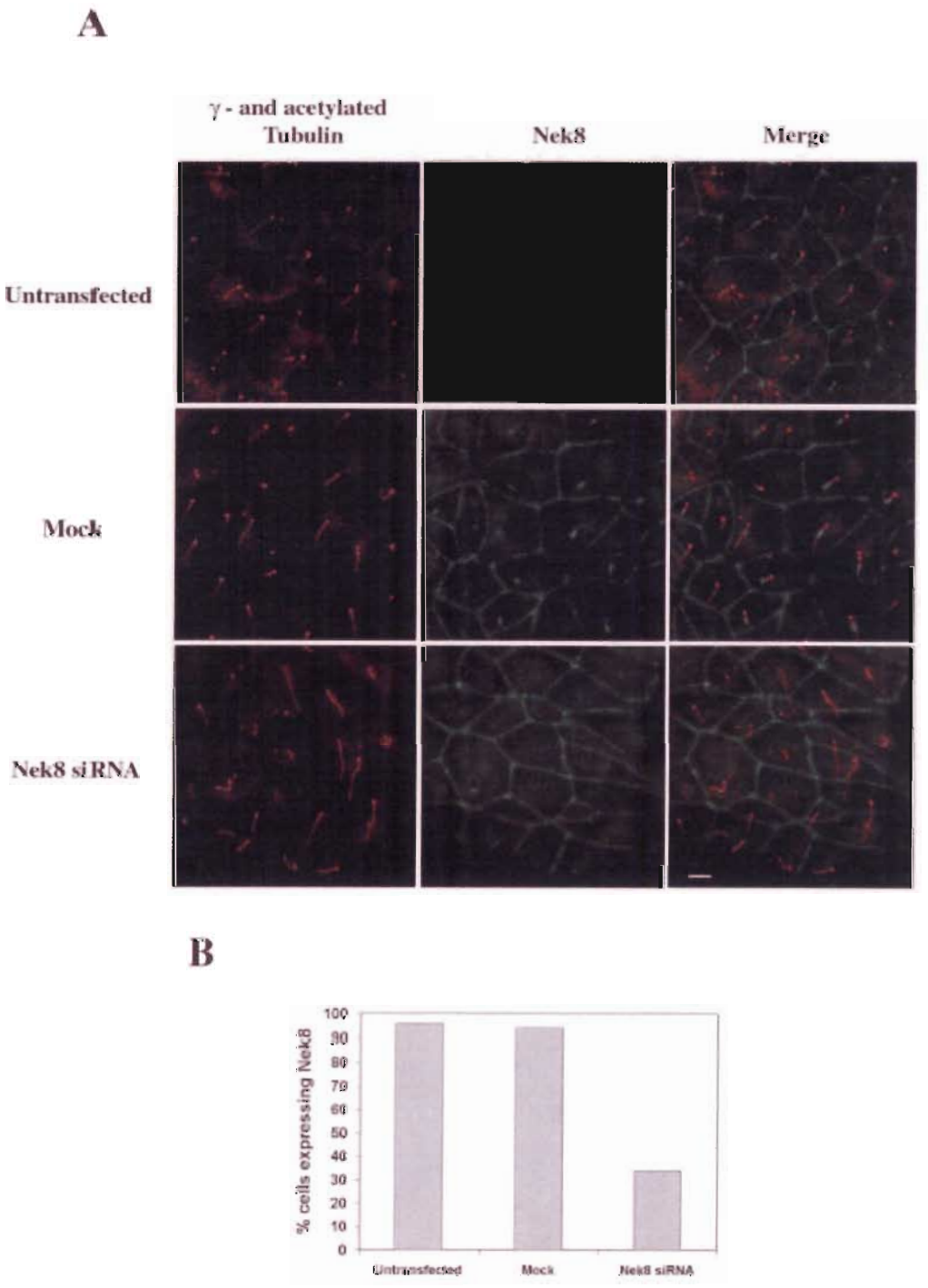

(A) IMCD-3 cells were transfected with siRNA targeting mNek8 and incubated for 96 h. Cells were stained with antibodies against γ- and acetylated tubulin (red) and mNek8 (green). Bar = 5 μm. **(B)** Quantification of mNek8 loss from cilia. Two hundred cells from each experimental sample were analyzed for the presence of mNek8 signal in the cilium.

Acknowledgments

This work was funded by an operating grant from the Canadian Institutes of Health Research (MOP 37861) to L.M.Q. M.R.M. and M.L.T are supported by graduate fellowships from the Michael Smith Foundation for Health Research and the Natural Sciences and Engineering Research Council of Canada. We are deeply indebted to David Beier for the mNek8 antibody, Yumay Chen for the mNek1 antibody, and Jerome Rattner for the M4491 anti-serum. We also thank Michel Leroux and his laboratory members for the use of their facilities.

References

1. Pazour GJ: Intraflagellar transport and cilia-dependent renal disease: The ciliary hypothesis of polycystic kidney disease. *J Am Soc Nephrol* 15: 2528–2536, 2004

2. Pazour GJ, Dickert BL, Vucica Y, Seeley ES, Rosenbaum JL, Witman GB, Cole DG: *Chlamydomonas* IFT88 and its mouse homologue, polycystic kidney disease gene Tg737, are required for assembly of cilia and flagella. *J Cell Biol* 151: 709–718, 2000

3. Guay-Woodford LM: Murine models of polycystic kidney disease: Molecular and therapeutic insights. *Am J Physiol Renal Physiol* 285: F1034–F1049, 2003

4. Quarmby LM, Mahjoub MR: Caught Nek-ing: Cilia and centrioles. *J Cell Sci* 2005, in press

5. O'Connell MJ, Krien MJE, Hunter T: Never say never. The NIMA-related protein kinases in mitotic control. *Trends Cell Biol* 13: 221–228, 2003

6. Osmani AH, O'Donnell K, Pu RT, Osmani SA: Activation of the nimA protein kinase plays a unique role during mitosis that cannot be bypassed by absence of the bimE checkpoint. *EMBO J* 10: 2669–2679, 1991

7. Faragher AJ, Fry AM: Nek2A kinase stimulates centrosome disjunction and is required for formation of bipolar mitotic spindles. *Mol Biol Cell* 14: 2876–2889, 2003

8. Quarmby LM, Parker JDK: Cilia and the cell cycle? *J Cell Biol* 169: 707–710, 2005

9. Mahjoub MR, Rasi MQ, Quarmby LM: A NIMA-related kinase, Fa2p, localizes to a novel site in the proximal cilia of *Chlamydomonas* and mouse kidney cells. *Mol Biol Cell* 15: 5172–5286, 2004

10. Bradley BA, Quarmby LM: A NIMA-related kinase, Cnk2p, regulates both flagellar length and cell size in *Chlamydomonas*. *J Cell Sci* 118: 3317–3326, 2005

11. Liu S, Lu W, Obara T, Kuida S, Lehoczky J, Dewar K, Drummond IA, Beier DR: A defect in a novel Nek-family kinase causes cystic kidney disease in the mouse and in the zebrafish. *Development* 129: 5839–5846, 2002

12. Mack GJ, Rees J, Sandblom O, Balczon R, Fritzler MJ, Rattner JB: Autoantibodies to a group of centrosomal proteins in human autoimmune sera reactive with the centrosome. *Arthritis Rheum* 41: 551–558, 1998

13. Ou Y, Rattner JB: A subset of centrosomal proteins are arranged in a tubular conformation that is reproduced during centrosome duplication. *Cell Motil Cytoskeleton* 47: 13–24, 2000

14. Kubo A, Sasaki H, Yuba-Kubo A, Tsukita S, Shiina N: Centriolar satellites: Molecular characterization, ATP-dependent movement toward centrioles and possible involvement in ciliogenesis. *J Cell Biol* 147: 969–980, 1999

15. Pazour GJ, San Agustin JT, Follit JA, Rosenbaum JL, Witman GB: Polycystin-2 localizes to kidney cilia and the ciliary level is elevated in orpk mice with polycystic kidney disease. *Curr Biol* 12: R378–R380, 2002

16. Yoder BK, Hou X, Guay-Woodford LM: The polycystic kidney disease proteins, polycystin-1, polycystin-2, polaris, and cystin, are co-localized in renal cilia. *J Am Soc Nephrol* 13: 2508–2516, 2002

17. Ward CJ, Yuan D, Masyuk TV, Wang X, Punyashthiti R, Whelan S, Bacallao R, Torra R, LaRusso NF, Torres VE, Harris PC: Cellular and subcellular localization of the ARPKD protein; fibrocystin is expressed on primary cilia. *Hum Mol Genet* 12: 2703–2710, 2003

18. Wang S, Luo Y, Wilson PD, Witman GB, Zhou J: The autosomal recessive polycystic kidney disease protein is localized to primary cilia, with concentration in the basal body area. *J Am Soc Nephrol* 15: 592–602, 2004

19. Atala A, Freeman MR, Mandell J, Beier DR: Juvenile cystic kidneys (jck): A new mouse mutation which causes polycystic kidneys. *Kidney Int* 43: 1081–1085, 1993 3488 Journal of the American Society of Nephrology J Am Soc Nephrol 16: 3485–3489, 2005

20. The International Polycystic Kidney Disease Consortium: Polycystic kidney disease: The complete structure of the PKD1 gene and its protein. *Cell* 81:289 –298, 1995

21. Ward CJ, Hogan MC, Rossetti S, Walker D, Sneddon T, Wang X, Kubly V, Cunningham JM, Bacallao R, Ishibashi M, Milliner DS, Torres VE, Harris PC: The gene mutated in autosomal recessive polycystic kidney disease encodes a large, receptor-like protein. *Nat Genet* 130: 259 – 269, 2002

22. Mochizuki T, Wu G, Hayashi T, Xenophontos SL, Veldhuisen B, Saris JJ, Reynolds DM, Cai Y, Gabow PA, Pierides A, Kimberling WJ, Breuning MH, Deltas CC, Peters DJ Somlo S: PKD2, a gene for polycystic kidney disease that encodes an integral membrane protein. *Science* 272: 1339–1342, 1996

23. Hou X, Mrug M, Yoder BK, Lefkowitz EJ, Kremmidiotis G, D'Eustachio P, Beier DR, Guay-Woodford LM: Cystin, a novel cilia-associated protein, is disrupted in the cpk mouse model of polycystic kidney disease. *J Clin Invest* 109: 533–540, 2002

24. Mochizuki T, Saijoh Y, Tsuchiya K, Shirayoshi Y, Takai S, Taya C, Yonekawa H, Yamada K, Nihei H, Nakatsuji N, Overbbek PA, Hamada H, Yokoyama T: Cloning of inv, a gene that controls left/right asymmetry and kidney development. *Nature* 395: 177–181, 1998

25. Pei Y: Molecular genetics of autosomal dominant polycystic kidney disease. *Med Clin Exp* 26: 252–258, 2003 J Am Soc Nephrol 16: 3485–3489, 2005

CHAPTER 3: MUTATIONS IN NIMA-RELATED KINASE NEK8 CAUSES NEPHRONOPHTHISIS IN HUMANS AND AFFECTS CILIARY AND CENTROSOMAL LOCALIZATION

Edgar A. Otto[1*], Melissa L.Trapp[2*], Ulla T. Schultheiss[1], Lynne M. Quarmby[2], & Friedhelm Hildebrandt[1,3]

[1]Departments of Pediatrics and of [3]Human Genetics, University of Michigan, Ann Arbor, MI, USA. [2]Departement of Molecular Biology and Biochemistry, Simon Fraser University, Burnaby, BC, Canada

* equal contribution

Rationale and Contribution

In this submitted manuscript, the aim was to identify mutations in human Nek8 as a cause of nephronophthisis. My contributions were performing all *in vitro* experiments using vectors provided by the co-authors, assembling figures and writing portions of the materials and methods, results, and supplemental data, included here as Figure 3-4.

Abstract

Nephronophthisis (NPHP), an autosomal recessive kidney disease, is the most frequent genetic cause of chronic renal failure in the first 3 decades of life. Mutations in 6 genes (*NPHP1-6*) have been identified and homologous mouse models for *NPHP2* and *NPHP3* have been described. Another mouse model of recessive cystic kidney disease is the *jck* mouse, which is caused by the homozygous missense mutation G448V, in a highly conserved RCC1 domain in

Nek*8*. Under the hypothesis that mutations of *NEK8* might cause NPHP in humans, we performed mutational analysis of all *NEK8* exons in a worldwide cohort of 188 unrelated patients with NPHP by direct sequencing. We identified 3 different amino acid changes L330F, H425Y, and A497P in human *NEK8*, which were absent from at least 80 healthy control individuals. All three mutations are within the RCC1 domain of Nek8, and the mutation H425Y is positioned within the same RCC1 repeat as the murine *jck* mutation. To test their functional significance, we introduced all three mutations into full length mouse *Nek8* (*mNek8*) GFP-tagged cDNA constructs. In transient overexpression experiments using inner medullary collecting duct (IMCD-3) cells, sub-cellular localization of mutant Nek8 was investigated and compared to wild-type Nek8 expression. All mutant forms of Nek8 showed defects in ciliary localization to varying degrees. The mNek8 mutant H431Y (corresponding to human H425Y) was completely absent from cilia and showed decreased localization to the centrosomes. Overexpression of these mutants did not affect overall ciliogenesis, mitosis, or centriole number. Our finding that Nek8, when mutated, causes nephronophthisis type 9 strengthens the link between proteins mutated in cystic kidney disease in humans and their localization at cilia and centrosomes.

Introduction

Nephronophthisis (NPHP) is an autosomal recessive kidney disease, which leads to kidney cyst formation and progressive renal failure. NPHP is the most frequent genetic cause for end-stage renal failure (ESRF) in the first 3 decades of life. Recently, functions of primary cilia, basal bodies, and

centrosomes have been implicated in the pathogenesis of NPHP (Watnick and Germino, 2003; Hildebrandt and Otto, 2005). In humans, 6 causative genes, *NPHP1-6* (MIM #256100, #602088, #604387, #606966, #609237, #610142) have been identified by positional cloning (Hildebrandt *et al.*, 1997; Otto *et al.*, 2002; Mollet *et al.*, 2002; Otto *et al.*, 2003; Olbrich *et al.*, 2003; Otto *et al.*, 2005; Sayer *et al.*, 2006). In mice, several monogenetic models of recessive cystic kidney disease, have been described. Seven proteins were identified as mutated in these murine disease models: Nphp2/inversin in *inv*, Nphp3 in *pcy*, cystin in *cpk*, bicaudal C in *bpk* and *jcpk*, polaris/Tg737 in *orpk*, Nek1 in *kat*, and Nek8 in *jck* mice (Guay-Woodford *et al.*, 2003). Because of phenotypic disease similarities between human NPHP and murine disease models, we examined by mutational analysis the genes encoding cystin (O'Toole *et al.*, 2007), polaris/Tg737 (Otto, unpublished), and bicaudal C (Otto, unpublished) as candidate genes by mutational analysis in patients with NPHP but failed to identify any causative mutations. The spontaneously arisen renal cystic mouse model *jck* is caused by a homozygous G448V substitution in the conserved RCC1 domain of the *Nek8* gene (Liu *et al.*, 2002). Nek1 and Nek8 are members of the NIMA (never in mitosis A)-related kinase (Nek) family. Neks are cell cycle kinases that are thought to coordinate the regulation of cilia and cell-cycle progression (Quarmby & Mahjoub, 2005). Like all known nephrocystins (NPHP proteins), Nek8 localizes to primary cilia but seems not to be required for ciliary assembly (Mahjoub *et al*, 2005). Knockdown of Nek8 led to the formation of pronephric cysts in zebrafish embryos, and *in vitro* expression of mutated Nek8 resulted in enlarged,

multinucleated cells (Liu *et al.*, 2002). On the basis of the renal cystic disease phenotype of Nek8 missense mutation in mice and knock-down in zebrafish and of the ciliary/centrosomal localization of Nek8 and the known nephrocystins we evaluated *NEK8* as a candidate gene for human NPHP. We identified 3 different functionally significant missense mutations in evolutionary conserved amino acids.

Materials and Methods

Human subjects. We obtained blood samples, pedigree, and clinical information after receiving informed consent (www.renalgenes.org) from 188 patients/families with NPHP and their parents. Approval for human subjects research was obtained from the University of Michigan Institutional Review Board. In all patients the diagnosis NPHP was based on the following criteria: i) clinical course with characteristic clinical signs of NPHP including chronic renal failure, polyuria, polydipsia, anemia, and growth retardation; ii) renal ultrasound or renal biopsy compatible with the diagnosis of NPHP as judged by a (pediatric) nephrologist; iii) pedigree compatible with autosomal recessive inheritance. Homozygous *NPHP1* deletions were excluded in all patients, applying a multiplex PCR approach (Hildebrandt *et al.*, 2001).

PCR amplification and sequencing. We screened for *NEK8* mutations by direct sequencing from one strand using exon flanking primers in a touchdown PCR reaction for all 15 exons. Sequences and PCR conditions are available upon request. PCR products were purified using spin columns according to the manufacturer's instructions (Marligen) and directly sequenced using the dideoxy

chain-termination method on an automatic capillary genetic analyzer (Applied Biosystems). DHPLC analysis was performed as described and was >95% sensitive (Wagner *et al.* 1999).

Cell Culture. IMCD-3 cells were cultured in humidified 37°C incubator with 5% CO_2 in 1:1 DMEM/Ham's F12 media with 10% FBS (all from Invitrogen).

GFP constructs and transfection. The L336F, H431Y, and A503P mutagenized mouse Nek8 (*mNek8*) cDNA constructs (corresponding to human amino acid positions L330F, H425Y, and A497P, respectively) were digested with *Blp*I and *Xba*I, and the resulting Nek8 fragment containing the mutation was subcloned into the *Blp*I/*Xba*I digested pEGFP-C2 (BD Biosciences Clontech) vector containing *mNek8* with an N-terminal GFP. The reading frame and mutations were verified by sequencing. The plasmids were then purified by an Endotoxin-free Maxiprep kit (Qiagen). Transient transfections were performed using Lipofectamine 2000 (Invitrogen) according to manufacturer's protocol with the following exception: Cells grown on coverslips were incubated with DNA complexes in OptiMEM (Invitrogen) for 4-6 hours, then washed with PBS and incubated in DMEM/Ham's F12 media for 16-24 hours. Transfection efficiency ranged from 30-62%.

Western blot: Samples were prepared by adding 1x SDS sample buffer (10% glycerol, 50 mM Tris (pH6.8), 2 mM EDTA, 2% SDS, 144 mM 2-mercaptoethanol, 0.01% bromophenol blue) to transfected IMCD-3 cells and the suspension was sonicated to shear genomic DNA. The samples were electrophoresed on an 8% SDS-PAGE gel and transferred to Trans-Blot transfer

membrane (BioRad) using a wet transfer apparatus. The nitrocellulose membrane was blocked using 5% skim milk in TBS-T for 1 hour, and then incubated in Mouse anti-GFP antibody (1000-fold dilution, Roche) overnight at 4oC. The membrane was then washed with TBS-T and incubated in HRP-conjugated goat anti-mouse antibody for 1 hour at room temperature. GFP-conjugated proteins were then visualized using an enhanced chemiluminescence kit (Amersham Biosciences) and X-OMAT film (Kodak).

Immunofluorescence. The transfected cells grown on coverslips were fixed with -20°C methanol for 10 minutes and then rehydrated with PBS. They were subsequently incubated for 1 h with the following primary antibodies: polyclonal rabbit anti-γ tubulin (500-fold dilution, Sigma), monoclonal mouse anti-γ tubulin (1,000-fold dilution, Sigma) and monoclonal mouse IgG2b anti-acetylated tubulin (7,500-fold dilution, Sigma). After washing in PBS, the cells were incubated for 1 h with one or more of the following secondary antibodies: Alexa 594-conguated goat anti-mouse IgG2b (1,000-fold dilution, Molecular Probes), Alexa 594-conjugated goat anti mouse all IgG (2,000-fold dilution, Molecular Probes) and Cy5-conjugated donkey anti-rabbit (500-fold dilution, Jackson ImmunoResearch Laboratories). Cell nuclei were stained with 4-6-diamidino-2-phenylindole (DAPI, 1 ug/mL). Coverslips were mounted using an antifade medium containing 0.1 mg/ml Mowiol (Calbiochem, San Diego, CA), 50% glycerol, and 100 mM Tris, pH 8.5 (Mahjoub *et al.* 2005). Microscopy was performed using the Delta Vision system (Applied Precision) as described previously (Mahjoub *et al.*, 2004).

Cell quantification. In three independent experiments, transfected and untransfected cells were categorized as ciliated with a pair of centrioles, lacking cilia with a pair of centrioles, undergoing mitosis, multinucleate, or having an aberrant number of centrioles, including none at all. The ciliated, mononucleate cells with low to medium levels of expression were then quantified for localization of GFP-mutant-Nek8 to cilia, centrosomes, to the perinuclear region, and/or to the cell periphery.

Results

Mutational screening of all exons of *NEK8* in 188 patients with NPHP revealed 3 different nucleotide changes that alter the deduced amino acid sequence of human *NEK8* (C988T, L330F, heterozygous; C1273T, H425Y, homozygous; G1489C, A497P, heterozygous) in 3 patients from different families (Table 3-1, Figure 3-1A). The changes were absent from at least 80 healthy control individuals. Mutation analysis of all known *NPHP* genes for these 3 patients revealed an additional homozygous mutation in the *NPHP5* gene (424-425delTT, F142fsX1460) in the patient F408 who carries the L330F change in NEK8 heterozygously (Otto *et al.*, 2005). Screening of additional 400 patients with NPHP for homozygosity typing 3 highly polymorpic microsatellite markers at the *NEK 8* locus yielded 2 individuals with homozygosity (Otto, submitted). None of these had any further NEK8 mutations. All 3 mutated amino acids (L330, H425, and A497 show evolutionary conservation and are identical in human, mouse, xenopus, and zebrafish. Additionally, the H425 is conserved in the chordate *Ciona intestinalis* (Figure 3-1B) The equivalent numbering of the L330F,

H425Y, and A497P human mutants is L336F, H431Y, and A503P in mouse, respectively.

Transient transfection of IMCD-3 cells with wild-type GFP-Nek8 shows cytoplasmic, centrosomal, ciliary, and perinuclear localization, while the mutant GFP-Nek8 constructs L336F and H413Y show decreased localization to the cilia (Figure 3-2A, Figure 3-3). The H431Y GFP-Nek8 mutant also shows reduced localization to the centrosome while the other mutations did not (Figure 3-2A, Figure 3-3). Transient transfection of GFP alone, wild-type GFP-Nek8, or GFP-Nek8 mutants in IMCD-3 cells had no effect on whether cells were ciliated (scored as % ciliated cells in the population). We did not detect an effect on mitosis or number of centrioles (Figure 3-2B). All transfections had expected band sizes by Western blot (Figure 3-4). Transient transfection of IMCD-3 cells with N-terminal myc-tagged wild-type, L336F, H431Y, or A503P Nek8 vectors resulted in similar observations as the GFP-tagged vectors, with all forms of Nek8 causing multinucleated cells and no effect on ciliation, mitosis, or centriole number (see Figure A2-4).

Discussion

Nephronophthisis is renal cystic disease with extensive genetic locus heterogeneity. Except for *NPHP1*, individual genes are mutated only in a few patients in the range of 1-3% of all cases. As an example, to date only 9 cases were described with *NPHP3* mutations, only in 3 of which both alleles were detected. Another rare cause for NPHP are mutations in *NPHP2/Inversin* which have been identified in only 8 patients (Otto *et al.*, 2003, O'Toole *et al.*, 2007).

After screening more than 600 patients with NPHP we identified 3 missense mutations in NEK8 in 3 unrelated patients, one of which was homozygous, and for two of which the second *NEK8* allele was not detected. Therefore, we consider Nek8 as another rare cause for NPHP (NPHP type 9). The mutation H425Y (mNek8_H431Y) found in a NPHP patient (# F601) homozygously is localized in close proximity to the murine *jck* mutation (G448V) in a highly conserved RCC1 (regulator of chromosome condensation) repeat. The role of the RCC1 domain in Nek8 is still unknown. Interestingly the retinitis pigmentosa GTPase regulator protein (RPGR), which is known to be in a complex with NPHP5, contains an RCC1 domain as well.

All mutations found in NEK8 including the *jck* cystic mouse model are "missense" mutations. Loss of function mutations, which are common in NPHP1-6, have not been found in NEK8. There is no Nek8 knockout mouse model to address the question if such a mutation would be compatible with life and whether the phenotype will be comparable with the *jck* phenotype.

Our experiments showed that overexpression of Nek8 gives rise to multinucleated cells regardless whether wild-type or mutated Nek8 is transfected into cultured cells, which is in conflict to findings that cells expressing *jck* mutant Nek8 differ compared to wild-type Nek8 regarding cell enlargement and multinucleation (Liu *et al.*, 2002). The authors did indeed not find multinucleated tubule cells in *jck* mice (Liu *et al.*, 2002).

The cellular basis of renal cyst formation is still not fully understood. Recent evidence supports a unifying theory of renal cystic disease on the basis

of ciliary/centrosomal localization (reviewed by Pazour, 2004; Watnick & Germino, 2003; Hildebrandt & Otto, 2005).

In this study we show that mutations in the kinase Nek8 decreases or abolishes its localization to the cilium. We speculate, that ciliary localization of Nek8 is crucial for proper cilia signaling, which then might affect downstream events such as cell cycle progression (Bowers and Boylan, 2004; Quarmby and Parker, 2005). Loss of cilary localization of Nek8 was reported in primary kidney epithelial cells derived from *jck* mice (Smith *et al.*, 2006). We have recently found decreased ciliary localization of Nek8 in lumenal cilia of *jck* homozygous mouse kidney tubules, but not in heterozygous (unaffected) mice (Trapp *et al.*, submitted). One patient with a heterozygous *NEK8* mutation (L330F) carries an additional homozygous frameshift mutation in *NPHP5*. The heterozygous Nek8 mutation might act as potential genetic modifier of the kidney phenotype in this patient. Alternatively, like in Bardet-Biedl syndrome, oligogenicity or triallelic inheritance may be necessary in order to manifest the disorder (Katsanis *et al.*, 2001).

Acknowledgements

We sincerely thank the affected individuals and their families for participation. We acknowledge R.H. Lyons for excellent large-scale sequencing. We are grateful to the following physicians for contribution of materials and clinical data from patients: H. Gadner, Vienna, Austria; J. Ehrich, Hannover, Germany; F. Frey, Bern, Switzerland. This research was supported by grants from the National Institutes of Health to F.H. (DK1069274, DK1068306,

DK064614) and a grant from the Kidney Foundation of Canada to L.Q. M.T. is supported by a graduate fellowship from the Michael Smith Foundation for Health Research and the Natural Sciences and Engineering Research Council of Canada. F.H. is a Frederick G. L. Huetwell Professor.

References

Bowers AJ, Boylan JF: Nek8, a NIMA family kinase member, is overexpressed in primary human breast tumors. *Gene* 328: 135-142, 2004

Guay-Woodford LM: Murine models of polycystic kidney disease: molecular and therapeutic insights. *Am J Physiol Renal Physiol 285*: F1034-1049, 2003

Hildebrandt F, Otto E, Rensing C, Nothwang HG, Vollmer M, Adolphs J, Hanusch H, Brandis M: A novel gene encoding an SH3 domain protein is mutated in nephronophthisis type 1. *Nat Genet 17*: 149-153, 1997

Hildebrandt F, Otto E: Cilia and centrosomes: a unifying pathogenic concept for cystic kidney disease? *Nat Rev Genet 6*: 928-940, 2005.

Hildebrandt F, Rensing C, Betz R, Sommer U, Birnbaum S, Imm A, Omran H, Leipoldt M, Otto E; Arbeitsgemeinschaft fur Paediatrische Nephrologie (APN) Study Group: Establishing an algorithm for molecular genetic diagnostics in 127 families with juvenile nephronophthisis. *Kidney Int 59*: 434-445, 2001

Katsanis N, Lupski JR, Beales PL: Exploring the molecular basis of Bardet-Biedl syndrome. *Hum Mol Genet 2001*:10:2293-2299, 2001

Liu S, Lu W, Obara T, Kuida S, Lehoczky J, Dewar K, Drummond IA, Beier DR: A defect in a novel Nek-family kinase causes cystic kidney disease in the mouse and in zebrafish. *Development 129*: 5839-5846, 2002

Mahjoub MR, Qasim Rasi M, Quarmby LM: A NIMA-related kinase, Fa2p, localizes to a novel site in the proximal cilia of Chlamydomonas and mouse kidney cells. *Mol Biol Cell 15*: 5172-5186, 2004

Mahjoub MR, Trapp ML, Quarmby LM: NIMA-related kinases defective in murine models of polycystic kidney diseases localize to primary cilia and centrosomes. *J Am Soc Nephrol 16*: 3485-3489, 2005

Mollet G, Salomon R, Gribouval O, Silbermann F, Bacq D, Landthaler G, Milford D, Nayir A, Rizzoni G, Antignac C, Saunier S: The gene mutated in juvenile nephronophthisis type 4 encodes a novel protein that interacts with nephrocystin. *Nat Genet 32*: 300-305, 2002

Olbrich H, Fliegauf M, Hoefele J, Kispert A, Otto E, Volz A, Wolf MT, Sasmaz G, Trauer U, Reinhardt R, Sudbrak R, Antignac C, Gretz N, Walz G, Schermer B, Benzing T, Hildebrandt F, Omran H: Mutations in a novel gene, *NPHP3*, cause adolescent nephronophthisis, tapeto-retinal degeneration and hepatic fibrosis. *Nat Genet 34*: 455-459, 2003

O'Toole JF, Otto EA, Hoefele J, Helou J, Hildebrandt F: Mutational analysis in 119 families with nephronophthisis. *Pediatr Nephrol 22*: 366-370, 2007

Otto E, Hoefele J, Ruf R, Mueller AM, Hiller KS, Wolf MT, Schuermann MJ, Becker A, Birkenhager R, Sudbrak R, Hennies HC, Nurnberg P, Hildebrandt F: A gene mutated in nephronophthisis and retinitis pigmentosa encodes a novel protein, nephroretinin, conserved in evolution. *Am J Hum Genet 71*: 1161-1167, 2002

Otto EA, Loeys B, Khanna H, Hellemans J, Sudbrak R, Fan S, Muerb U, O'Toole JF, Helou J, Attanasio M, Utsch B, Sayer JA, Lillo C, Jimeno D, Coucke P, De Paepe A, Reinhardt R, Klages S, Tsuda M, Kawakami I, Kusakabe T, Omran H, Imm A, Tippens M, Raymond PA, Hill J, Beales P, He S, Kispert A, Margolis B, Williams DS, Swaroop A, Hildebrandt F: Nephrocystin-5, a ciliary IQ domain protein, is mutated in Senior-Løken syndrome and interacts with RPGR and calmodulin. *Nat Genet 37*: 282-288, 2005

Otto EA, Schermer B, Obara T, O'Toole JF, Hiller KS, Mueller AM, Ruf RG, Hoefele J, Beekmann F, Landau D, Foreman JW, Goodship JA, Strachan T, Kispert A, Wolf MT, Gagnadoux MF, Nivet H, Antignac C, Walz G, Drummond IA, Benzing T, Hildebrandt F: Mutations in *INVS* encoding inversin cause nephronophthisis type 2, linking renal cystic disease to the function of primary cilia and left-right axis determination. *Nat Genet 34*: 413-420, 2003

Pazour GJ: Intraflagellar transport and cilia-dependent renal disease: the ciliary hypothesis of polycystic kidney disease. *J Am Soc Nephrol 15*:2528-2536, 2004

Quarmby LM, Parker JDK: Cilia and the cell cycle? J Cell Biol 169: 707–710, 2005

Quarmby LM, Mahjoub MR: Caught Nek-ing: cilia and centrioles. J Cell Sci 118: 5161-5169, 2005

Sayer JA, Otto EA, O'Toole JF, Nurnberg G, Kennedy MA, Becker C, Hennies HC, Helou J, Attanasio M, Fausett BV, Utsch B, Khanna H, Liu Y, Drummond I, Kawakami I, Kusakabe T, Tsuda M, Ma L, Lee H, Larson RG, Allen SJ, Wilkinson CJ, Nigg EA, Shou C, Lillo C, Williams DS, Hoppe B, Kemper MJ, Neuhaus T, Parisi MA, Glass IA, Petry M, Kispert A, Gloy J, Ganner A, Walz G, Zhu X, Goldman D, Nurnberg P, Swaroop A, Leroux MR, Hildebrandt F: The centrosomal protein nephrocystin-6 is mutated in Joubert syndrome and activates transcription factor ATF4. *Nat Genet 38*: 674-681, 2006

Smith LA, Bukanov NO, Husson H, Russo RJ, Barry TC, Taylor AL, Beier DR, Ibraghimov-Beskrovnaya O. Development of polycystic kidney disease in juvenile cystic kidney mice: insights into pathogenesis, ciliary abnormalities, and common features with human disease. *J Am Soc Nephrol 17*: 2821-2831, 2006

Trapp ML, Galtseva A, Manning DK, Beier DR, Rosenblum ND, Quarmby LM: Defects in ciliary localization of Nek8 in a subset of kidney tubules is associated with cystogenesis. Submitted.

Wagner T, Stoppa-Lyonnet D, Fleischmann E, Muhr D, Pages S, Sandberg T, Caux V, Moeslinger R, Langbauer G, Borg A, Oefner P: Denaturing high-performance liquid chromatography detects reliably BRCA1 and BRCA2 mutations. *Genomics* 62: 369-376, 1999

Watnick T, Germino G: From cilia to cyst. *Nat Genet 34*: 355-362, 2003

Table 3-1 *NEK8* mutations and clinical characteristics in three patients with NPHP.

Family #	Ethnic origin	Nucleotide change[a]	Deduced protein change[a]	Exon (allele)	Parental consan-guinity	Age at ESRF [yr]	Renal cysts	Eye involvement	Mutation absent from controls[b]
F408[c]	Swiss	C988T	L330F	7 (heterozygous)	-	24	ND	RP, blind at age 24	0/80, DHPLC
F601	Kurdish	C1273T	H425Y	9 (homozygous)	+	3	Microcysts (renal biopsy consistent with NPHP	No	0/85, *Nco*I
F612	Austrian	G1489C	A497P	11 (heterozygous)	-	14	ND	No	0/85, *Blp*I

[a]Numbering based on *NEK8* cDNA position in human reference sequences NM_178170.2, +1 corresponds to the A of the ATG translation initiation codon. [b]All mutations were absent from at least 80 healthy control subjects. *Blp*I or *Nco*I restriction enzyme digest or DHPLC were used for examination of healthy control samples. [c]The patient of family F408 carries an additional homozygous *NPHP5* mutation (Otto *et al.*, 2005). DHPLC, Denaturing high performance liquid chromatography; RP, retinitis pigmentosa; ND, no data available.

Figure 3-1 Human mutations in NEK 8 and evolutionary conservation

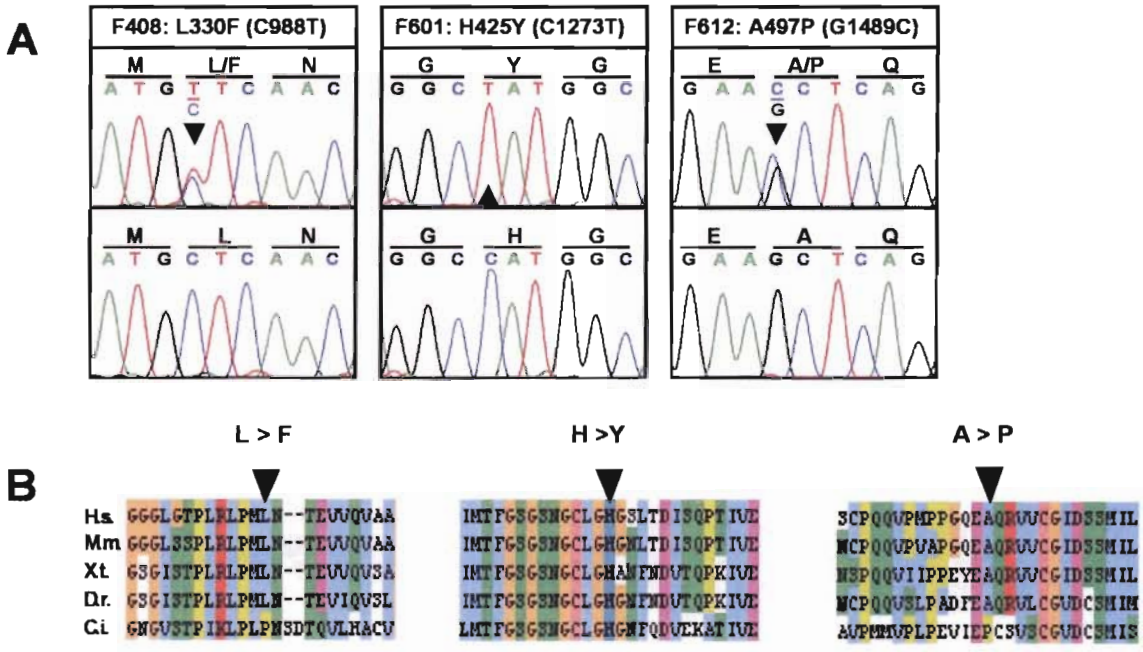

A) Chromatograms of 3 different *NEK8* mutations detected in 3 individuals with nephronophthisis. Family number, amino acid sequence change, and mutated nucleotide are given above sequence traces. Wild-type sequences are shown below mutated sequences. Reading frame is indicated by underlining codon triplets in the upper panel and mutated nucleotides are indicated by an arrowhead. The two mutations L330F and A497P occurred in the heterozygous and H425Y in the homozygous state. All mutations were absent from at least 80 healthy control individuals. **B)** Alignment of the Nek8 protein sequence of regions mutated in patients with homologues from various species. Mutated amino acid are indicated with arrowheads. The amino acid sequences are aligned with those of *Homo sapiens* (H.s.), *Mus musculus* (M.m), *Xenopus tropicalis* (X.t.), *Danio rerio* (D.r.), and *Ciona intestinalis* (C.i.).

Figure 3-2 *in vitro* expression of GFP-Nek8 mutations

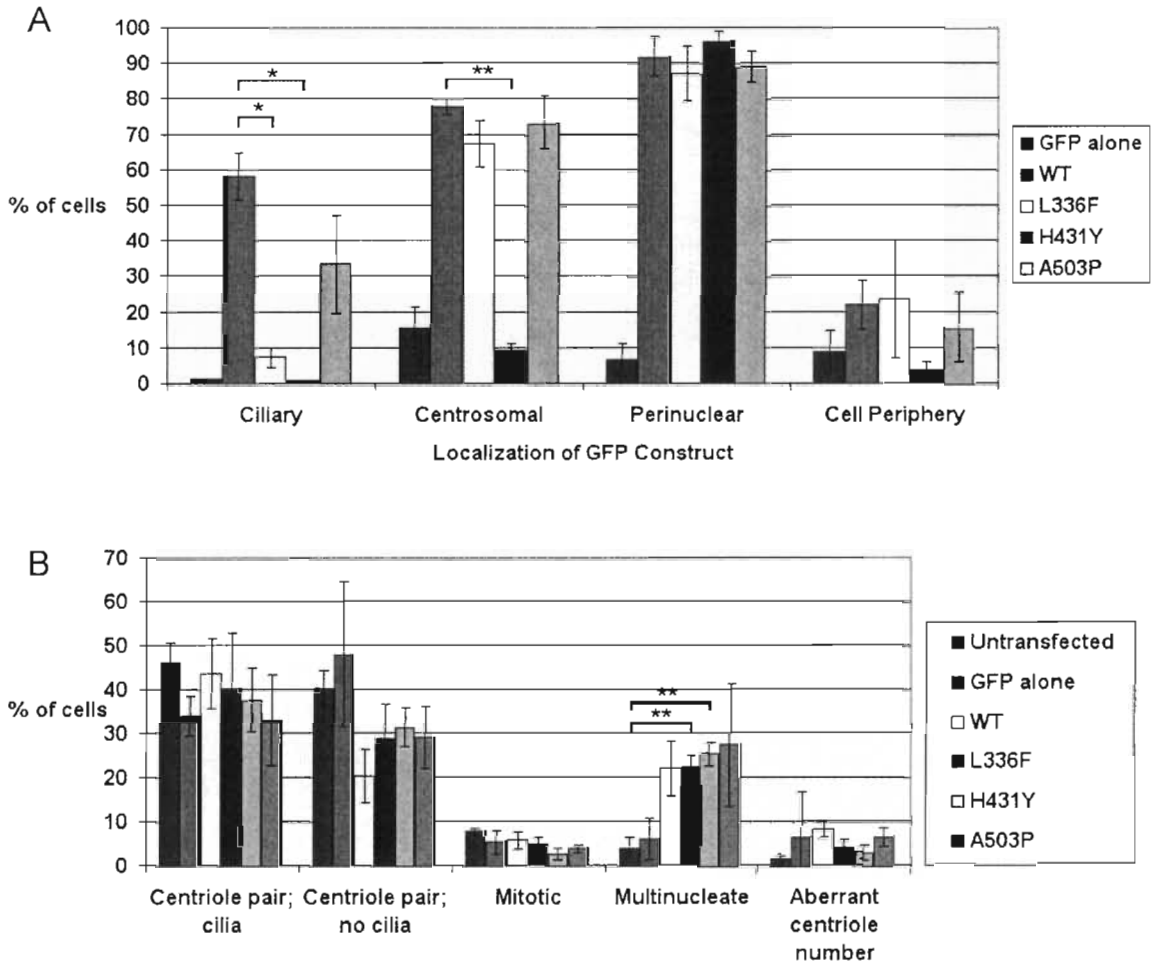

A) Quantification of differential sub-cellular localization of GFP-tagged Nek8 constructs. Transiently transfected ciliated, mononucleate IMCD-3 cells with low to medium levels of expression were quantified for ciliary, centrosomal, perinuclear and cell peripheral localization of GFP-mutant-Nek8. The total number of cells counted from three independent experiments was N=45, 50, 55, 55, and 45 for GFP alone, wild-type (WT), L336F, H431Y, and A503P, respectively. Error bars = SEM. Note that ciliary localization was significantly reduced for mutant constructs L336F and H431Y compared to the wild-type. Centrosomal localization was significantly reduced for mutant H431Y. Statistical significance was assessed using T-test assuming 2-sample unequal variances with 2-tailed probability. * $p=0.01$, ** $p<0.001$. **B) Overexpression of Nek8 has no effect on ciliogenesis.** Transfected and untransfected cells were categorized as ciliated with a pair of centrioles, lacking cilia with a pair of centrioles, undergoing mitosis, multinucleate, or having an aberrant number of centrioles, including none at all. N=total number of cells counted from three independent experiments. The total number of cells counted from three independent experiments was N=1095, 150, 300, 250, 300, and 258 for untransfected, GFP alone, WT, L336F, H431Y, and A503P, respectively. Error bars = SEM.

Figure 3-3 Mutant forms of Nek8 have defects in sub-cellular localization

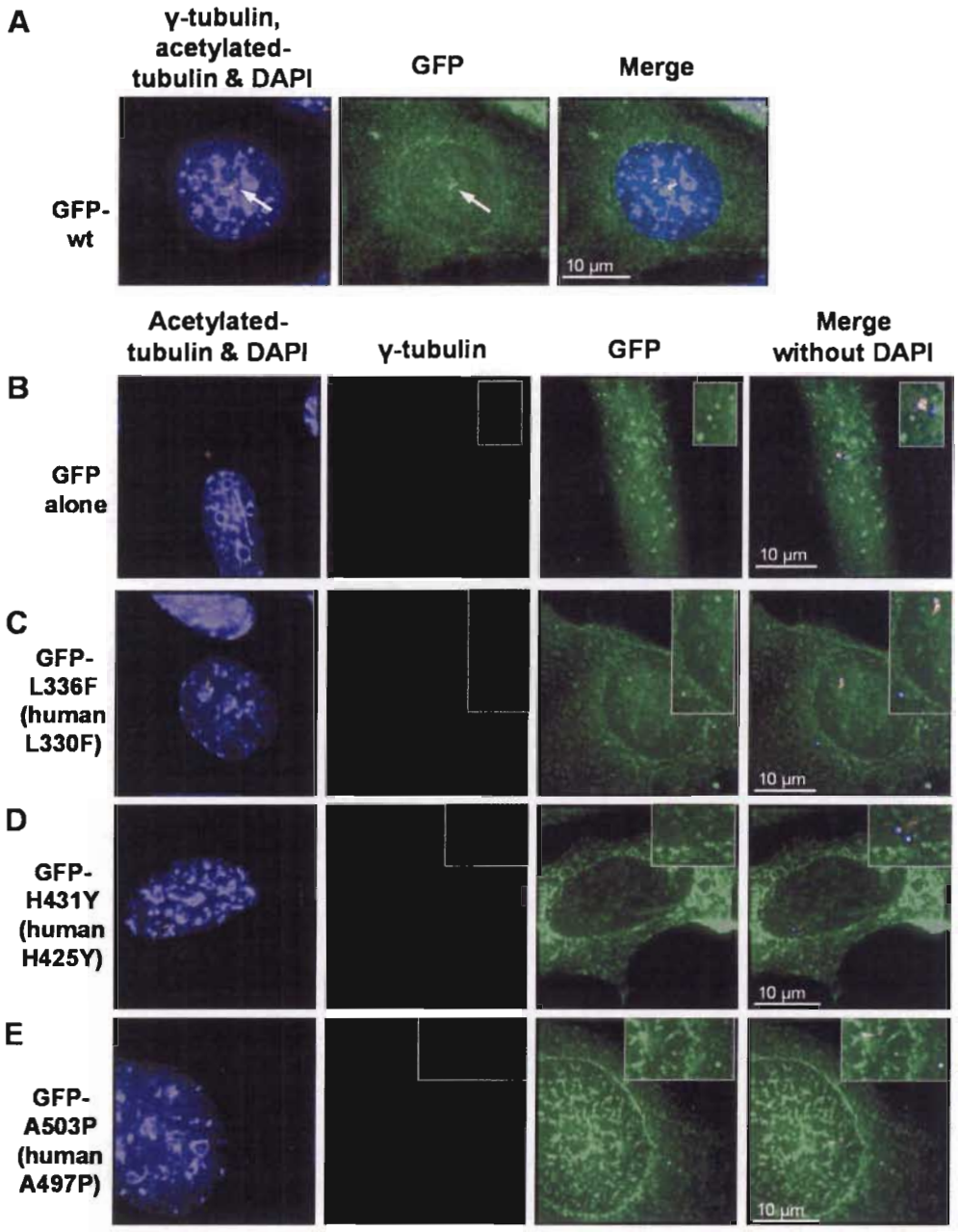

Transient overexpression of N-terminal GFP-tagged mouse Nek8 cDNA in inner medullary collecting duct (IMCD-3) cells. **A)** Cells were stained for anti-acetylated tubulin (red) to visualize cilia (arrows) and anti-γ-tubulin (red) to mark centrosomes (arrowheads) and DAPI to indicate the nucleus (blue). Wild-type GFP-Nek8 (green) localizes to the cytoplasm, centrosomes (arrowheads) and cilia (arrows). **B-E)** Expression of GFP alone and mutant GFP-Nek8 constructs. Note that amino acid numbering differs in murine *mNek8* and human *NEK8* (Table 1). Cells were fixed and stained for anti-acetylated tubulin for cilia (red) and for anti-γ-tubulin for centrosomes (blue) and DAPI (blue). **B)** GFP alone localizes to the cytoplasm, but not to cilia or centrosomes. **C)**The GFP-L336F Nek8 mutant was detected in the cytoplasm and centrosomes, but not in cilia. **D)** The GFP-H431Y Nek8 mutant is not associated with either centrosomes or cilia, in this example. **E)** GFP-A503P localizes to the cytoplasm and centrosomes, but not to cilia in this example. Insets are 2x magnification in B) and D) and 1.5x magnification in C) and E).

Figure 3-4 Western blot of GFP-Nek8 Constructs.

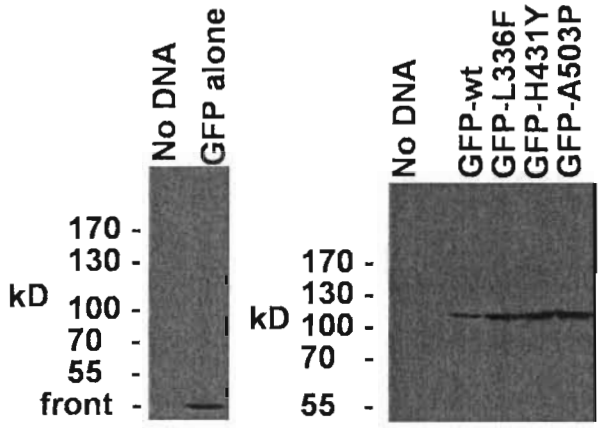

Western blot of transfected IMCD-3 cell extracts using anti-GFP antibody shows expected band size of 102 kDa for the GFP-Nek8 fusion proteins and 27 kDa for GFP alone.

CHAPTER 4: DEFECTS IN CILIARY LOCALIZATION OF NEK8 IN A SUBSET OF KIDNEY TUBULES IS ASSOCIATED WITH CYSTOGENESIS

Melissa L. Trapp[1], Alevtina Galtseva[2], Danielle K. Manning[3], David R. Beier[3], Norman D. Rosenblum[2,4], Lynne M. Quarmby[1].

[1]Department of Molecular Biology and Biochemistry, Simon Fraser University, Burnaby, BC, Canada. [2]Program in Developmental and Stem Cell Biology, The Hospital for Sick Children; Department of Physiology, University of Toronto, Toronto, ON, Canada. [3]Genetics Division, Brigham and Women's Hospital, Harvard Medical School, Boston, Massachusetts, USA. [4]Department of Paediatrics, University of Toronto, Toronto, ON, Canada.

Rationale and Contribution

In this submitted manuscript, our aim was to determine the effect of mutations in Nek8 and the localization of endogenous Nek8 *in vivo*. My contributions were performing all experiments with reagents provided by the co-authors and writing the manuscript.

Abstract

Mutations in human Nek8 are associated with a rare form of the juvenile renal cystic disease, nephronophthisis and mutations in murine Nek8 cause renal cysts in *jck* mice. The etiology of renal cysts involves dysfunctional ciliary signaling and we have previously reported that Nek8 localizes to the primary cilium in mouse kidney epithelial cells. In order to investigate the cell biological consequences of kinase-deficient and *jck* mutant forms of Nek8, we transiently

expressed GFP-tagged constructs in a mouse kidney epithelial line. We find that mutations in the kinase and C-terminal domains of Nek8 corresponded to decreased ciliary localization while not affecting assembly and maintenance of cilia. These data correspond to our observations of endogenous Nek8 within the cilium in a subset of uretic bud and collecting duct tubules in the medullary and cortical region of the developing mouse kidney. Compared to kidneys from heterozygous (unaffected) mice, kidneys from homozygous *jck* mice revealed reduced ciliary localization of Nek8. These data indicate that the ciliary localization of Nek8 in a subset of uretic bud-derived kidney tubules is essential for maintaining tubule integrity in the mammalian kidney.

Introduction

The cystic renal diseases, including polycystic kidney disease (PKD) and nephronophthisis (NPH) are caused by defects in ciliary signaling, but the signaling pathways involved have not been elucidated. Many of the proteins which carry the mutations that cause cystic kidney disease localize to the cilium or the centrosome (1). Additionally, defects in the assembly and maintenance of the cilium (ciliogenesis) cause cystic kidney disease (2). Mutations in the NIMA-related kinase, Nek8 are associated with the formation of renal cysts in both humans (in NPH type 9) and mice (in the *j*uvenile *c*ystic *k*idney (*jck*) model) (3,4).

Neks form a family of evolutionarily conserved cell cycle kinases that are defined by a conserved N-terminal Ser/Thr kinase domain and a variable C-terminal domain (5, 6). The C-terminus of Nek8 contains a RCC1 (regulator of

chromatin condensation) domain, usually involved in protein-protein interactions. The causal mutation in *jck* mice is a missense mutation (G448V) in the RCC1 domain (4). Similarly, three independent human mutations in the same domain are associated with a rare form of the juvenile cystic kidney disease, NPH type 9 (3). We have previously reported that Nek8 localizes to the primary cilium in mouse kidney epithelial cells (7).

In order to understand the pathogenesis of kidneys inflicted with a mutant Nek8, we examined mouse Nek8 in the context of the organ itself. The study of metanephric kidney organogenesis has elucidated key developmental mechanisms, such as reciprocal induction between mesenchyme and epithelium, branching morphogenesis, mesenchymal-to-epithelial transition, and nephrogenesis (8). These processes require many signaling pathways such as the FGF, Wnt, and BMP familes, and specific regional control of these signals is necessary for coordinating growth and structure of the kidney (9). The temporal and spatial patterns of Nek8 expression provide clues to its function during development and therefore, how mutations in Nek8 can cause cystic kidney diseases.

Herein we report that ciliary localization of Nek8 is restricted to tubules in the uretic bud lineage of the developing mouse kidney, consistent with the onset of cystogenesis in these tissues (4). We find subcellular mis-localization of transiently expressed kinase-deficient and *jck* mutant forms of Nek8 and note that these proteins do not have dominant effects on the assembly or maintenance of cilia in a mouse kidney epithelial line. These two lines of

evidence lead to the prediction that Nek8 is mislocalized in the jck kidney. Indeed, we observed reduced ciliary localization of Nek8 in homozygous *jck* kidneys. Our data indicate that defects in ciliary localization of Nek8 in a subset of uretic bud-derived kidney tubules is associated with cystogenesis.

Materials and Methods

Cell Culture: Mouse inner medullary collecting duct (IMCD-3) cells were cultured in a humidified 37°C incubator with 5% CO_2 in a 1:1 mix of DMEM and Ham's F12 media with 10% FBS (all from Invitrogen).

Mouse Lines: CD1/129 mice were housed in the Animal Facility of The Hospital for Sick Children (Toronto, Canada) and C57BL/6J heterozygous and homozygous *jck* mice were housed in the NRB Animal Facility (Boston, USA). Animal experiments were approved by the ethics committee at The Hospital for Sick Children and the Harvard Medical area standing committee on animals. Kidneys from different developmental stages from CD1/129 mice and C57BL/6J heterozygous and homozygous *jck* mice were dissected and embedded in paraffin using standard procedures. Sections were mounted on slides using a microtome.

GFP Constructs: The K33M (presumptive kinase deficient) and G448V (*jck*) mouse Nek8 (mNek8) cDNA constructs in pcDNA3.1 were PCR amplified with SacI and SalI-flanking restriction sites, digested and subcloned into the SacI/SalI digested pEGFP-C2 vector (BD Biosciences Clontech) with an N-terminal GFP. The reading frame and mutations were verified by sequencing.

The vectors were then purified by an Endotoxin-free Maxiprep kit (Qiagen). Transient transfections were performed using Lipofectamine 2000 (Invitrogen) according to manufacturer's protocol with the following exception: Cells grown on coverslips were incubated with DNA complexes in OptiMEM (Invitrogen) for 4-6 hours, then washed with PBS and grown in DMEM/Ham's F12 media for 16-24 hours. Transfection efficiency ranged from 9-35%.

Western blot: Transfected IMCD-3 cells were resuspended in 1x SDS sample buffer (10% glycerol, 50mM Tris (pH6.8), 2mM EDTA, 2% SDS, 144mM 2-mercaptoethanol, 0.01% bromophenol blue (all from Sigma)) and the suspension was sonicated to shear genomic DNA. The samples were separated by electrophoresis in an 8% SDS-PAGE gel and transferred to Trans-Blot membrane (BioRad) using a wet transfer apparatus. The nitrocellulose membrane was blocked using 5% skim milk in TBS-T for 1 hour, followed by incubation in mouse anti-GFP antibody (clones 7.1 and 13.1, 0.4µg/mL, Roche) overnight at 4°C. The membrane was then washed with TBS-T and incubated in HRP-conjugated goat anti-mouse antibody for 1 hour at room temperature. GFP-conjugated proteins were visualized using an enhanced chemiluminescence kit (Amersham Biosciences) and X-OMAT film (Kodak).

Indirect immunofluorescence of tissue culture cells: Transfected cells grown on coverslips were fixed by -20°C methanol for 10 minutes, and then rehydrated by PBS. They were subsequently stained for immunofluorescence using monoclonal mouse anti-gamma tubulin (clone GTU-88, 1,000-fold dilution, Sigma) and monoclonal mouse IgG2b anti-acetylated tubulin (clone 6-11B-1,

7,500-fold dilution, Sigma) as primary antibodies and Alexa 594-conjugated goat anti mouse all IgG (2,000-fold dilution, Molecular Probes) as a secondary antibody. Cell nuclei were stained with 4-6-diamidino-2-phenylindole (DAPI, 1 µg/mL). Coverslips were mounted using Mowiol (Calbiochem).

Indirect immunofluorescence of kidney sections: Slide-mounted paraffin wax-embedded 5µm kidney sections were deparaffinized through incubations in xylene (Fisher Scientific), then sequentially with 100%, 95%, 70%, and 50% ethanol and washed in PBS. Slides were microwaved in a pressure cooker in 10 mM sodium citrate (pH 6.0) and cooled. After three PBS washes, slides were incubated in blocking solution (PBS, 3% BSA (Sigma), 4.8% heat-inactivated goat serum (Invitrogen), 0.02% Tween-20 (Sigma)) for 1 hour and incubated overnight at 4°C with one or more of the following primary antibodies and lectin in blocking solution: Rabbit polyclonal anti-mouse Nek8 (2000-fold dilution, (4)), mouse monoclonal anti-acetylated tubulin (clone 6-11B-1, 500-fold dilution, Sigma), mouse monoclonal anti-calbindin-D-28K (clone CB-955, 100-fold dilution, Sigma), mouse monoclonal anti-NCAM (clone NCAM-0B11, 50-fold dilution, Sigma) and FITC-conjugated Dolichos Biflorus Agglutinin (DBA; 20 ug/mL, Vector Labs). After three PBS washes, slides were incubated with one or more of the following secondary antibodies in blocking solution: Alexa 594-conjugated goat anti mouse all IgG (1,000-fold dilution, Molecular Probes), Alexa 488-conjugated goat anti rabbit (500-fold dilution, Molecular Probes), and Alexa 568-conjugated goat anti-rabbit (500-fold dilution, Molecular Probes). Slides were washed in PBS, incubated in DAPI (10 µg/mL), and mounted in Vectashield

hardest mounting medium (Vector Labs). Fluorescence microscopy was performed using the Delta Vision system (Applied Precision) as described previously (10). Heterozygous and homozygous *jck* kidney sections were stained with haematoxylin and eosin and imaged under brightfield illumination.

Quantification of cellular phenotypes of transiently transfected cells: In three independent experiments, immunostained untransfected and transfected cells were categorized as ciliated with a pair of centrioles, lacking cilia with a pair of centrioles, undergoing mitosis, multinucleate, or having an abnormal number of centrioles, including none at all. The ciliated, mononucleate cells with low to medium levels of expression were then quantified for localization of GFP constructs to cilia, centrosomes, a perinuclear region, and/or cell periphery. Statistical significance was assessed using a two-sample T-test assuming unequal variances with two-tailed probability and calculated using Microsoft Excel 2003.

Quantification of Nek8 expression in developing kidney: Different embryonic stages of immunostained mouse kidney sections were scored for the presence or absence of Nek8 in the lumenal cilia of tubules in the medullary and cortical regions judged by co-localization with acetylated tubulin or lumenal orientation to cellular markers. At least three different sections from different kidneys were examined for each stage. In homozygous *jck* kidney sections, Nek8 localization was scored as positive if at least one cilium of a tubule contained Nek8.

Results

Transiently Expressed Mutant Forms of Nek8 Are Mis-Localized, but Have No Effect on Overall Ciliary Assembly

A mouse kidney epithelial cell line (IMCD-3 cells) was transiently transfected with GFP-tagged full length mouse Nek8 cDNA, encoding wild type or mutant forms of the protein. Transiently expressed GFP was cytoplasmic, but GFP-tagged wild type Nek8 localized to cilia (58% of cells, p=0.014), centrosomes (78%, p=0.046), a perinuclear region (92%, p=0.0023), and possibly also to the cell periphery (22%, p=0.26) (Fig. 1, Fig. 2A). However, when either the presumptive kinase dead K33M or the jck G448V mutations were introduced into GFP-Nek8, the protein showed decreased localization to the cilia (19%, p=0.092 and 25%, p=0.029 respectively). Kinase deficient GFP-Nek8 also shows reduced localization to the centrosomes (6%, p=0.00019) and possibly cell periphery (1.5%, p=0.096) while the *jck* mutation did not (40%, p=0.97 and 23%, p=0.97, respectively) (Fig. 1, Fig.2A). These data suggest that the K33M and *jck* mutations in Nek8 affect the subcellular localization of this protein, and the K33M mutation is more severe.

Members of the NIMA-related kinase (Nek) family function in both cell cycle and ciliary regulation, while localizing to cilia and/or centrosomes (11). To investigate the cellular effects of transient expression of mutant forms of Nek8, we quantified the percentage of transfected cells that had a pair of centrioles with a cilium, had a pair of centrioles without a cilium, were mitotic, were multinucleate, or had an abnormal number of centrioles (Fig. 2B). Transfection of GFP-wild type Nek8 and GFP-mutant Nek8 had no effect on ciliogenesis, as

the percentage of transfected ciliated cells was similar to GFP alone ($p>0.69$). There was no obvious effect on mitosis ($p>0.15$) or number of centrioles ($p>0.44$, Fig 2B). In addition, transfection of any form of GFP-Nek8 caused multinucleate cells, which is possibly due to a defect in cytokinesis, as the total number of cells in mitosis and spindle formation in transfected cells appeared normal. Liu *et al.* (4) previously reported that overexpression of kinase deficient and *jck* Nek8 caused multinucleate cells, but we now demonstrated that overexpression of wild type Nek8 causes the same phenotype; therefore this phenotype is not likely to be related to the etiology of renal cysts. Note that because the quantification was mutually exclusive, the decrease of cells in the category "2 centrioles, no cilia" in GFP-Nek8 wt, K33M and *jck* transfectants was due to an increase in multinucleate cells, which contained a range of ciliated and non-ciliated cells. Expression of the mutant constructs was many fold higher than endogenous Nek8 expression (data not shown). Nevertheless, our data indicate that overexpression of wild-type, kinase-deficient, or *jck* Nek8 do not have dominant effects on ciliogenesis.

Spatiotemporal Nek8 Expression in Developing Kidney

Mutations in the RCC1 domain of Nek8 cause renal cysts in both mouse models and human NPH patients. To investigate the *in vivo* role of endogenous Nek8 in developing mouse kidney, we examined its localization pattern through indirect immunofluorescence of kidney sections at different embryonic stages. We found Nek8 localized to the majority of lumenal cilia within a given tubule or

not at all in other ciliated tubules (Fig. 3). Also, Nek8 did not localize to the entire cilium, occurring in patches as previously reported in tissue culture cells (7).

Primary cilia are known to project into the lumen of kidney tubules and are expressed by mesenchymal, stromal and epithelial cell types within the developing mouse kidney (A.G. unpub. data). Analysis of temporal expression showed Nek8 was absent in cilia in early stages of kidney development (E13.5-14.5) and appeared within lumenal cilium at E15.5 in a subset of ciliated tubules in the medullary and cortical regions (Table 1). Nek8 also localized to more medullary tubules than cortical tubules throughout development (Table 1). In addition, a roughly increasing percentage of ciliated tubules of the medulla and cortex express Nek8 as development proceeds, to a maximum of 60-72% of medullary tubules and 40-56% of cortical tubules expressing Nek8 (Table 1). Because Nek8 is expressed from E15.5, we hypothesize that the effects of a mutation could manifest at an earlier time point than previously reported (4,12).

In order to identify the subset of tubules expressing Nek8, E18.5 kidney sections were stained with a variety of kidney cell type markers. Nek8 was not expressed by tubules derived from mesenchyme demarked as NCAM-positive cells (0% co-staining, N=91) although NCAM-positive cells still contain cilia (Fig. 4C,D). The majority of Nek8-containing tubules positively stain for calbindin (89%, N=38) and Dolichos Biflorus Agglutinin (DBA, 82%, N=28), indicating tubules of uretic bud origin and/or collecting ducts contain Nek8 in their cilia (Fig. 4A,B). Conversely, only 36% of DBA (N=42) and 65% of calbindin-positive (N=60) tubules within the kidney expressed Nek8. Thus, Nek8 is specifically

expressed in tubules of uretic bud origin and/or collecting ducts, but not all uretic bud tubules or collecting ducts express Nek8.

Reduced Ciliary Nek8 Localization in Early *jck* Kidneys

Having established that Nek8 localizes to cilia of the developing kidney, we examined whether this was affected in mutant *jck* mice. Sectioned kidneys of post-natal day 7 mice reveal the earliest reported example of cysts within the *jck* mouse. In haematoxylin and eosin stained sections, cysts are primarily localized to the corticomedullary region (Fig. 5), a phenotype characteristic of human nephronophthisis, in which Nek8 has recently been identified as a causal mutation (3).

Indirect immunofluorescence of kidney sections showed that wild type and heterozygous *jck* ciliated tubules expressed Nek8 in the majority of cilia within a given tubule (Fig.6 A,B). In homozygous *jck* ciliated tubules, Nek8 localized to fewer cilia within a given tubule in both cystic and interestingly, non-cystic tubules (Fig 6 C,D). Only 29% of medullary and 23% of cortical non-cystic ciliated tubules of the *jck* homozygote expressed Nek8 whereas 69% of medullary and 49% of cortical ciliated tubules had ciliary Nek8 in heterozygous littermates (Table 2). Cystic tubules in the *jck* homozygote also had decreased ciliary Nek8 localization similar to non-cystic tubules (26%, Table 2). Furthermore, the decreased percentage of tubules expressing Nek8 in *jck* homozygotes provides a conservative estimation of the overall effect of the mutation because any ciliated tubule with at least one patch of Nek8 co-localizing with the cilia was scored as a tubule which expressed Nek8. Thus, in *jck* homozygous mice, Nek8 is

expressed in fewer tubules and these tubules have fewer cilia that co-localize with Nek8. This result correlates with our cell culture data in which GFP-*jck* shows reduced ciliary localization (Fig.1 and Fig.2) and with previously published data reporting the lack of ciliary Nek8 localization in *jck* mouse kidney primary culture cells (12).

Discussion

The Effect of the *jck* Mutation on Nek8 in the Developing Kidney

The *jck* missense mutation was responsible for decreased ciliary localization of Nek8 both *in vitro* and *in vivo*. In *jck* homozygous mice, reduced ciliary localization was observed in both cystic and non-cystic tissue. This result correlates with loss of apical Nek8 localization reported in Liu *et al.* (4) and Nek8 absence in cilia of primary kidney cell culture reported by Smith *et al.* (12). However, because some cilia within the *jck* kidney still co-localized with Nek8, this suggests that the *jck* mutation is hypomorphic, and reduces the ability of Nek8 to localize to cilia in both cystic and non-cystic tubules.

Similar loss of ciliary Nek8 localization was observed in over-expression studies with the K33M, kinase-deficient mutation. In addition, kinase deficient Nek8 failed to localize to the centrosomes, unlike wild type and *jck* forms of the protein. These data indicate that, in addition to the RCC1 domain, kinase activity is required for ciliary targeting via the centrosome. Dependence of the kinase domain for correct sub-cellular localization has been demonstrated with another family member, Nek1, which carries the causal mutation of the *kat* (kidney,

anemia, testes) mouse model of cystic kidney disease (13,14). We conclude that ciliary Nek8 plays an essential role in normal signaling between cilia and the machinery of cell differentiation/proliferation and that inadequate expression of Nek8 in cilia leads to the formation of cysts.

Contribution of Nek8 to Ciliogenesis

The etiology of renal cysts remains enigmatic, but we do have a few hints. In *Tcf2* mice mutant for HNF1β, a transcription factor for genes involved in PKD, it was found that a defect in oriented cellular division, a hallmark of the planar cell polarity pathway, preceded cyst formation in kidney tubules (15). Other defects in PKD include increased proliferation and apoptosis, as well as defects in mechanosensation of lumenal flow in kidney tubules (16). Failure to build a cilium can also cause polycystic kidneys, such as the *orpk*/Tg737 mouse that is defective in intraflagellar transport, a process necessary for assembly, maintenance, and disassembly of the cilium (17). Yet, the presence of cilia in *jck* mice, *in vitro* overexpression of Nek8, and in RNAi knockdown of Nek8 (7) indicates that Nek8 plays no role in the assembly or maintenance of cilia.

Although others have reported lengthened cilia in *jck* mice (12), we did not observe differences in ciliary length between wild type and *jck* Nek8 in both cell culture and stained kidney sections. We note, however, that ciliary length is highly variable within cell culture (MT unpubl. obs.) and within the kidney in different cell types and different stages of development (AG unpubl. obs.).

Specific Expression of Nek8 in Developing Kidneys

The earliest developmental stage at which we observed Nek8 in the cilia of embryonic mouse kidneys was E15.5. At this stage, Nek8 appears in a subset of tubules of uretic bud origin and/or collecting ducts and continues to be expressed until at least post-natal day 7. However, cells associated with tubules in this lineage are ciliated earlier than E15.5, indicating temporal as well as spatial specificity of Nek8 expression.

The spatial localization of endongenous Nek8 is consistent with the collecting bud origin of *jck* cysts at post natal day 14 (4) and the collecting duct, distal tubule, and the Loop of Henle origin of cysts at 26 days after birth (12). This suggests a cell autonomous function of Nek8, as defects in ciliary localization due to the *jck* mutation correlates with cyst formation of that tubule.

Onset of Nek8 expression coincides with a series of events occurring at E15.5, including epithelial-to-mesenchymal transition, nephrogenesis, and onset of kidney function and urine flow (18). It is tempting to speculate that Nek8 may play a role in these processes, perhaps in conjunction with other cystoproteins which are expressed in the developing kidney. Polycystin-1 is expressed at the basal surface of uretic bud epithelium in the developing kidney medulla in humans and mice (19, 20). Polycystin-2 is expressed from mouse E14.5 in the uretic bud, at P0 in distal tubules, and in the adult in the the distal convoluted tubule and collecting ducts (21, 22). Both polycystin-1 and polycystin-2 seem to be absent from the nephrogeneic mesenchyme, S-bodies, and glomeruli, similar to our findings with Nek8 (19, 21). Fibrocystin-1, defective in autosomal

recessive PKD, is found in mouse uretic bud branches from E15-E19, and in medullary and cortical collecting ducts and the ascending Loop of Henle in adult human kidney (23). Inversin, which is defective in nephronophthisis (NPHP) type 2, localizes to cortical collecting ducts and strongly to the medulla to the ascending Loop of Henle and distal tubules of the adult kidney (24). Specific spatiotemporal expression in the developing kidney has not been demonstrated for NPHP1 (nephrocystin), NPHP3, NPHP4 (nephroretinin), NPHP5 (IQCB1), or NPHP6 (CEP290).

We propose that Nek8 is an essential component of a ciliary signaling pathway that promotes and maintains correct tubule morphogenesis. Identification of the targeting mechanism of Nek8, through identification of proteins that interact with the RCC1 domain as well as substrates for the kinase activity of Nek8, will reveal important elements of the elusive signaling pathway which is defective in cystogenesis.

Acknowledgements

We thank the Rosenblum lab members, especially Lin Chen for invaluable assistance. We also thank Michel Leroux and his lab members for the use of their tissue culture facilities. M.L.T. is supported by graduate fellowships from the Michael Smith Foundation for Health Research and the Natural Sciences and Engineering Research Council of Canada. This work was funded by an operating grant from the Kidney Foundation of Canada to L.M.Q.

References

1. Hildebrandt F, Otto E: Cilia and centrosomes: a unifying pathogenic concept for cystic kidney disease? *Nat Rev Genet* 6: 928-940, 2005

2. Pazour GJ: Intraflagellar transport and cilia-dependent renal disease: the ciliary hypothesis of polycystic kidney disease. *J Am Soc Nephrol* 15: 2528-2536, 2004

3. Otto EA, Trapp ML, Schultheiss UT, Quarmby LM, Hildebrant F: Mutations in NIMA-related kinase NEK8 causes nephronophthisis in humans and affects ciliary and centrosomal localization. Under revision.

4. Liu S, Lu W, Obara T, Kuida S, Lehoczky J, Dewar K, Drummond IA Beier DR: A defect in a novel Nek-family kinase causes cystic kidney disease in the mouse and in the zebrafish. *Development* 129: 5839-5846, 2002

5. Parker JDK, Bradley BB, Mooers AO, Quarmby LM: Phylogeny of the NIMA-related family of kinases (Neks): an ancient gene family associated with cilia Submitted.

6. O'Connell MJ, Krien MJE, Hunter T: Never say never. The NIMA-related protein kinases in mitotic control. *Trends Cell Biol* 13: 221-228, 2003

7. Mahjoub MR, Trapp ML, Quarmby LM: NIMA-Related Kinases Defective in Murine Models of Polycystic Kidney Diseases Localize to Primary Cilia and Centrosomes. *J Am Soc Nephrol* 16: 3485-3489, 2005

8. Dressler GR: The cellular basis of kidney development. *Ann Rev Cell Dev Biol* 22: 509-529, 2006

9. Bouchard M: Transcriptional control of kidney development. *Differentiation* 72: 295-306, 2004

10. Mahjoub MR, Rasi MQ, Quarmby LM: A NIMA-related kinase, Fa2p, localizes to a novel site in the proximal cilia of Chlamydomonas and mouse kidney cells. *Mol Biol Cell* 15: 5172-5286, 2004

11. Quarmby LM, Mahjoub MR: Caught Nek-ing: cilia and centrioles. *J Cell Sci* 118: 5161-5169, 2005

12. Smith LA, Bukanov NO, Husson H, Russo RJ, Barry TC, Taylor AL, Beier DR, Ibraghimov-Beskrovnaya O: Development of polycystic kidney disease in juvenile cystic kidney mice: insights into pathogenesis, ciliary abnormalities, and common features with human disease. *J Am Soc Nephrol* 17: 2821-2831, 2006

13. Upadhya P, Birkenmeier EH, Birkenmeier CS, Barker JE: Mutations in a NIMA-related kinase gene, Nek1, cause pleiotropic effects including a progressive polycystic kidney disease in mice. *Proc Natl Acad Sci* 97: 217-221, 2000

14. White MC, Quarmby LM: The NIMA-family kinase, Nek1, cycles through the nucleus and affects the stability of centrosomes and cilia. Under revision.

15. Fischer E, Legue E, Doyen A, Nato F, Nicolas JF, Torres V, Yaniv M, Pontoglio M: Defective planar cell polarity in polycystic kidney disease. *Nat Genet* 38: 21-23, 2006

16. Bissler JJ, Dixon BP: A mechanistic approach to inherited polycystic kidney disease. *Pediatr Nephrol* 20: 558-566, 2005

17. Pazour GJ, Dickert BL, Vucica Y, Seeley ES, Rosenbaum JL, Witman GB, Cole DG: Chlamydomonas IFT88 and its mouse homologue, polycystic kidney disease gene tg737, are required for assembly of cilia and flagella. *J Cell Biol* 151: 709-718, 2000

18. Davies JA, Bard JB: The development of the kidney. *Curr Top Dev Biol* 39: 245-301, 1998

19. Polgar K, Burrow CR, Hyink DP, Fernandez H, Thornton K, Li X, Gusella GL, Wilson PD: Disruption of polycystin-1 function interferes with branching morphogenesis of the ureteric bud in developing mouse kidney. *Dev Biol* 286: 16-30, 2005

20. Guillaume R, D'agati V, Daoust M, Trudel M: Murine Pkd1 is a developmentally regulated gene from morula to adulthood: Role in tissue condensation and patterning. *Dev Dyn* 214: 337-348, 1999

21. Foggensteiner L, Bevan AP, Thomas R, Coleman N, Boulter C, Bradley J, Ibraghimov-Beskrovnaya O, Klinger K, Sandford R: Cellular and subcellular distribution of polycystin-2, the protein product of the PKD2 gene. *J Am Soc Nephrol* 11: 814-827, 2000

22. Chauvet V, Qian F, Boute N, Cai Y, Phakdeekitacharoen B, Onuchic LF, Attie-Bitach T, Guicharnaud L, Devuyst O, Germino GG, Gubler MC: Expression of PKD1 and PKD2 transcripts and proteins in human embryo and during normal kidney development. *Am J Pathol* 160: 973-983, 2002

23. Menezes LFC, Cai Y, Nagasawa Y, Silva AMG, Watkins ML, da Silva AM, Somolo S, Guay-Woodford LM, Germino GG, Onuchic LF. Polyductin, the *PKHD1* gene product, comprises isoforms expressed in plasma membrane, primary cilium, and cytoplasm. *Kidney Int* 66: 1345-1355, 2004

24. Nürnberger J, Kavapurackal R, Zhang SJ, Saez AO, Heusch G, Philipp T, Pietruck F, Kribben A: Differential tissue distribution of the Invs gene product inversin. *Cell Tissue Res* 323: 147-155, 2006

Table 4-1 Temporal expression of Nek8 in developing kidney.

Stage	Medullary tubules	Cortical tubules
E14.5	0% (N=11)	0% (N=16)
E15.5	42% (N=26)	13% (N=23)
E16.5	44% (N=55)	38% (N=53)
E18.5	60% (N=78)	29% (N=91)
P1	72% (N=110)	41% (N=100)
P7	66% (N=83)	56% (N=87)

Paraffin-embedded CD1/129 mouse kidney sections were stained with anti-acetylated tubulin to denote lumenal cilia and anti-Nek8 to denote endogenous expression. Percentages indicate the number of ciliated tubules expressing Nek8 in the medullary and cortical regions of wild type developing mouse kidney. N=Number of ciliated tubules counted.

Table 4-2 Decreased Nek8 expression in *jck* kidneys.

Phenotype	Medullary tubules	Cortical tubules
+ / jck **non-cystic**	69% (N=148)	49% (N=116)
jck / jck **non-cystic**	29% (N=49)	23% (N=52)
jck / jck **cystic**	26% (N=42)	

Paraffin-embedded sections of post-natal day 7 mouse kidneys from heterozygous (*+/jck*) and homozygous *jck* (*jck/jck*) mouse littermates were stained with anti-acetylated tubulin and anti-Nek8 antibodies. Percentages indicate the number of cystic and non-cystic tubules in the medulla and cortex of the kidney that express Nek8 in lumenal cilia. Any tubule with at least one cilium co-localizing with Nek8 was scored as positive. N=Number of ciliated tubules counted.

Figure 4-1 Overexpression of mutant forms of Nek8 shows differential localization.

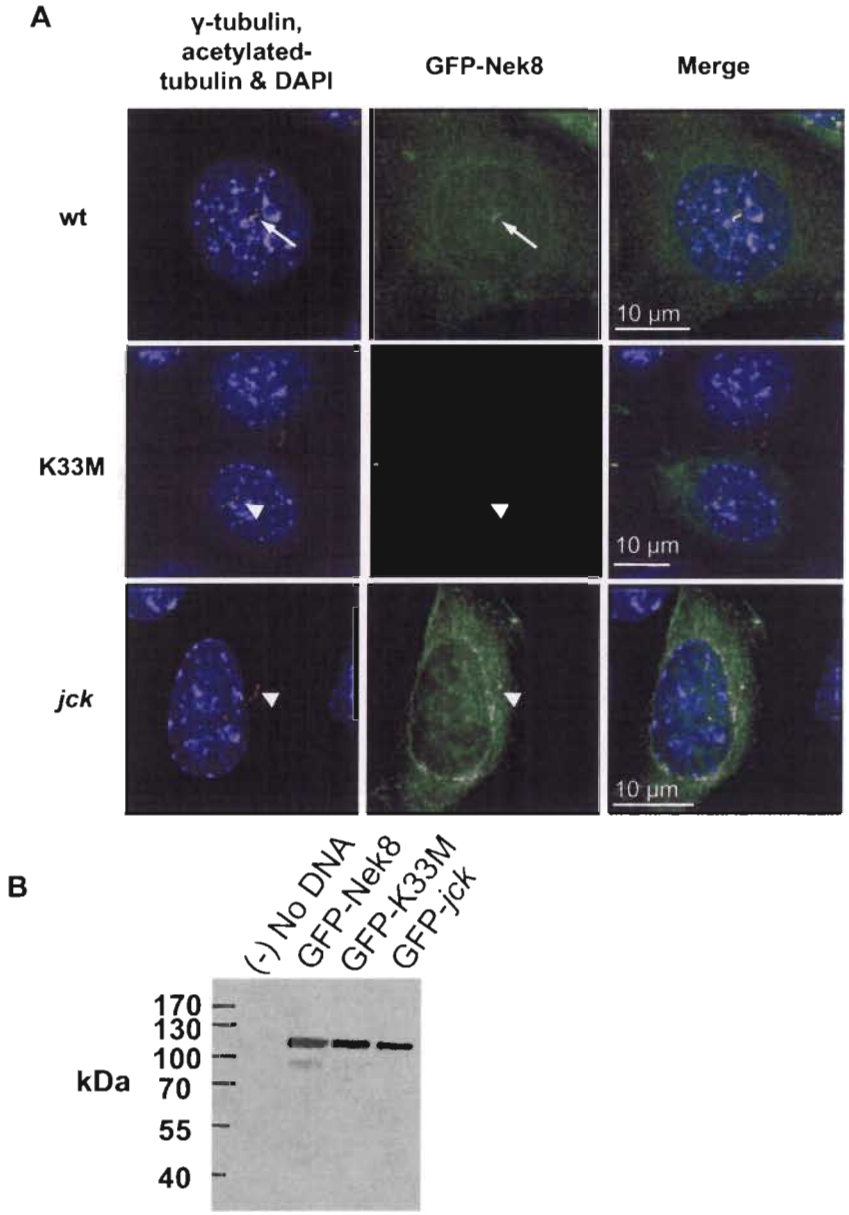

Transient overexpression of N-terminal GFP-tagged mouse Nek8 cDNA in mouse inner medullary collecting duct (IMCD-3) cells. **(A)** Cells were fixed and stained for anti-acetylated tubulin for cilia and anti-gamma tubulin for centrosomes (both red) and DAPI to indicate the nucleus (blue). Wild type GFP-Nek8 localizes to the cytoplasm, centrosomes and cilia (arrow). GFP-Kinase-deficient (K33M) Nek8 localizes to the cytoplasm, but not centrosomes and cilia (arrowhead) in this example. GFP-*jck* Nek8 localizes to the cytoplasm and centrosomes, but not cilia (arrowhead) in this example. **(B)** Western blot of transfected cell extracts using anti-GFP antibody shows expected band size of 102kDa for the GFP-Nek8 fusion proteins.

Figure 4-2 *in vitro* expression of GFP-Nek8 mutations

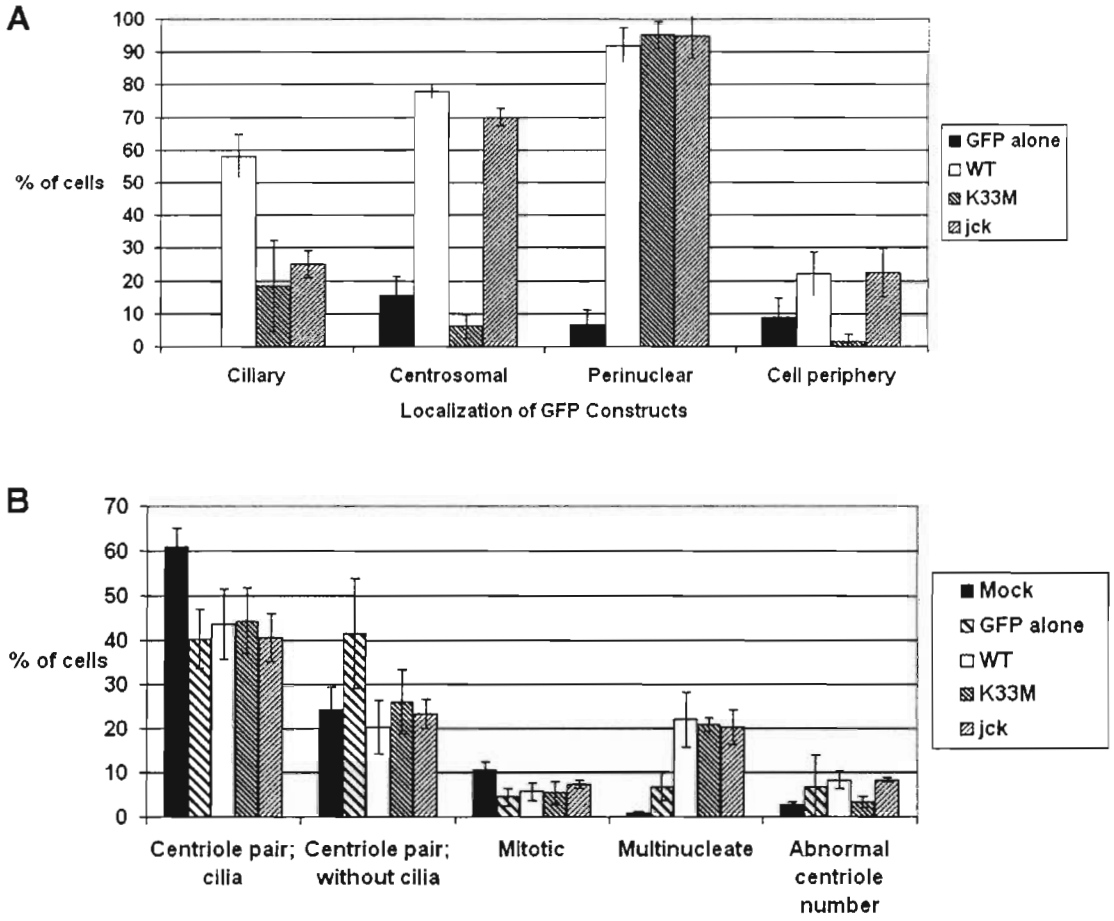

(A) Quantification of differential sub-cellular localization of GFP-tagged Nek8 constructs. Transiently transfected ciliated, mononucleate IMCD-3 cells with low to medium levels of expression were quantified for localization of various forms of GFP-Nek8 to cilia, centrosomes, a perinuclear region, and/or cell periphery. The total number of cells counted from three independent experiments was N=45, 50, 65 and 40 respectively for GFP alone, wt, K33M and *jck*. Error bars = SEM. **(B) Overexpression of Nek8 has no effect on overall ciliogenesis.** Transfected and untransfected IMCD-3 cells expressing various forms of GFP-Nek8 were categorized as ciliated with a pair of centrioles, lacking cilia with a pair of centrioles, undergoing mitosis, multinucleate, or having an abnormal number of centrioles, including none at all. The total number of cells counted from three independent experiments was N=950, 250, 300, 300 and 300 respectively for untransfected, GFP alone, wt, K33M, and *jck*. Error bars = SEM.

Figure 4-3 Variable spatial expression of Nek8 in developing mouse kidney.

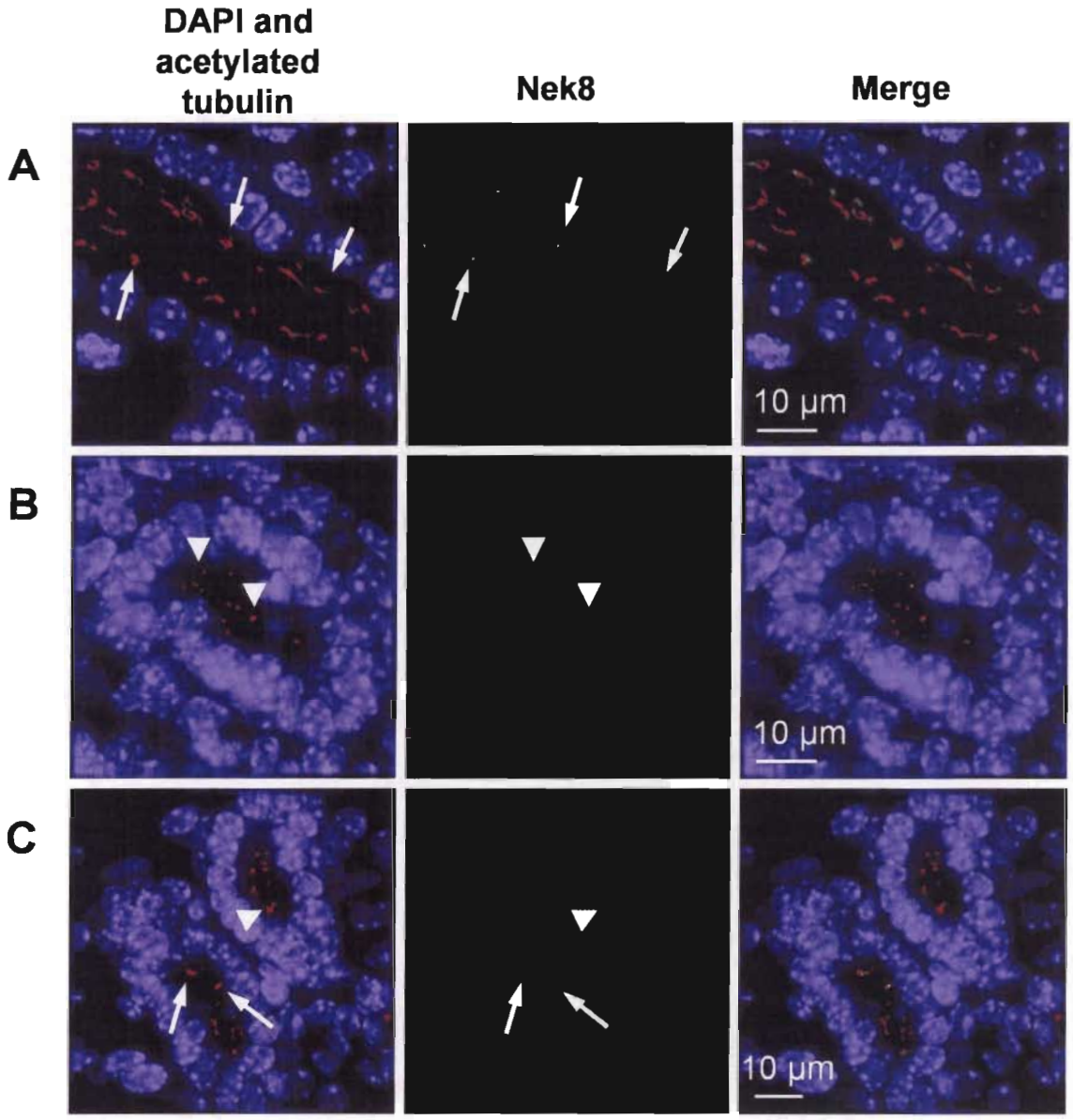

Paraffin embedded sections of CD1/129 mouse embryonic kidney were stained with DAPI for nuclei (blue), anti-acetylated tubulin for cilia (red), and anti-Nek8 for endogenous protein (green). **(A)** A medullary tubule from embryonic day 18.5 with Nek8 co-localizing with the majority of cilia (arrows). **(B)** A cortical tubule from embryonic day 16.5 with Nek8 absent in cilia (arrowheads). **(C)** Tubules from embryonic day 16.5. Nek8 co-localizes with the majority of cilia in a medullary tubule (arrows), but exhibits no co-localization with cilia in an adjacent tubule (arrowhead).

Figure 4-4 Tubules of uretic bud origin and/or collecting ducts express Nek8.

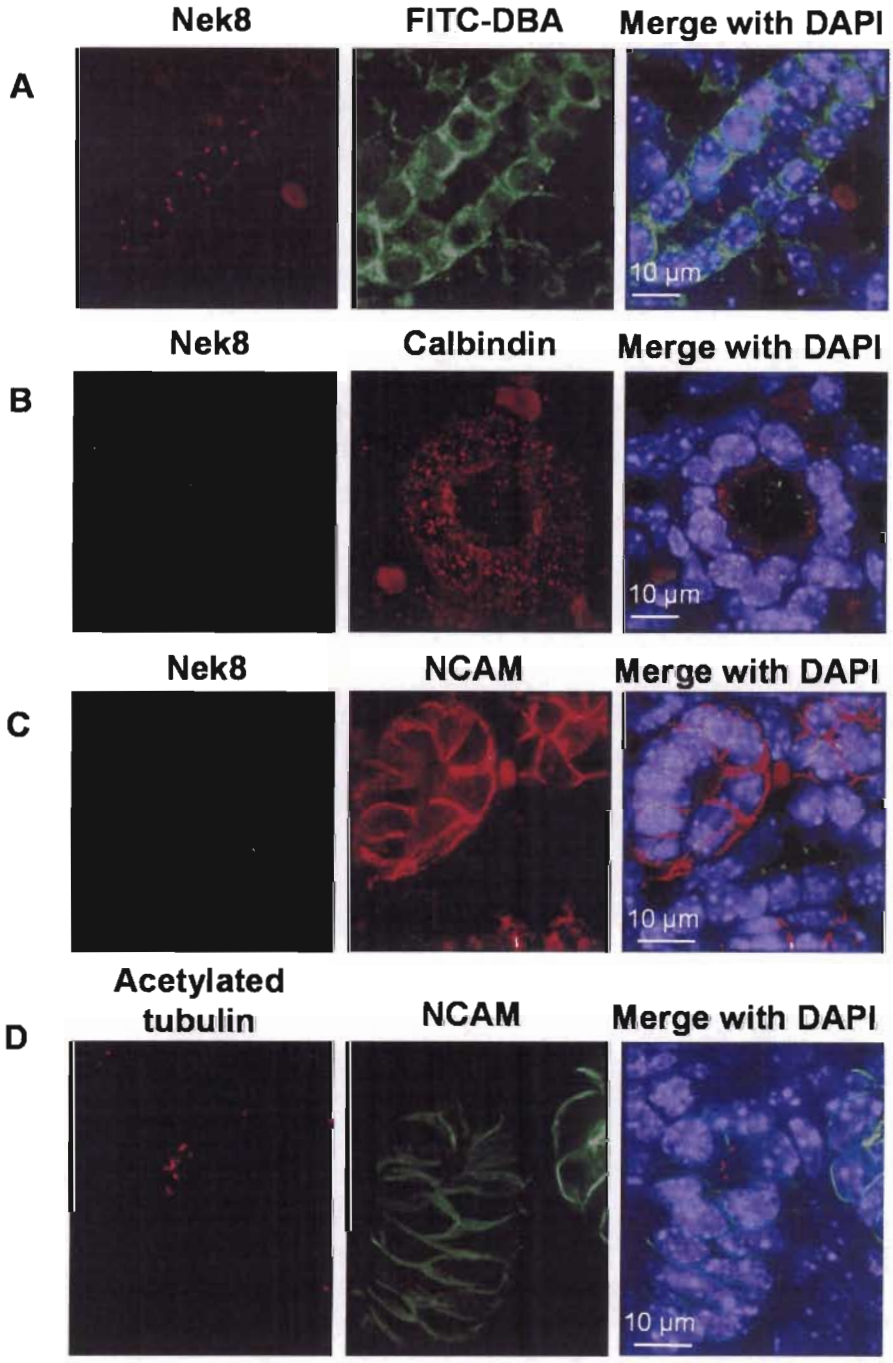

Paraffin-embedded sections of E18.5 CD1/129 mouse kidneys stained with anti-Nek8 antibody, markers denoting kidney cell types, and DAPI (blue). **(A)** An example of a tubule in the medulla labeled with FITC-conjugated dolichos biflorus agglutinin (DBA, green) expressing lumenal Nek8 (red). **(B)** An example of a tubule in the medulla labeled with anti-calbindin (red) expressing lumenal Nek8 (green). **(C)** Tubules in the cortex labeled with anti-NCAM (red) do not express lumenal Nek8 (green). **(D)** NCAM-positive tubules (green) stained with anti-acetylated tubulin (red) indicating cilia.

Figure 4-5 Early *jck* renal morphology.

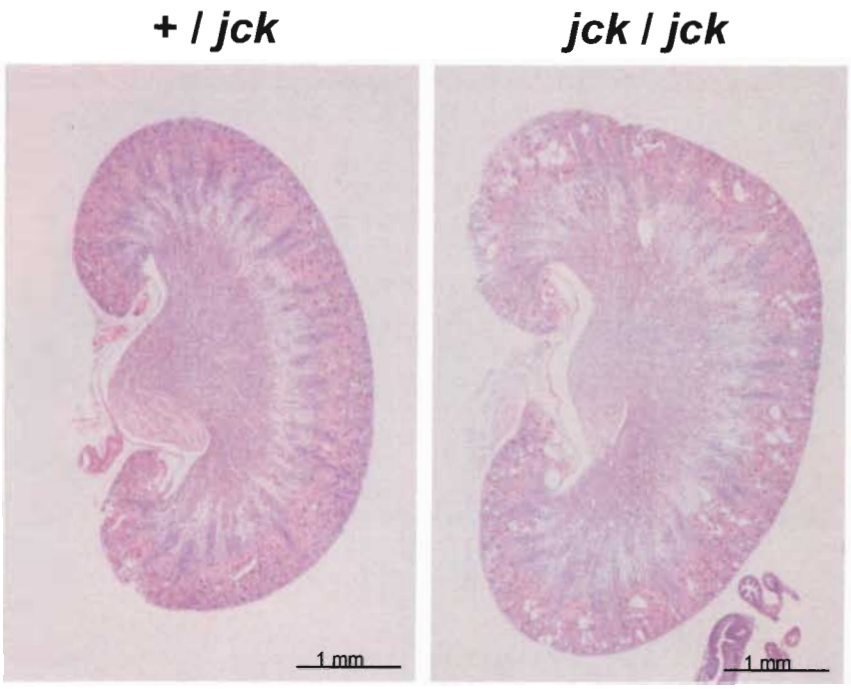

Paraffin-embedded sections of post-natal day 7 *jck* heterozygous (+/*jck*) and homozygous (*jck*/*jck*) mouse kidneys from littermates were stained with hematoxylin and eosin.

Figure 4-6 Differential Nek8 ciliary localization in diseased *jck* kidney.

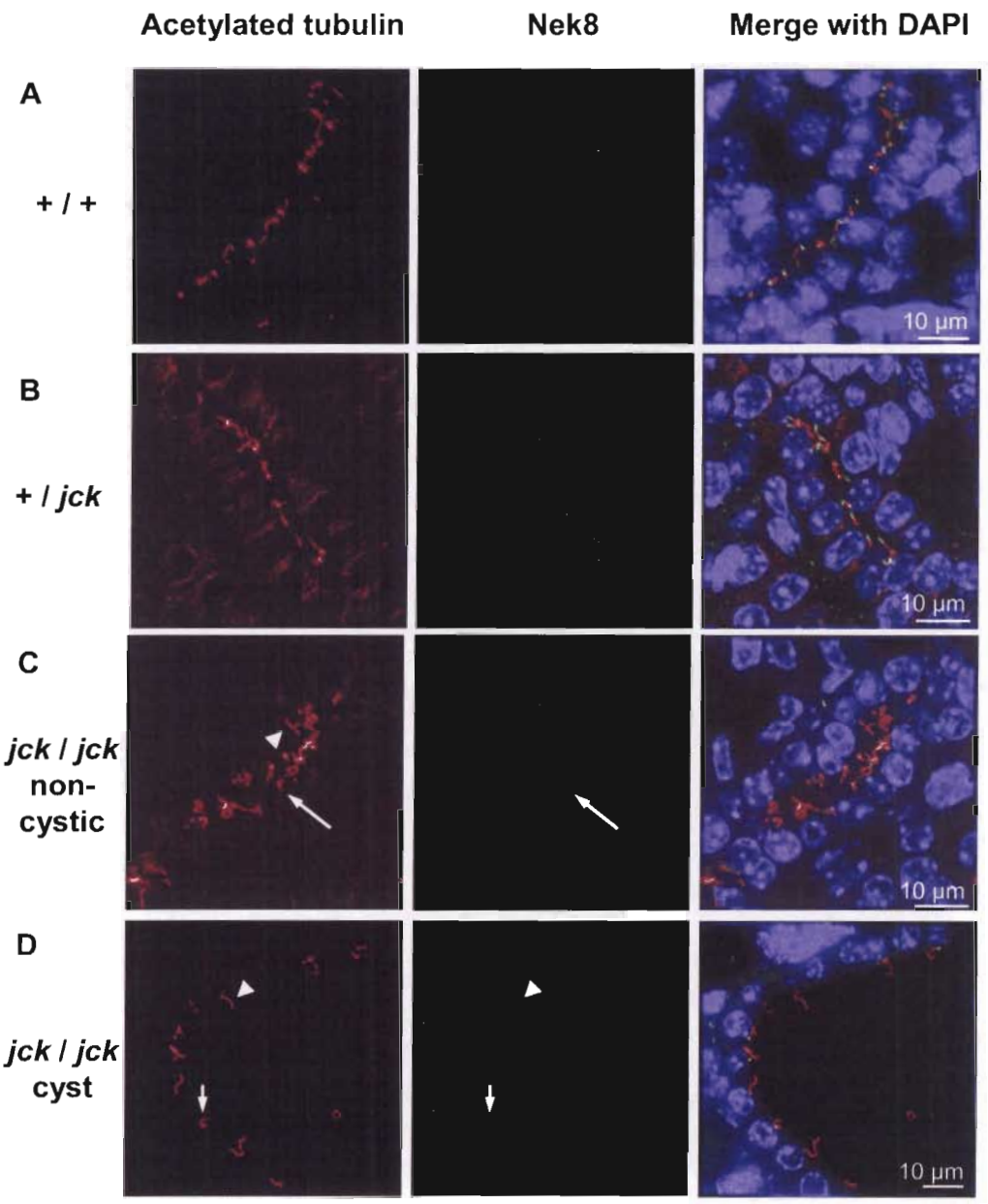

Paraffin-embedded sections of post-natal day 7 mouse kidneys from **(A)** wild type (+/+), **(B)** heterozygous (+/*jck*), and **(C,D)** homozygous *jck* (*jck*/*jck*) mice were stained with DAPI (blue), anti-acetylated tubulin for cilia (red), and anti-Nek8 for endogenous protein (green). The heterozygous and homozygous mice were littermates. Shown are ciliated tubules within the medulla. Arrows indicate Nek8 localization and arrowheads indicate lack of Nek8 in cilia.

CHAPTER 5: CONCLUSIONS

My work has shown that Nek8 is found in cilia *in vitro* and *in vivo* and is expressed in tubules of uretic bud origin during mouse kidney development. Mutations in Nek8 causing cystic kidney disease in *jck* mice and human nephronophthisis cause differential sub-cellular localization and defects in ciliary localization of Nek8 *in vivo* are associated with cystogenesis.

Much remains to be discovered about Nek8, and foremost, its interacting proteins and substrates. Nek8 likely shares a common signaling pathway with the nephrocystins; however, preliminary yeast two-hybrid data indicate that Nek8 does not bind NPHP1-5 (F. Hildebrandt, personal communication). It may be that Nek8 modifies the cystic kidney disease phenotype by compromising signaling pathways not directly involved with the nephrocystins, but still affect cystogenesis. Identifying proteins which bind Nek8 will also allow analysis into how the G448V, L336F, H431Y, and A503P mutations alter Nek8 function and why both the kinase activity and RCC1 domain is required for ciliary localization. More fundamentally, identifying protein interactors will specify the role of Nek8 in cilia.

It is interesting that all four naturally occurring cystogenic mutations in Nek8 are missense mutations, whereas NPH1-6 had frameshift and nonsense mutations associated with NPHP (See Table 1-1). Are Nek8 knockout or null mutations lethal? To answer this, it would be necessary to make a knockout

mouse or create an RNAi knockdown cell culture line (see Appendix 3). With Nek8 levels lowered, effects on cell cycle or other effects associated with PKD, such as insensitivity to flow, could be determined.

The molecular mechanism of ciliopathies remains enigmatic. The polycystins and some nephrocystins localize to more subcellular regions than cilia, such as cell-cell junctions, focal adhesions, and the nucleus (Hildebrandt and Otto, 2005); what is the site controlling cystic renal disease progression? To answer these questions biochemically, a cell fractionation scheme could isolate these complexes and identify interacting proteins. Genetically, selective disruption of structural components of cilia, focal adhesions, or cell-cell junctions could potentially rule out their necessity in the disease pathology. However, these subcellular locations are likely highly interconnected through regulatory pathways, and therefore, separating their functions would be difficult.

More research remains on the role of the polycystin and nephrocystin signaling pathways in renal cystogenesis including identification of the cause and effect of cystogenesis. Many cellular processes are associated in cyst formation, including proliferation, apoptosis, ciliogenesis, PCP, and the second messengers cAMP and calcium (Torres and Harris, 2007). It is important to note that cyst formation is a default pathway *in vivo* and *in vitro* (Karihaloo *et al.* 2005).

Polycystins are expressed during kidney development and may be responsible for some aspect of nephrogenesis, the formation and elongation of the nephric tubule (Polgar *et al.* 2005; Guillaume *et al.* 1999; Foggensteiner *et al.* 2000; Chauvet *et al.* 2002). However, additional signals responsible for tubule

elongation and nephron patterning in addition to the pathways responsible for maintaining tubular integrity, including proper length and diameter, remain to be elucidated.

This work also touches on more fundamental topics, such as differentiation of the primary cilium into specific proximal and distal regions. Proteins, such as NPHP1/nephrocystin-1 localizing to the transition zone (Fliegauf *et al.* 2006), Nek8 localizing specifically to the proximal region (Mahjoub *et al.* 2005) and Fa2p localizing to the site of flagellar autotomy (Mahjoub *et al.* 2004) indicate that 1) such a differentiation exists and 2) localization to distinct regions of the cilia are controlled and perhaps, conserved throughout evolution. Additional evidence on tubulin modifications supports non-conformity along the proximal-distal axis of the cilium. Staining of polyglycylated tubulin in mouse organ sections indicates that short chain glycylation of tubulin is restricted to the bottom portion of the primary cilium (Dossou and Hallworth, 2006). Other tubulin modifications include glutamylation, acetylation, and detyrosination (van Dijk *et al.* 2007; Polevoda and Sherman, 2002; Phung *et al.* 2006). The *C. elegans* singlet microtubules at the distal tip of sensory cilia also illustrate a discontinuity along the ciliary length (Snow et al., 2004). What other proteins display this variance and what is the role of proximal-distal discontinuity in cilia?

The ultimate goal in the etiology of ciliopathies is to determine the precise mechanism between cilia and the cell cycle as well as other signaling pathways and to identify all regulators of these pathways. Is IFT, which is required for ciliogenesis, the central regulator of all ciliary signaling pathways? Genomic and

proteomic analysis have identified kinases, phosphatases, chaperones, E3 ligases, GTPases, membrane channels, receptors, nucleotide exchange factors and many diverse non-structural components located in the cilium (Pazour *et al.* 2006, Keller *et al.* 2006). The next step is to build an "interactome" describing the hierarchal organization and interaction of ciliary proteins. In addition to elucidating novel ciliary pathways, much remains to be studied on already identified ciliary pathways, such as the Shh and Wnt pathways. How are cilia related to the planar cell polarity pathway and does the PCP pathway control ciliogenesis or *vice versa*?

Finally, what regulates entry into the cilium? The compilation of a ciliary proteome provides a dataset of ciliary specific genes that may be analyzed for a small amino acid consensus sequence. However, it may be that entry is not be regulated by a general ciliary transport molecule, but the ability to target to the centrosome, and then consecutively target to the cilium through protein-protein interactions.

The cilium has come a long way from just cell motility. It contains a wide variety of signaling molecules and shares a relationship with cell cycle progression. The importance of the cilium is highlighted by the numerous and diverse diseases that occur when the cilium is defective. A large amount of research has illustrated the necessity and complexity of the cilium, but indeed, there is still much to be learnt.

References

Chauvet V, Qian F, Boute N, Cai Y, Phakdeekitacharoen B, Onuchic LF, Attie-Bitach T, Guicharnaud L, Devuyst O, Germino GG, Gubler MC: Expression of PKD1 and PKD2 transcripts and proteins in human embryo and during normal kidney development. *Am J Pathol* 160: 973-983, 2002

Dossou SJY, Hallworth R: Extensive polyglycylation of tubulin is not essential for cilia function in mammals. *Mol Biol Cell* 17: 2320a, 2006

Fliegauf M, Horvath J, von Schnakenburg C, Olbrich H, Muller D, Thumfart J, Schermer B, Pazour GJ, Neumann HP, Zentgraf H, Benzing T, Omran H: Nephrocystin specifically localizes to the transition zone of renal and respiratory cilia and photoreceptor connecting cilia. *J Am Soc Nephrol* 17: 2424-2433, 2006

Foggensteiner L, Bevan AP, Thomas R, Coleman N, Boulter C, Bradley J, Ibraghimov-Beskrovnaya O, Klinger K, Sandford R: Cellular and subcellular distribution of polycystin-2, the protein product of the PKD2 gene. *J Am Soc Nephrol* 11: 814-827, 2000

Guillaume R, D'agati V, Daoust M, Trudel M: Murine Pkd1 is a developmentally regulated gene from morula to adulthood: Role in tissue condensation and patterning. *Dev Dyn* 214: 337-348, 1999

Hildebrandt F, Otto E: Cilia and centrosomes: A unifying pathogenic concept for cystic kidney disease? *Nat Rev Genet* 6: 928-940, 2005

Karihaloo A, Nickel C, Cantley LG: Signals which build a tubule. *Nephron Exp Nephrol* 100: e40-e45, 2005

Keller LC, Romijn EP, Zamora I, Yates JR, Marshall WF: Proteomic analysis of isolated *Chlamydomonas* centrioles reveals orthologs of ciliary disease genes. *Curr Biol* 15: 1090-1098, 2005

Mahjoub MR, Rasi MQ, Quarmby LM: A NIMA-related kinase, Fa2p, localizes to a novel site in the proximal cilia of Chlamydomonas and mouse kidney cells. *Mol Biol Cell* 15: 5172-5286, 2004

Mahjoub MR, Trapp ML, Quarmby LM: NIMA-Related Kinases Defective in Murine Models of Polycystic Kidney Diseases Localize to Primary Cilia and Centrosomes. *J Am Soc Nephrol* 16: 3485-3489, 2005

Pazour GJ, Agrin N, Leszyk J, Witman GB: Proteomic analysis of a eukaryotic cilium. *J Cell Biol* 170: 103-113, 2005

Phung AD, Soucek K, Kubala L, Harper RW, Chloe Bulinski J, Eiserich JP: Posttranslational nitrotyrosination of alpha-tubulin induces cell cycle arrest and inhibits proliferation of vascular smooth muscle cells. *Eur J Cell Biol* 85: 1241-1252, 2006

Polevoda B, Sherman F: The diversity of acetylated proteins. *Genome Biol* 3: 1-0006, 2002

Polgar K, Burrow CR, Hyink DP, Fernandez H, Thornton K, Li X, Gusella GL, Wilson PD: Disruption of polycystin-1 function interferes with branching morphogenesis of the ureteric bud in developing mouse kidney. *Dev Biol* 286: 16-30, 2005

Snow JJ, Ou G, Gunnarson AL, Walker MR, Zhou HM, Brust-Mascher I, Scholey JM: Two anterograde intraflagellar transport motors cooperate to build sensory cilia on *C. elegans* neurons. *Nat. Cell Biol* 6: 1109-1113, 2004

Torres VE, Harris PC: Polycystic kidney disease: genes, proteins, animal models, disease mechanisms and therapeutic opportunities. *J Intern Med.* 261: 17-31, 2007

van Dijk J, Rogowski K, Miro J, Lacroix B, Edde B, Janke C: A targeted multienzyme mechanism for selective microtubule polyglutamylation. *Mol Cell* 26: 437-48, 2007

APPENDICES

Appendix 1: Truncation analysis of Nek8

Rationale

Work in previous chapters has established that Nek8 localizes to the cilia both *in vitro* and *in vivo*. To further understand the functional targeting domain of Nek8, cDNA truncations were constructed and expressed *in vitro* by Laura Hilton, in fulfilment of an undergraduate individual study semester under my supervision.

Materials and Methods

The kinase domain (encompassing nucleotides 1-855, amino acids 1-285, with a 32kDa predicted size) and the C-terminal domain (encompassing nucleotides 856-2097, amino acids 286-698, with a 43kDa predicted size) of mouse Nek8 was PCR amplified from full length Nek8 in pEGFP-C2 with SacI and SalI flanking primers. The PCR products were sequentially digested with SacI and SalI restriction enzymes and ligated into SacI/SalI-cut pEGFP-C2 (Clontech) with an N-terminal GFP tag. Vectors were transformed into Mach1 *E. coli* (Invitrogen), verified by sequencing and purified with an endotoxin-free maxiprep kit (Qiagen). Transfection into IMCD-3 cells, immunofluorescence, and cellular quantification were performed as previously described in earlier chapters. Averages were taken from three independent experiments. The full length Nek8

control failed to express in these experiments, and previous values are used for comparison.

Results and Discussion

Nek8 truncations were successfully transfected into IMCD-3 cells, shown by Western blot (Figure A1- 1) of the predicted sizes of 59kD for the GFP-kinase fusion and 70kD for the GFP-C-terminus fusion.

Figure A1- 1 Expression of GFP-Nek8 truncations

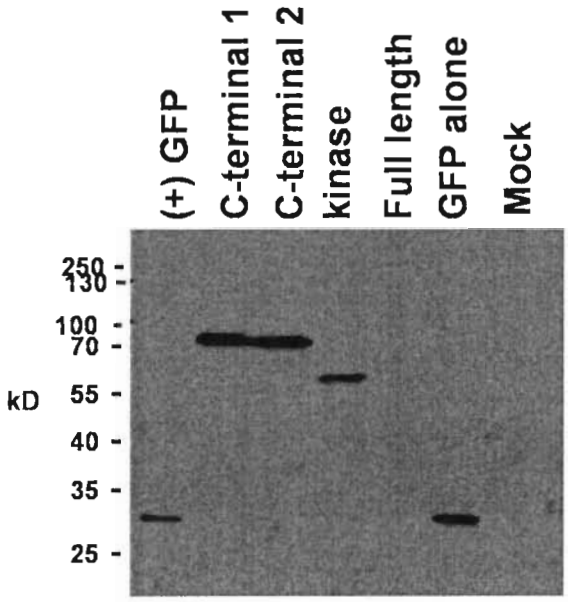

Representative anti-GFP Western blot of IMCD-3 cells transfected with GFP-tagged C-terminal domain (1 and 2), kinase domain (KIN 1-2), full length Nek8, and GFP alone (EGFP). Mock transfected cells and a positive control ((+) GFP) are shown. Note that all bands were of predicted size, except full length Nek8, which failed to express in these experiments.

Indirect immunofluorescence of transfected IMCD-3 cells showed that expression of GFP-kinase and GFP-C-terminus did not significantly affect ciliogenesis, mitosis, or the number of centrosomes, relative to GFP alone and untransfected controls (Table A1- 1), similar to full length GFP-Nek8 expression.

However, whereas expression of full length GFP-Nek8 caused multinucleate cells, only 7% of GFP-kinase and 8% of GFP-C-terminus transfected cells had this phenotype. It appears that multinucleate cells is due to an overexpression of wild-type and mutated Nek8 (see previous chapters), but requires both kinase and C-terminal domains.

Table A1- 1 Phenotype of overexpression of Nek8 truncations

	Mock	GFP alone	Full length Nek8	Kinase Domain	C-terminal Domain
Ciliated	56%	34%	44%	53%	45%
Mitotic	9%	5%	6%	7%	7%
Abnormal centriole number	4%	7%	8%	4%	4%
Multinucleate	1%	6%	22%	7%	8%
N=	535	150	300	250	230

Transfected and untransfected cells were categorized as ciliated with a pair of centrioles, lacking cilia with a pair of centrioles, undergoing mitosis, multinucleate, or having an aberrant number of centrioles, including none at all. N=total number of cells from three independent experiments.

Indirect immunofluorescence was used to define the ciliary localization domain of Nek8. Both the kinase and C-terminal domains had decreased localization to cilia compared to full length Nek8 (Figure A1- 2, Table A1-2). In addition, the C-terminal domain showed decreased centrosomal localization, and the kinase domain showed increased cell peripheral localization versus full length Nek8 (Figure A1- 2, Table A1-2).

Figure A1- 2 Immunofluorescence of Nek8 truncations

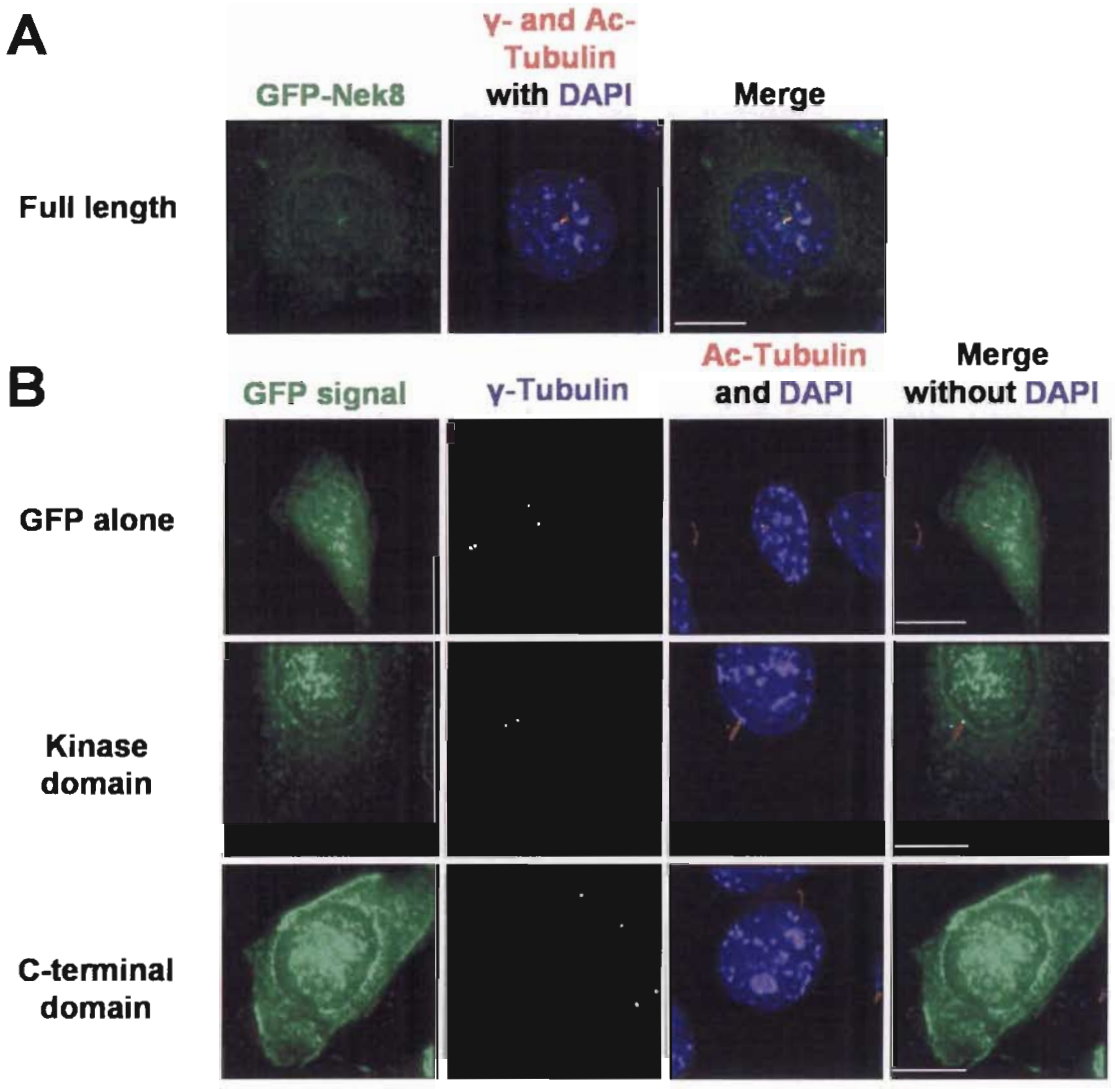

IMCD-3 cells transfected with GFP-tagged constructs. **(A)** Full length Nek8 transfected cells were stained for γ- and acetylated-tubulin to visualize centrosomes and cilia (red), and DAPI to mark nuclei. This example shows ciliary, centrosomal, and perinuclear localization. **(B)** Cells were stained for γ-tubulin to mark centrosomes (blue in merge), acetylated-tubulin to mark cilia (red), and DAPI to mark nuclei (blue). EGFP-kinase domain localizes to centrosomes and the perinuclear region in this example, while EGFP-C-terminal domain localizes to the perinuclear region and cell periphery in this example. Bar = 10μm

Through *in vitro* expression of truncated domains of Nek8, it appears that the kinase and C-terminal RCC1 domains of Nek8 alone are insufficient for ciliary localization, while each domain by itself retains some ability to localize to centrosomes, the cell periphery, and perinuclear region.

Table A1- 2 Differential localization of Nek8 truncations

	GFP alone	Full Length Nek8	Kinase Domain	C-terminal Domain
Ciliary	0%	58%	2%	2%
Centrosomal	16%	78%	52%	15%
Perinuclear	7%	92%	69%	65%
Cell Periphery	9%	22%	40%	19%
N=	45	50	42	46

The ciliated, mononucleate cells with low to medium levels of expression were then quantified for localization of GFP-mutant-Nek8 to cilia, centrosomes, to the perinuclear region, and/or to the cell periphery. N=number of cells counted from 3 independent experiments.

These findings agree with results in previous chapters in which mutations in the kinase domain (K33M) or the C-terminal domain (G448V, L336F, H431Y, A503P) of full length Nek8 cause decreased ciliary and centrosomal localization. However, it is important to consider whether the truncated domains of Nek8 fold properly or are even functional; yet, the crystal structure and protein interactors and substrates of Nek8 are undetermined. In addition, these studies were performed in a cell line with endogenous Nek8, and therefore the effects of expression of these truncations may not be dominant.

Appendix 2: Epitope-tagged Nek8

Rationale

This work addressed a problem that arose from transient transfection *in vitro* where expression levels affected GFP-Nek8 localization. For instance, high levels of expression caused GFP-Nek8 to localize to cytoplasmic and perinuclear puncta, medium levels caused multinucleate cells and prevents GFP-Nek8 localization to cilia, and low levels allowed the localization to cilia, centrosomes, etc. as reported in earlier chapters (see Figure A2-1). This range of expression occurred within every transfected population of cells. The solution was to co-transfect wild type and mutant Nek8, to verify that mutant Nek8 was non-ciliary, while wild type was ciliary within the same cell.

Figure A2- 1 Expression levels affect Nek8 localization

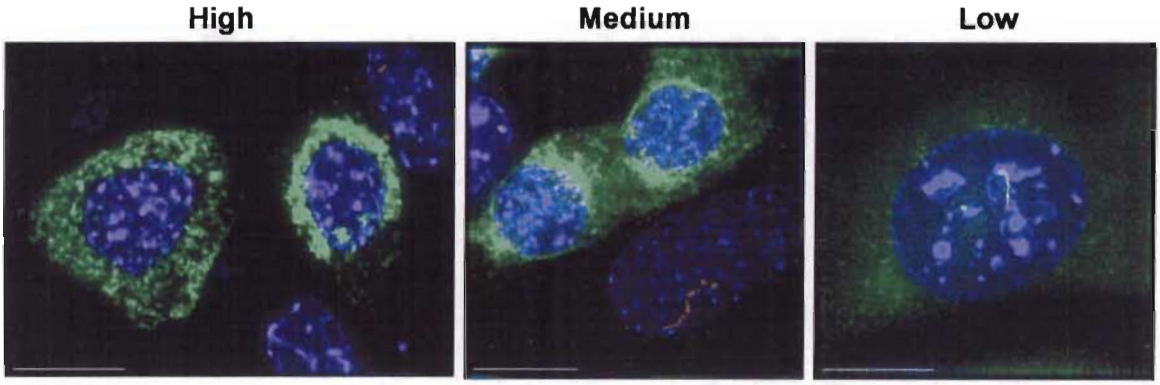

IMCD-3 cells transfected with GFP-Nek8 (green) were stained for γ- and acetylated tubulin (red), and DNA (blue). High, medium, and low reflect the expression levels of individual cells. Note that the lower expression levels required a longer picture exposure. Bar = 10 μm

Materials and Methods

Full length wild-type, K33M, G448V, L336F, H431Y, and A503P mouse Nek8 cDNA in pEGFP-C2 was PCR amplified using primers flanked by EcoRI and SalI. PCR products were sequentially digested with EcoRI and SalI restriction enzymes and ligated into pCMV-HA and pCMV-myc (Clontech) cut with the same enzymes, thus fusing the HA and myc epitopes to the N-terminus of Nek8 (denoted HA-Nek8 and myc-Nek8). Vectors were transformed into Mach1 *E. coli* (Invitrogen), selected on ampicillin-containing media (Sigma), verified by restriction endonuclease digest and DNA sequencing, and purified with an endotoxin-free maxiprep kit (Qiagen). Transient transfection was performed as previously, with 4 µg of total DNA used for co-transfection of pEGFP-Nek8 and pCMV-myc or pCMV-HA Nek8. Immunofluorescence was performed as previously, using monoclonal rat anti-HA (100-fold dilution, clone 3F10, Roche) and monoclonal mouse IgG1 anti-myc (250-fold dilution, clone 9E10, Clontech) primary antibodies and Alexa 488-conjugated goat anti-rat (1,000-fold dilution, Molecular Probes) and Alexa 647-conjugated goat anti-mouse IgG1 (500-fold dilution, Molecular Probes) secondary antibodies. Quantitative analysis was performed as previously, in chapters 3 and 4.

Results and Discussion

IMCD-3 cells successfully expressed both GFP-Nek8 and HA- and myc-Nek8 when co-transfected (Figure A2-2).

Figure A2- 2 HA- and myc-tagged Nek8 co-expression with GFP-Nek8

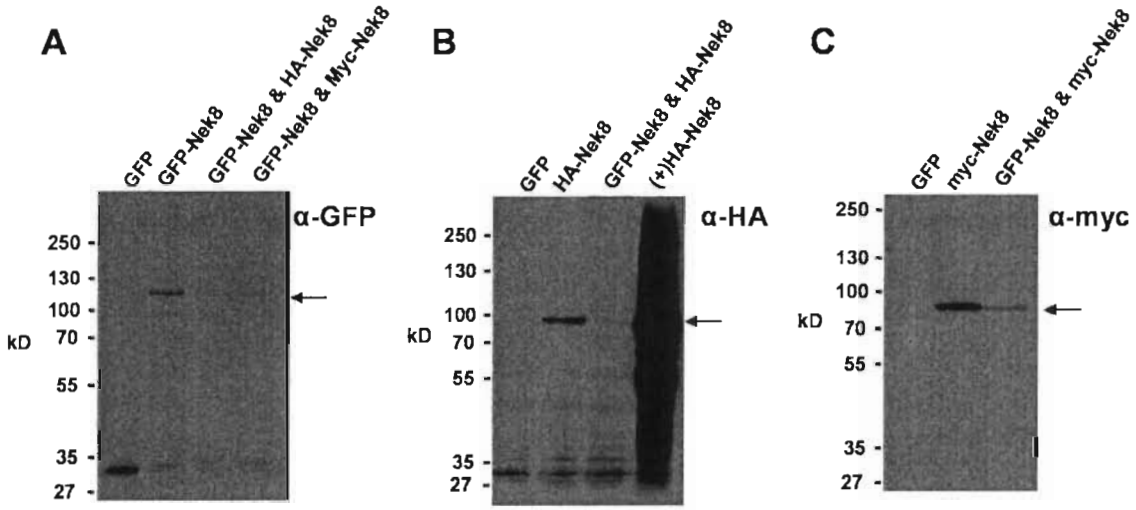

Western blot analysis of IMCD-3 cells transfected with wild type Nek8. **(A)** Anti-GFP blot shows expected sizes for GFP alone (27kD) and GFP-Nek8 (102kD) in GFP-Nek8 alone and co-transfected lanes. **(B)** Anti-HA blot shows expected size for HA-Nek8 (76kD) in HA-Nek8 alone and co-transfected lanes. (+) HA-Nek8 = positive control from a different Nek8-HA vector. **(C)** Anti-myc blot shows expected size for myc-Nek8 (76kD) in myc-Nek8 alone and co-transfected lanes. Note that half the amount of vector DNA was used in co-transfections.

Using indirect immunofluorescence, both the HA-Nek8 and myc-Nek8 fusion proteins failed to localize to cilia (Figure A2-3). This was unexpected, as GFP-Nek8 localized to cilia in 58% of transfected cells (see Figure 4-2). It may be that the small HA and myc epitopes interfere with folding or function of the Nek8 kinase domain, which is required for ciliary localization, while the GFP domain does not.

When IMCD-3 cells were transfected with only myc-Nek8 constructs, there was no effect on ciliation, mitosis, or number of centrosomes for wild type and mutant forms (Figure A2-4). Also similar to GFP-Nek8, overexpression of any form of myc-Nek8 (wild type or mutant) caused multinucleate cells (Figure A2-4).

Figure A2- 3 HA- and myc-tagged Nek8 fail to localize to cilia

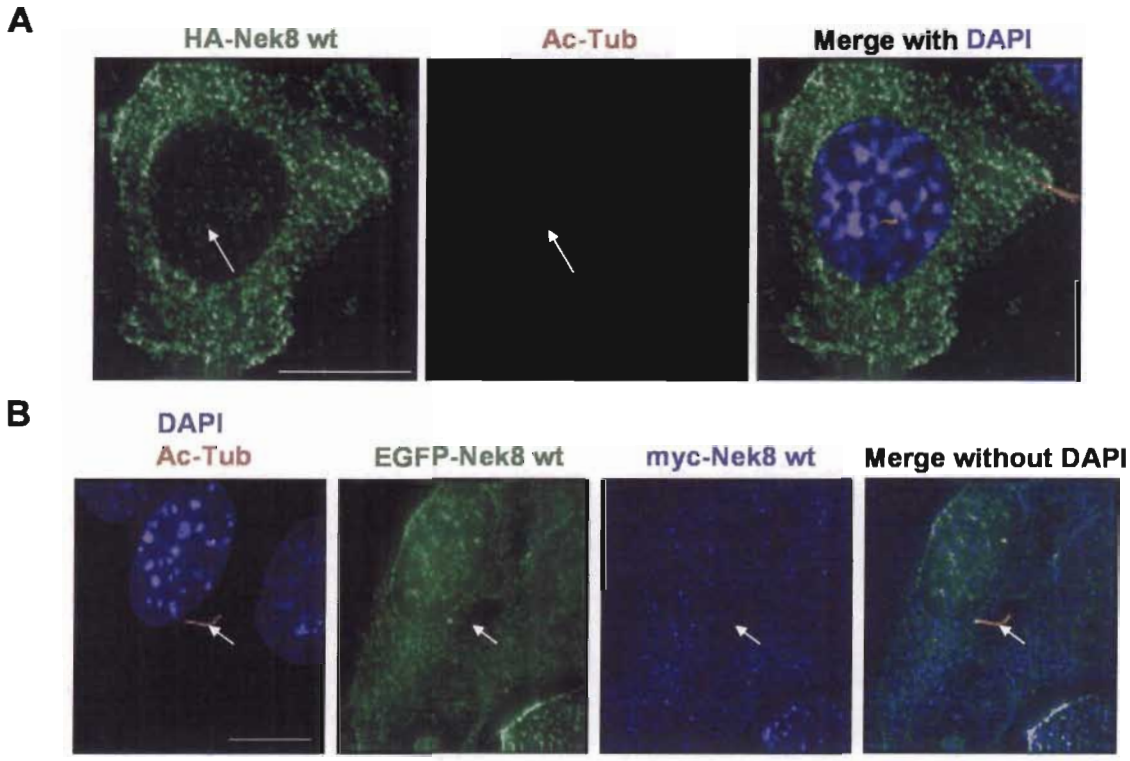

(A) HA-Nek8 transfected IMCD-3 cell stained for acetylated tubulin (red), HA-Nek8 (green), and nuclei (blue). **(B)** EGFP-Nek8 and myc-Nek8 co-transfected IMCD-3 cell stained for acetylated tubulin (red), myc-Nek8 (blue), and nuclei (blue with Ac-tub). Bar = 10 μm

Figure A2- 4 Myc-Nek8 expression

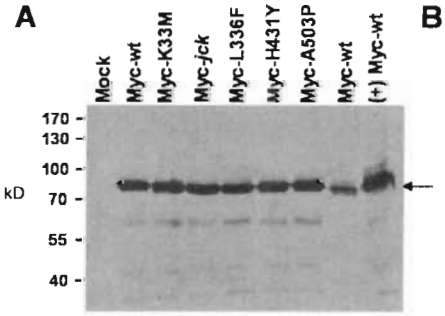

B

	Mock	WT	L336F	H431Y	A503P
With cilia	64%	54%	39%	47%	45%
Without cilia	25%	20%	20%	24%	19%
Mitotic	10%	3%	4%	4%	3%
Multinucleate	1%	22%	36%	22%	29%
Abnormal centrosomes	0.5%	1%	1%	3%	4%
N=	400	100	100	100	100

(A) Anti-myc western blot of pCMV-myc transfected IMCD-3 cells. Shown is expected size of 76kD for myc-Nek8 (arrow) wild type and mutants. **(B)** Quantification of phenotype of pCMV-myc transfected IMCD-3 cells, judged by immunofluorescence of cells stained for myc-Nek8, acetylated tubulin, and DAPI. N=number of cells counted.

Appendix 3: RNAi Knockdown of Nek8

Rationale

This work addressed a second problem that arises from transient transfection *in vitro* where endogenous Nek8 could be compensating for any phenotypes resulting from exogenous mutant Nek8 expression. The solution was to acquire Nek8 knockout cell line for transfection of mutant constructs, thus removing endogenous contribution of Nek8 function.

Methods and Materials

The two shRNA vectors used for RNAi contained 21bp sequences of exons 2 and 8 of mouse Nek8 mRNA, designated as pRNAi-E2 and pRNAi-E8. The targeting oligonucleotides consisting of BamHI-antisense-loop-sense-termination-HindIII motif were GATCCCGTACTCCATAGCAATCATGAGGTTGATATCCGC CTCATGATTGCTATGGAGTATTTTTTCCAAA for exon 2 and GATCCCATAATGCCTCGGTC TGTCAAGTTGATATCCGCTTGACAGACCGAGGCATTATTTTTTTCCAAA for exon 8, along with the reverse complements with BamHI and HindIII overhangs. Page-purified oligos were annealed together at 95°C for 10 min. in 1x SSC (150mM sodium chloride, 15mM sodium citrate, pH 7.0) and ligated into BamHI/HindIII-cut pRNAinT-H1.2/Neo (Genscript) which carries neomycin and ampicillin resistance, a TetO1 operator upstream of the cloning site, and a reporter coral GFP expression cassette under the CMV promoter. Vectors were transformed into Mach1 *E. coli* (Invitrogen), selected in ampicillin-containing media, verified by restriction endonuclease digest and DNA sequencing, and purified with an

endotoxin-free maxiprep kit (Qiagen). Transient transfection in IMCD-3 cells was performed as previously. Stably transfected clones were isolated by dilution of cells resistant to antibiotic, grown on 10cm dishes, selectively trypsinized (0.05% Trypsin, with EDTA 4Na, 1X, Invitrogen) within greased glass cloning rings, and grown in 24-well plates. Western blots were performed as described in chapter 4 and used rabbit anti-Nek8 antibody (2000-fold dilution, Liu *et al.* 2002). The methodology is outlined in Figure A3-1 and Figure A3-2.

A stable tetracycline repressor (TetR) IMCD-3 cell line was made by transfection of the FspI digested, linearized pcDNA6/TR (Invitrogen) and selection of clones in blasticidin-containing media. Tetracycline was used at 1 µg/mL in media containing certified tetracycline-free fetal bovine serum. RT-PCR verifying TetR expression was conducted using primers (ACAGCGCATTAGAGCTGCTT and CCCCTTCTAAAGGGCAAAAG) to amplify an 186bp portion of TetR transcript. RNA was isolated and cDNA was prepared from IMCD-3 cells using TRIzol (Invitrogen) and RevertAid H Minus First Strand cDNA Synthesis Kit (Fermentas) according to manufacturer's protocol.

Figure A3- 1 Methodology for a Nek8 knockdown IMCD-3 cell line

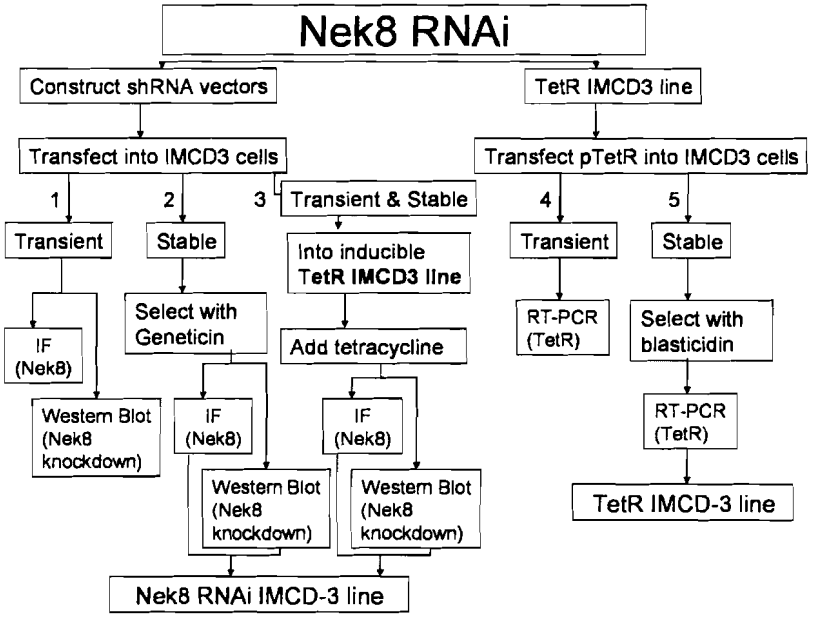

Nek8 knockdown was attempted in IMCD-3 cells and in a TetR IMCD-3 cell line. Transfection into IMCD-3 cells was performed 1) transiently 2) stably through Geneticin selection and 3) into a TetR cell line, both transiently and stably. Introducing the TetR into IMCD-3 cells was done 4) transiently and 5) stably through blasticidin selection. Successful transfections were monitored by anti-Nek8 immunofluorescence and Western blot and by RT-PCR against the TetR protein. Abbreviations: IF=immunofluorescence, TetR=tetracycline repressor, RT-PCR=reverse transcriptase polymerase chain reaction.

Figure A3- 2 Co-transfection scheme for Nek8 knockdown IMCD-3 cell line

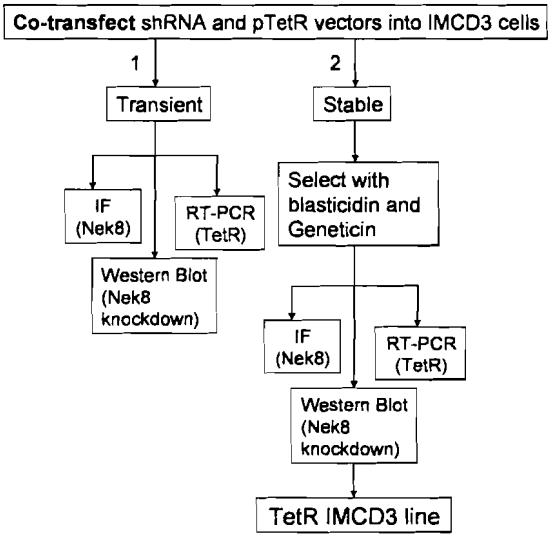

The pRNAi-E2 and pRNAi-E8 vectors are cotransfected with pcDNA6/TR at a 1:6 ratio. The 1) transient transfection was performed while the 2) stable transfection and double selection has yet to be done. Successful transfections were monitored by anti-Nek8 immunofluorescence and Western blot and by RT-PCR against the TetR transcript. Abbreviations: IF= immunofluorescence, TetR=tetracycline repressor, RT-PCR=reverse transcriptase polymerase chain reaction.

Results and Discussion

Short hairpin RNAi constructs targeting exons 2 and 8 of Nek8 (pRNAi-E2 and pRNAi-E8) were transfected transiently into IMCD-3 cells and after a 96h incubation period, a modest knockdown of Nek8 was observed by Western blot (Fig A3-3A). However, when transfected cells were selected by Geneticin, no knockdown was observed for either construct (not shown). It could be that persistent Nek8 knockdown was lethal to the cell line and the antibiotic-resistant cells which grew had likely selectively integrated the RNAi vector without the targeting short hairpin.

It was necessary to make a Nek8 knockdown cell line that was inducible. Linearized and circular TetR vectors were transfected into IMCD-3 cells and selected in blasticidin-containing media. Clones were isolated and stable expression of TetR transcript was successful in two clones from the linearized transfection, TRL5 and TRL7, as monitored by RT-PCR (Figure A3-3B). The IMCD-3 TRL5 cell line, which appeared to have higher TetR expression, was transiently transfected with pRNAi-E2 and pRNAi-E8. Nek8 knockdown was observed after 24h incubation with tetracycline when compared with empty vector-transfected cells, but is inconclusive when compared to cells without tetracycline (Figure A3-3C). Transfected TRL5 cells were grown in Geneticin-containing media and twelve pRNAi-E2 and six pRNAi-E8 clones were isolated. However, when incubated in tetracycline-containing media for 24h or 72h, no Nek8 knockdown was observed (Figure A3-3D).

Figure A3- 3 Towards an inducible Nek8 knockdown IMCD-3 cell line

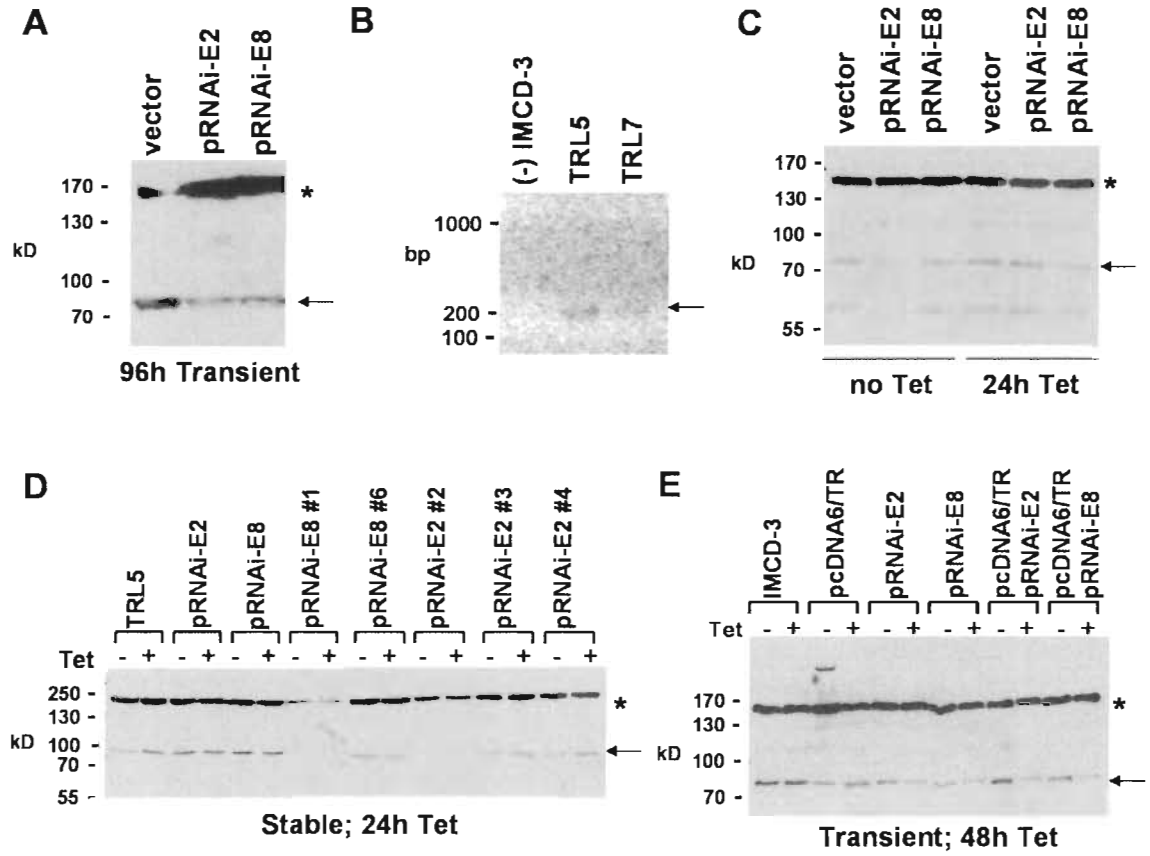

(A) Anti-Nek8 western blot of the transient transfection of pRNAi vectors into IMCD-3 cells after 96h incubation. **(B)** RT-PCR of TetR cDNA from IMCD-3 cells untransfected [(-) IMCD-3] and transfected with linearized pcDNA6/TR (TRL) and selected on blasticidin (clones 5 and 7). Arrow indicates expected band size of 186bp. **(C)** Anti-Nek8 western blot of the TetR IMCD-3 cell line (TRL5) transiently transfected with pRNAi vectors after 24h incubation in Tet-containing media **(D)** Anti-Nek8 western blot of selected clones (indicated by #) from stable transfection of TetR IMCD-3 cell line (TRL5) with pRNAi-E2 and pRNAi-E8 after 24h incubation in Tet-containing media. Similar results were found with 72h incubation. **(E)** Anti-Nek8 western blot of IMCD-3 cells transiently co-transfected with pcDNA6/TR and pRNAi vectors after 48h incubation with Tet-containing media. *=non-specific antibody-reactive band used as internal loading control. Expected size of Nek8 is 75 kD (arrows). Abbreviations: Tet=tetracycline

Stable knockdown of Nek8 in a TetR background may not have been achieved due to insufficient expression of TetR in the TRL5 cell line, allowing leaky expression of shRNA and lethality due to decreased Nek8 protein. Therefore, IMCD-3 cells were co-transfected with both TetR and pRNAi vectors in a 6:1 ratio (see Figure A3-2 for methodology). In transiently co-transfected

cells, Nek8 knockdown was visible after 48h in tetracycline-containing media for both pRNAi-E2 and pRNAi-E8 constructs versus no-tetracycline controls (Figure A3-3E). However, this experiment is unrepeated as of yet.

The next step towards making an inducible Nek8 knockdown IMCD-3 cell line is to doubly select co-transfected cells on blasticidin and Geneticin-containing media (see Figure A3-2). This would eliminate cells transfected with only one vector, as well as select for cells containing a high expression of TetR, assuming Nek8 knockdown is lethal. Clones of resistant cells would be isolated and tested for inducible Nek8 knockdown. This cell line could then be transfected with mutant Nek8 constructs and the effects analyzed.

Appendix 4: Domain Analysis of Nek8

Rationale

This work aims to explore the role of NPHP and *jck* mutations in the structure of Nek8, by examining the C-terminal RCC1 (regulator of chromatin condensation 1) domain through proteomics.

Methods and Materials

To predict the three-dimensional structure of the RCC1 domain of Nek8, the protein prediction programs, 3D PSSM (three-dimensional position-specific scoring matrix) and its successor, Phyre (protein homology/analogy recognition engine, Kelley *et al.* 2000) were used. The five predicted RCC1 repeats consisting of amino acids 414-698 of Nek8 were threaded onto the RCC1 protein crystal structure (PDB structure 1A12) using 3D PSSM, and later, the entire C-terminus of Nek8 consisting of amino acids 259-698 was queried using Phyre. The top hits for the structural analysis from Phyre were RCC1 (e-value 1.1e-10), galactose oxidase (e-value 0.0024, PDB structure 1K3I), and Groucho/Transducin-like enchancer protein 1 (TLE1, e-value 0.0083, PDB structure 1GXR) – all 7-bladed beta-propellers. The predicted Nek8 RCC1 domain structure was visualized using Swiss PdbViewer 3.7 (GlaxoSmithKline).

Results and Discussion

Mouse Nek8 contains 5 predicted RCC1 repeats and the RCC1 protein contains 7 RCC1 repeats, which are 50 amino acids in length and consists of beta-strands. When the five repeats of Nek8 are threaded onto the RCC1

protein crystal structure (PDB structure 1A12) using 3D PSSM, there is a large gap which suggests more residues are needed to make a complete RCC1 domain (Figure A4-1).

The following evidence supports a 7-bladed Nek8 RCC1 domain. Human and *Xenopus* Nek8 contain 5 predicted RCC1 repeats which differ in location to mouse Nek8 and are further upstream, although mouse Nek8 is 93% identical and 96% similar to human Nek8. Additionally, when the sequence of Nek8 is queried using Blast, the C-terminus is assigned 7 RCC1 domains. RCC1 domains are similar to the beta-propellor, WD40 domains. Searching through the PDB database, I found that the WD40 domain-containing Groucho/TLE1 has only 5 *predicted* WD40 repeats but has a crystal structure showing 7 blades. It is likely that Nek8 RCC1 domain contains 2 additional non-canonical RCC1 repeats upstream of the 5 predicted repeats.

The structure of the Nek8 RCC1 domain was predicted using the entire C-terminal domain using Phyre (Figure A4-2). However, only a 2-repeat portion of the Nek8 queried sequence was modeled on RCC1. The most complete Nek8 RCC1 structure was modeled on Groucho/TLE1 and is similar to that modeled on gaslactose oxidase. Nevertheless, the residues mutated in NPH (L336F, H431Y, and A503P) and the *jck* mouse model (G448V) were visualized using the 3D-PSSM-predicted RCC1 and Phyre-predicted Groucho/TLE1-based models. It appears that L336, H431, and G448 are at the periphery of the RCC1 domain and A503 is nearby (Figure A4-1, Figure A4-2). It is likely that the disease-

related missense mutations alter Nek8 function by affecting its ability to bind interacting partners and do not significantly destabilize the RCC1 domain.

Figure A4- 1 Nek8 RCC1 domain modelled on RCC1 protein

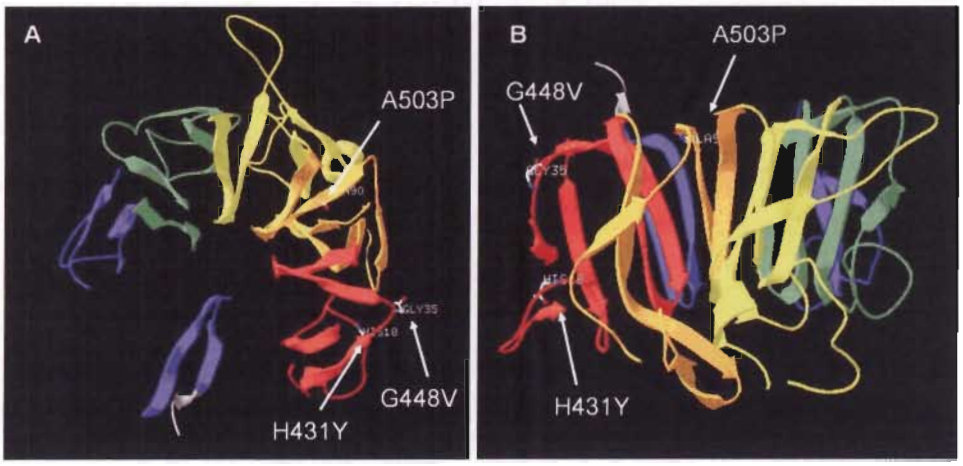

3D-PSSM-predicted structure of Nek8 RCC1 domain. The five predicted RCC1 repeats are shown in red (aa 416-467), orange (aa 468-519), yellow (aa 520-585), green (aa 586-637), and blue (aa 638-690). Grey is C-terminal sequence following the last predicted repeat. Shown are the locations of mutations associated with NPH (H431Y and A503P) and the *jck* mouse model (G448V). The L336F mutation is not shown because it occurs before the predicted RCC1 repeats.

Figure A4- 2 Nek8 RCC1 domain modelled on Groucho/TLE1 WD40 domain

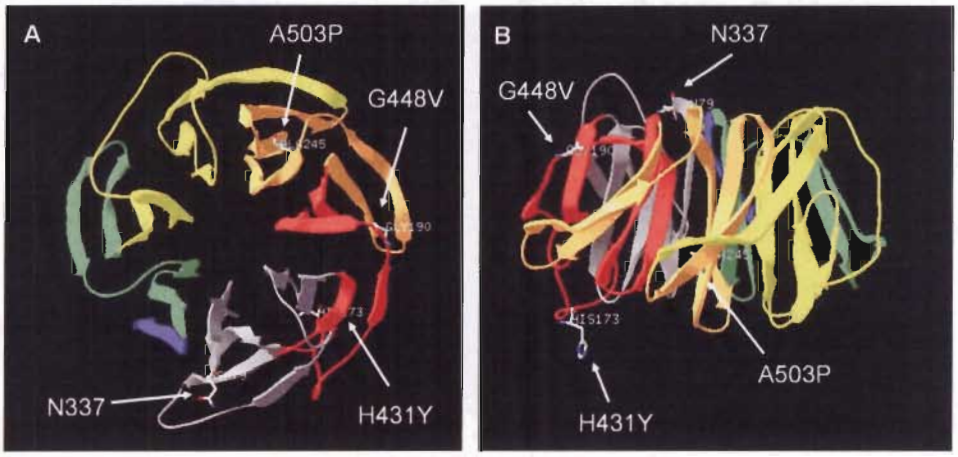

Phyre-predicted structure of Nek8 RCC1 domain. The five predicted RCC1 repeats are shown in red (aa 416-467), orange (aa 468-519), yellow (aa 520-585), green (aa 586-637), and blue (aa 638-690). Grey is C-terminal sequence preceding the first predicted repeat. Shown are the locations of mutations associated with NPH (H431Y and A503P) and the *jck* mouse model (G448V). Note that the prediction program initiated threading at Arg337, so the adjacent Leu336 is not visualized.

Appendix 5: Exogenous Nek3 Expression

Rationale

There is a correlation between the NIMA-related kinase family and cilia and centrosomes (Quarmby and Mahjoub, 2005 and Parker *et al.* 2007). This work examined transiently transfected mouse Nek3 in IMCD-3 cells to determine if GFP-tagged Nek3 localized to either cilia or centrosomes.

Methods and Materials

Mouse Nek3 IMAGE cDNA (Invitrogen) was subcloned into pEGFP-C2 by Moe Mahjoub. Transfection into IMCD-3 cells and immunofluoresence was performed as previously detailed in chapters 2 to 4.

Results and Discussion

Transient transfection of GFP-Nek3 in IMCD-3 cells showed the predicted size by Western blot (Figure A5-1B). GFP-Nek3 did not localize to cilia or centrosomes, but rather, to the cell periphery and the leading edge. GFP-Nek3 transfected cells also seemed to have more lamellopodia/filopodia than mock transfected controls (Figure A5-1A). However, Nek3 does not appear to be endogenously expressed in IMCD-3, NIH 3T3, HeLa, or HEK 293 cells, judged by Western blot using anti-mouse Nek3 antibody (2,500-fold dilution, BD Biosciences, Figure A5-1C) and the transfected phenotype likely reflects ectopic expression. Nek3 has been reported to be overexpressed in breast cancer and functions in motility through the prolactin pathway by phosphorylating Vav2, a guanidine nucleotide exchange factor for the Rho family (Miller *et al.* 2007, Miller

et al. 2005). The localization and phenotype due to ectopic expression in IMCD-3 cells supports a role of Nek3 in cytoskeletal reorganization associated with metastasis.

Figure A5- 1 Exogenous GFP-Nek3 expression

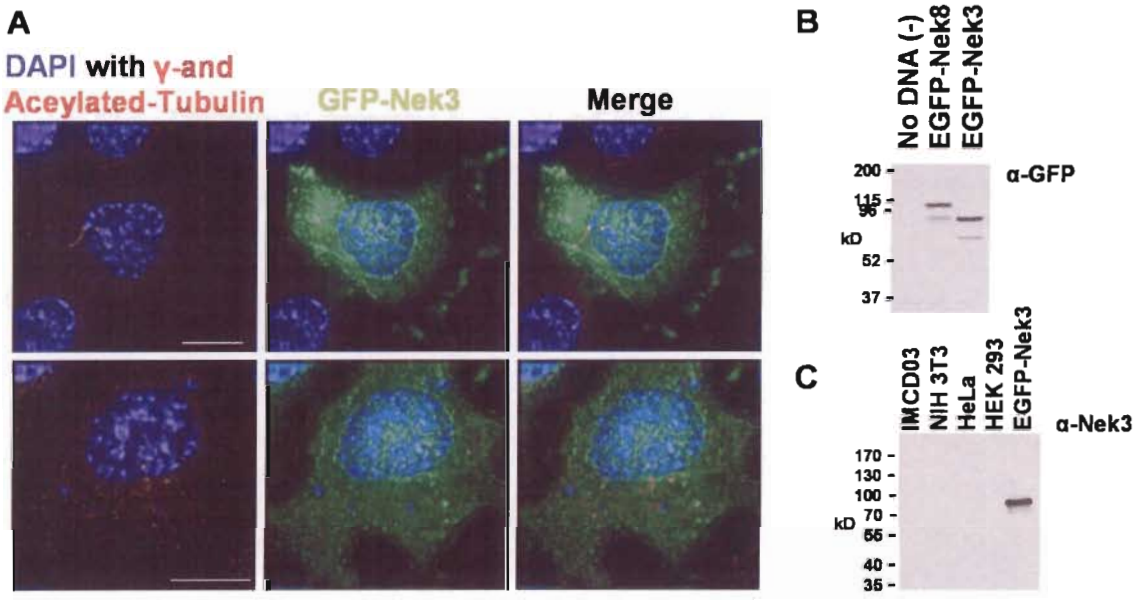

(A) IMCD-3 cells transfected with GFP-Nek3 (green) were stained for γ- and acetylated tubulin (red), and DNA (blue). Bar = 10 μm (B) Anti-GFP Western blot of cells tranfected with pEGFP constructs. The predicted sizes for GFP-Nek8 and GFP-Nek3 were 102kD and 83kD, respectively. (C) Western blot of endogenous Nek3 protein. Nek3 had an expected size of 56kD.

Appendix References

Kelley LA, MacCallum RM, Sternberg MJ: Enhanced genome annotation using structural profiles in the program 3D-PSSM. *J Mol Biol* 299: 499-520, 2000

Liu S, Lu W, Obara T, Kuida S, Lehoczky J, Dewar K, Drummond IA Beier DR: A defect in a novel Nek-family kinase causes cystic kidney disease in the mouse and in the zebrafish. *Development* 129: 5839-5846, 2002

Miller SL, Antico G, Raghunath PN, Tomaszewski JE, Clevenger CV: Nek3 kinase regulated prolactin-mediated cytoskeletal reorganization and motility of breast cancer cells. *Oncogene* In Press.

Miller SL, DeMaria JE, Freier DO, Riegel AM, Clevenger CV: Novel association of Vav2 and Nek3 modulates signaling through the human prolactin receptor. *Mol Endocrinol* 19: 939-949, 2005

Parker JDK, Bradley BB, Mooers AO, Quarmby LM: Phylogeny of the NIMA-related family of kinases (Neks): an ancient gene family associated with cilia. Submitted.

Quarmby LM, Mahjoub MR: Caught Nek-ing: cilia and centrioles. *J Cell Sci* 118: 5161-5169, 2005